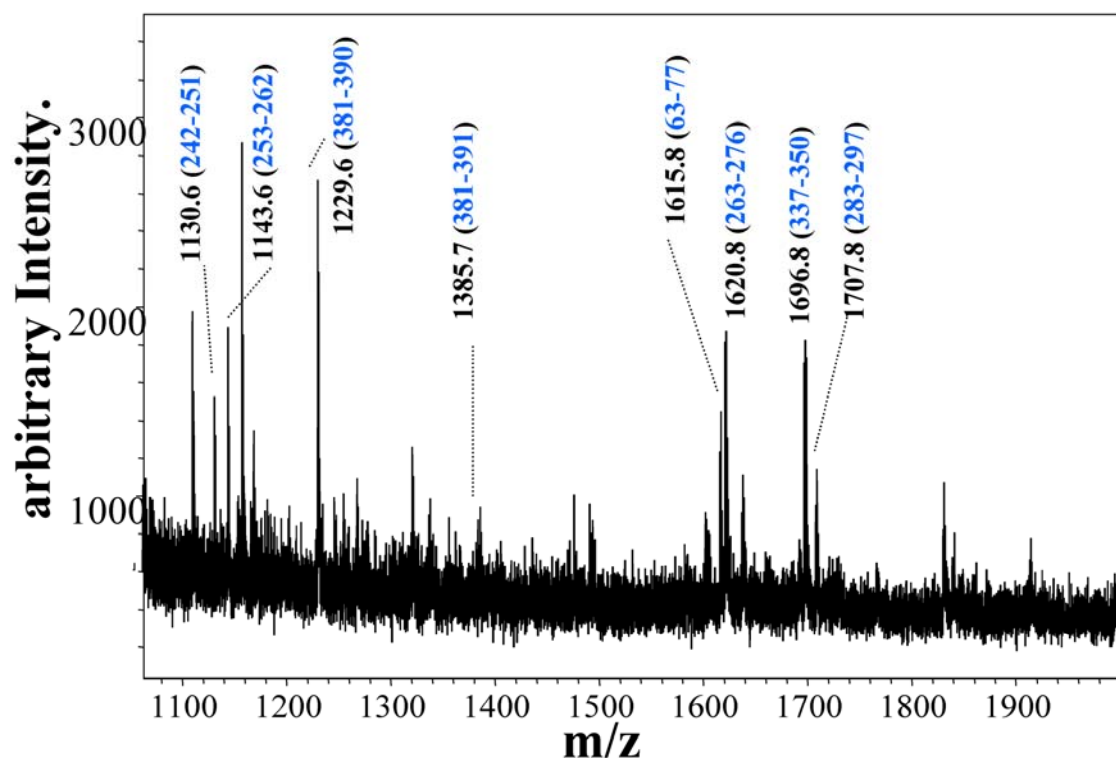# 2. Results.

By a proteomic screen, tubulin was identified as a Ca^{2+}-sensitive interacting protein of TRPV1. The interaction was confirmed and further characterized biochemically (chapter 2.1). Observations that C-terminus of TRPV1 interacts with and provides stability to the polymerized microtubules *in vitro* suggested that the TRPV1 is physically-linked with the microtubule cytoskeleton, and the microtubule cytoskeleton may be the down stream effectors of the receptor activation. Therefore, the effect of TRPV1 activation on the microtubule cytoskeleton was analyzed and characterized on a cellular context (chapter 2.3). Finally, if TRPV1-microtubule cytoskeleton interaction/ regulation can influence the axonal growth, was functionally analyzed at the level of growth cone morphology and movement (chapter 2.4). Additionally, an attempt was taken to identify and biochemically characterize the tubulin-binding site/s located at the C-terminal cytoplasmic domain of TRPV1 (chapter 2.2).

2.1. Identification and characterization of Tubulin as a Ca^{2+} sensitive interactor for TRPV1

In an attempt to identify the TRPV1 interacting proteins, which might be important for the channel function, regulation and/or signalling, a pull-down approach with MBP-fused cytoplasmic domains of TRPV1 was initially started by Han Si along with Ricarda Jahnel at the laboratory of Prof F. Hucho. For that purpose, both N- and C-terminal cytoplasmic domains of TRPV1 were expressed as MBP-fusion proteins and planned to use as baits to identify the TRPV1 interacting proteins.

This thesis work begins with the aim of identifying some of the TRPV1 interacting proteins. Using MBP-TRPV1-Nt, as bait to identify the interacting proteins was not feasible due to the difficulties associated with the expression of MBP-TRPV1-Nt in its full-length. Therefore, the major attention was shifted to identify the proteins that interact with the C-terminal cytoplasmic domain of TRPV1. Tubulin was identified as a protein that interacts with the TRPV1 with its C-terminal cytoplasmic domain but not with the N-terminal cytoplasmic domains. This interaction was confirmed by means of multiple biochemical experiments. The C-terminus of TRPV1 was observed to interact not only with soluble tubulin, but also with the polymerized microtubules. Under certain experimental conditions, C-terminus of TRPV1 was also observed to provide stability to the polymerized microtubules and exerts a Ca^{2+}-sensitivity.

2.1.1. Detection of Ca^{2+}-sensitive interactions of the TRPV1 C-terminal fragment.

Ca^{2+} plays an important role in the desensitisation of the TRPV1, and Ca^{2+}-influx through TRPV1 may trigger intracellular signalling events. Assuming that at least some of the protein-protein interactions of the TRPV1 might be Ca^{2+}- sensitive, pull-down assays were conducted with C-terminus of TRPV1 both in the presence and absence of Ca^{2+}. This is mainly due to difficulties to express and purify MBP-TRPV1-Nt (N-terminus of TRPV1) in large amount in its full-length size. The MBP-TRPV1-Ct fusion protein was for that purpose bound to an amylose resin, incubated with protein extracts from spinal cord, and the fusion protein along with interacting proteins was eluted from the resin with maltose. The soluble eluate was then precipitated with trichloroacetic acid and subjected to SDS-PAGE. Extracts

Figure 2.1. Identification of α– and β-tubulin as an interacting partner of the C-terminal of TRPV1. MBP-TRPV1-Ct (lane 2 and 3) or MBP alone (lane 4 and 5) immobilised on amylose beads and incubated with spinal cord extract overnight in the presence of 5 mM Ca^{2+} or absence of Ca^{2+}. Bound proteins were eluted with 10 mM maltose, and subjected to 10% SDS-PAGE. Proteins were visualised by silver stain (left side). Lane 1, spinal cord extract, lane 2, pull down eluate of proteins bound in the presence of Ca^{2+}, lane 3, pull down eluate in the absence of Ca^{2+}, lane 4 and 5 represent negative controls in the presence or absence of Ca^{2+}, showing non-specific binding to MBP alone immobilised on amylose beads. MBP-TRPV1-Ct (indicated by arrow) interacts with a 55 kDa protein (indicated by red coloured asterisk). Subsequent in-gel digestion and MALDI-MS analysis reveals the identity of that protein as β-tubulin. Western blot analysis with monoclonal antibodies against α–tubulin and β–tubulin (right side) of the same samples confirms the presence of tubulin as a TRPV1 interactor.

Measured mass (M)	Avg/ Mono	Computed mass	Error (ppm)	Residues start	to	Missed cut	Peptide sequence
1052.652	M	1052.601	48	310	318	0	YLTVAAIFR
1129.622	M	1129.588	31	242	251	0	FPGQLNADLR
1142.642	M	1142.627	14	253	262	0	LAVNMVPFPR
1228.652	M	1228.590	50	381	390	0	ISEQFTAMFR
1384.702	M	1384.692	8	381	391	1	ISEQFTAMFRR
1384.702	M	1384.692	8	380	390	1	RISEQFTAMFR
1615.792	M	1615.905	-70	307	320	2	HGRYLTVAAIFRGR
1619.762	M	1619.828	-40	263	276	0	LHFFMPGFAPLTSR
1695.772	M	1695.772	-31	337	350	0	NSSYFVEWIPNNVK
1706.822	M	1706.854	-19	283	297	0	ALTVPELTQQMFDSK

Figure 2.2. Peptide analysis of 55 kDa band observed as a Ca^{2+}-sensitive TRPV1 interacting protein. Peptide mass fingerprint obtained from MALDI-MS analysis of the peptide mixture derived from the protein corresponding to the 55 kDa band. Peptides matching with β-tubulin are indicated. Specific masses and sequences of the peptides are listed. Dr. Mathias Dreger did MALDI-MS analysis.

that contained predominantly soluble proteins from rat or pig spinal cord/brain, or from the DRG-derived cell line F11, were used as the sources for potential MBP-TRPV1-Ct-interacting proteins. In the presence of Ca^{2+}, a number of spinal-cord proteins were observed

to be pulled down with MBP-TRPV1-Ct, while some of these proteins were not pulled down to the same extent in the absence of Ca^{2+} (figure 2.1). None of these potential interacting proteins was observed in the absence of fusion protein in the fractions eluted from only amylose resin either in presence or in the absence of Ca^{2+}, or when MBP alone was used as bait (figure 2.1). These observations were reproduced multiple times in independent experiments.

2.1.2. Identification of tubulin as TRPV1 interacting protein.

To identify the proteins interacting with TRPV1, the corresponding protein bands pulled down by MBP-TRPV1-Ct were excised out of the gel and tryptically derived peptides were analysed by mass spectrometry. A protein pulled down in a Ca^{2+}-sensitive manner, corresponding to a 55 kDa protein band observable on the gel, was identified as tubulin β chain 15 from rat (figure 2.2). A total of 16 peptides covered 39% of the full-length protein sequence matched with NCBI accession number A25113 (figure 2.2). This result was further confirmed by Western blot analysis (figure 2.1). Monoclonal antibodies specific for α- and β-tubulin were used for Western blot analysis. Presence of α-tubulin was also revealed by Western blot analysis. Both tubulins bound to the MBP-TRPV1-Ct predominantly in the presence of Ca^{2+}, and α-tubulin was virtually only detected when the pull-down was conducted in the presence of Ca^{2+} (figure 2.1). The pull down of the tubulins by the MBP-TRPV1-Ct was observed from pig spinal cord-extracts as well as from F11 cell extracts (data not shown). The identification of other potential TRPV1-interacting proteins is ongoing and this thesis work focussed on the characterisation of the TRPV1-tubulin interaction.

2.1.3. Tubulin, but not actin, co-precipitates with full-length TRPV1 in anti-TRPV1 immunoprecipitation.

To confirm the interaction between TRPV1 and tubulin by an independent method, full-length TRPV1 was expressed by transient transfection in F11 cells, and immunoprecipitation experiments were performed. The F11 cell line, originating from rat DRG neuron and mouse neuroblastoma cells, reflects many properties of DRG neurons (Platika et al. 1985). This cell line was therefore used as a model system to express TRPV1 in a more "natural" environment and to explore how TRPV1 and the neuronal cytoskeleton are interrelated.

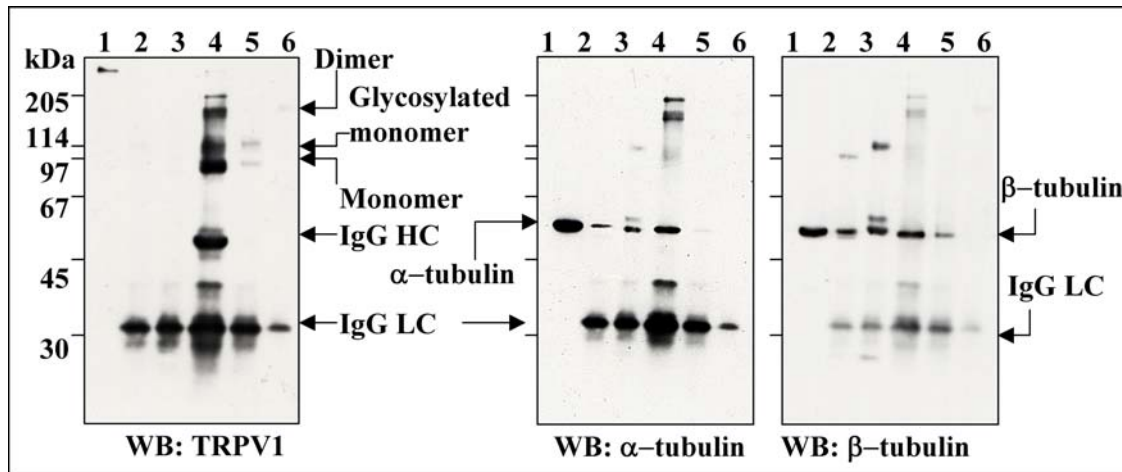Antibodies specific for TRPV1 precipitate monomer, glycosylated monomer, dimer

Figure 2.1.3. Tubulin co-immunoprecipitates with TRPV1. TRPV1 was transiently expressed in F11 cells. Soluble cell extract (lane 1) was immunoprecipitated by anti-N-terminal TRPV1 antibody (lane 2), anti C-terminal TRPV1 antibody (lane 3), anti α-tubulin (lane 4), anti β-tubulin (lane 5) and non-specific antibody (lane 6). Blots were probed for TRPV1 (left side), stripped off and probed for α-tubulin (middle) and β-tubulin (right) subsequently.
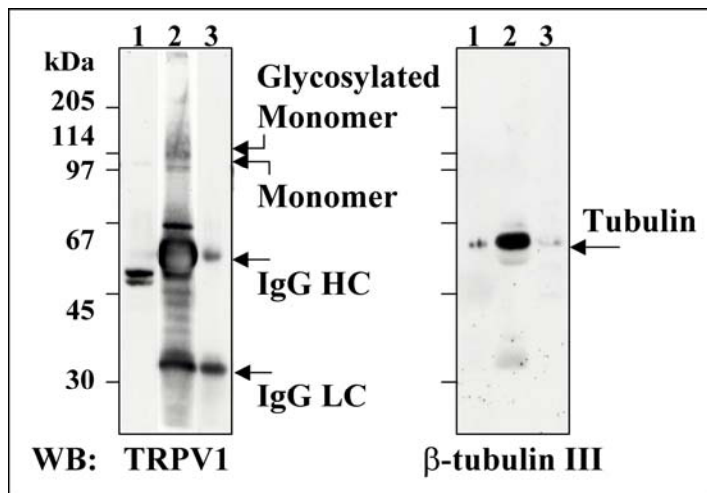

Figure 2.4. Co-immunoprecipitation of neuron-specific β-tubulin subtype III with TRPV1 from rat spinal-cord extract. Detergent solubilised rat spinal-cord extract (lane 1) was precipitated by anti-N-terminal TRPV1 antibody (lane 2) and non-specific antibody (lane 3). Blots were probed for TRPV1 (left side) and β-tubulin subtype III (right side).

and glycosylated dimer of TRPV1. Tubulin co-precipitated with TRPV1-specific antibodies, regardless whether N-terminus-specific anti-TRPV1 antibodies or C-terminus-specific anti-TRPV1 antibodies were used for immunoprecipitation (figure 2.3). Co-precipitation of tubulin from the same extract was not observed with non-specific antibodies, suggesting that the interaction between TRPV1 and tubulin is specific. Whether monoclonal antibodies specific for α-tubulin and β-tubulin are capable to co-precipitate TRPV1 with the tubulins was also tested. However, TRPV1 was not co-precipitated in those experiments (figure 2.3). From this observation it can be concluded that only a small subset of tubulin might interact with TRPV1, and TRPV1 was much less abundant in the preparation than tubulin.

Neuron-specific β-tubulin subtype III was also co-precipitated with TRPV1 from detergent-soluble spinal-cord extracts, suggesting that the tubulin-TRPV1 interaction not only occurs in transfected cells, but also in native tissue (figure 2.4). The anti-TRPV1 antibodies did not precipitate the tubulins from non-transfected cells (data not shown) confirming further that the observed tubulin-TRPV1-interaction is specific. Additionally, GFP-TRPV1 (fusion at N-terminus) or TRPV1-GFP (fusion at C-terminus) was expressed in F11 cells and immunoprecipitation was performed using anti-TRPV1 antibody. Equal amounts of tubulin were observed in both immunoprecipitates, indicating that both N- and C-
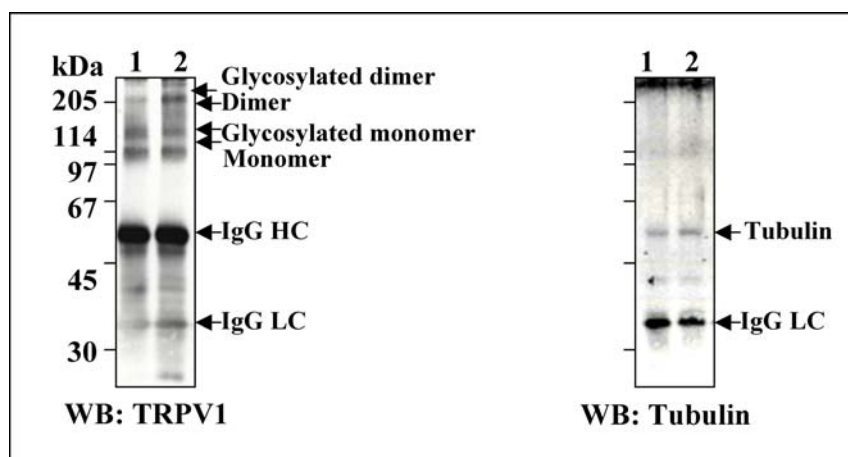
Figure 2.5. Tubulin co-immunoprecipitates with GFP-fused TRPV1. Antibodies specific for TRPV1 were used to precipitate GFP-TRPV1 (fusion at N-terminal, lane 1) or TRPV1-GFP (fusion at C-terminal, lane 2) transiently expressed in F11 cells. Blots were probed for TRPV1 (left side) and tubulin (right side). Tubulin co-immunoprecipitates with both GFP-TRPV1 and TRPV1-GFP, indicating that the free ends are probably not important for the interaction.
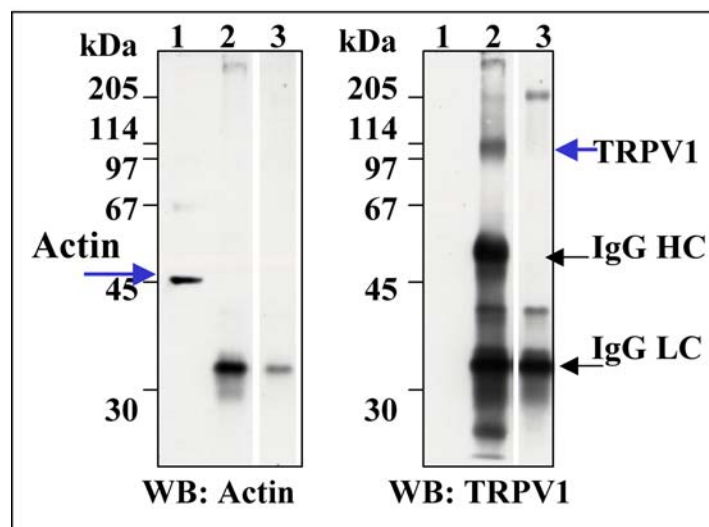
Figure 2.6. Actin does not co-precipitate with TRPV1.

TRPV1 was transiently expressed in F11 cells. Soluble cell extract (lane 1) was immunoprecipitated by anti-N-terminal TRPV1 antibody (lane 2), and non-specific antibody (lane 3). Blots were probed for actin (left side), stripped off and probed for TRPV1 (right) subsequently. No actin was detected in the TRPV1 immunoprecipitates.

terminal free ends are probably not important for the tubulin-TRPV1 interaction (figure 2.5).

Actin is another major constituent of cytoskeletal structures. In order to assess whether actin co-precipitates in anti-TRPV1 immunoprecipitation, the anti-TRPV1 immunoprecipitate was probed for the presence of actin. However, no actin was detected in the immunoprecipitates (figure 2.6). Taken together, the results suggest that tubulin, but not actin, is a component of the TRPV1 complex, and links the receptor to the microtubule cytoskeleton.

2.1.4. Purified tubulin binds to the C-terminal sequence of TRPV1, but not with the N-terminal portion of TRPV1

In the MBP-TRPV1-Ct pull-down assay with proteins from spinal cord extracts, it
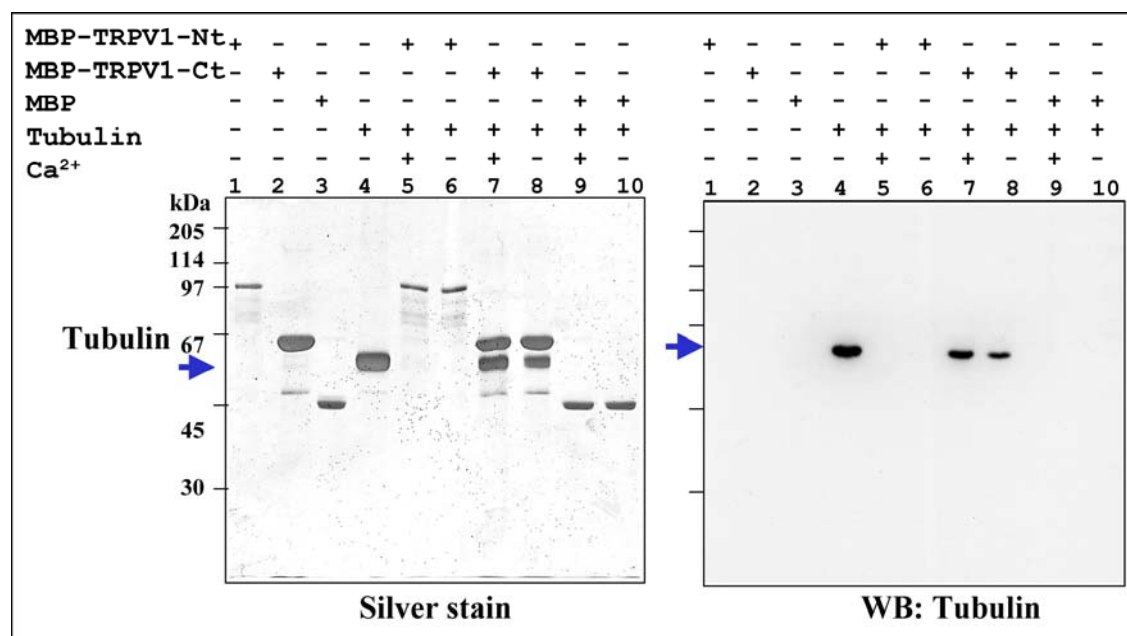
Figure 2.7. Purified tubulin interacts directly with MBP-TRPV1-Ct in a Ca^{2+}-sensitive manner, but not with MBP-TRPV1-Nt. MBP-TRPV1-Nt, MBP-TRPV1-Ct and MBP alone, all immobilized on amylose resin material, were incubated with purified tubulin dimers. MBP-TRPV1-Nt (lane 1), MBP-TRPV1-Ct (lane 2), MBP alone (lane 3) and tubulin dimers (lane 4). Tubulin dimers did not bind to the MBP-TRPV1-Nt (lanes 5 and 6) nor to the MBP alone (lanes 9 and 10), but bound to the MBP-TRPV1-Ct (lanes 7 and 8). Binding of tubulin dimers to MBP-TRPV1-Ct appeared to be slightly enhanced in the presence of Ca^{2+} (+) as compared to the situation in the absence of Ca^{2+} (–). The proteins were eluted from the amylose resin with 10 mM maltose and resolved by 10% SDS–PAGE. Proteins were stained with silver stain (left side). Western blot analysis (right side) of corresponding samples with anti-tubulin antibody YL1/2, confirming the presence of tubulin only in the MBP-TRPV1-Ct pull-down eluates. Arrow indicates the position of tubulin.
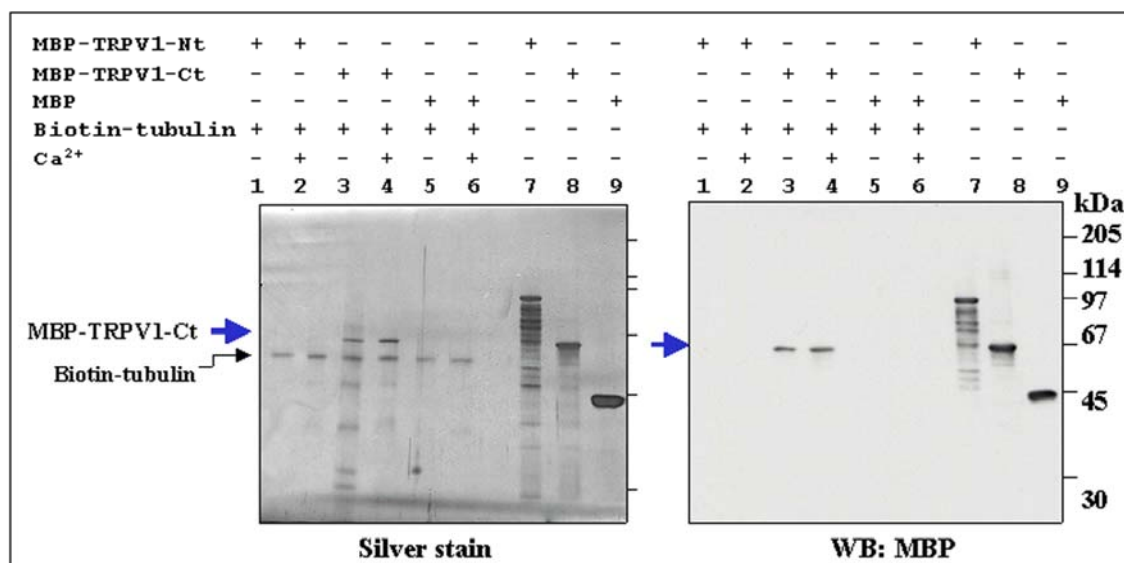
Figure 2.8. MBP-TRPV1-Ct is pulled down by biotinylated tubulin immobilized with streptavidin agarose. Biotinylated tubulin immobilized on streptavidin agarose was incubated with MBP-TRPV1-Nt (lane 1– 2), MBP-TRPV1-Ct (lane 3–4), or with MBP alone (lane 5–6) in the presence of Ca^{2+} (lane 1, 3 and 5) or in the absence of Ca^{2+} (lane 2, 4 and 6). Lanes 7–9 show the input of MBP-TRPV1-Nt, MBP-TRPV1-Ct and MBP, respectively. Only MBP-TRPV1-Ct was pulled down with the biotinylated tubulin. Right panel: Western blot analysis of samples corresponding to those in silver stain (left side) probed with the anti-MBP antibody. Among all the pull down samples, anti-MBP immunoreactivity shows up only in lanes 3 and 4, confirming that MBP-TRPV1-Ct, but not MBP-TRPV1-Nt or MBP alone, was pulled down with biotinylated tubulin.

was observed that tubulin interacts with the C-terminal domain of the TRPV1 along with other proteins. In order to test if the tubulin-TRPV1 interaction is direct and independent of other proteins, a soluble tubulin dimer fraction was prepared from porcine brain and a pull-down experiment was performed with this purified soluble tubulin. A considerable amount of purified tubulin was pulled down with MBP-TRPV1-Ct both in the presence and absence of Ca^{2+}, but not with MBP alone. Purified tubulin was also not pulled down by MBP-TRPV1-Nt (figure 2.7). This result was further confirmed by Western blot analysis using antibodies directed against tubulin (figure 2.7).

In reverse pull-down experiments using biotinylated tubulin immobilized on streptavidin agarose as a bait, it was found that MBP-TRPV1-Ct, but neither MBP-TRPV1-Nt nor MBP alone, bound to the tubulin (figure 2.8). This suggests that the TRPV1- tubulin interaction is direct and specific and is mediated by the C-terminal cytoplasmic domain, not by the N-terminal cytoplasmic domain of TRPV1.

2.1.5. TRPV1 cytosolic domains do not interact with soluble actin or neurofilament.

In order to explore if the cytoplasmic fragments of TRPV1 can directly interact with the other cytoskeleton elements, e.g. soluble actin and neurofilaments, direct binding experiments were performed with MBP-TRPV1-Ct or MBP-TRPV1-Nt with purified soluble actin and neurofilament preparation either in the presence or in the absence of Ca^{2+}. Neither binding of actin nor neurofilaments was detected with MBP-TRPV1-Ct or MBP-TRPV1-Nt under the same conditions (presence or absence of Ca^{2+}) where tubulin binds to the MBP-TRPV1-Ct. The absence of actin and neurofilaments in the pulled down eluates was further confirmed by Western blot analysis (figure 2.9).
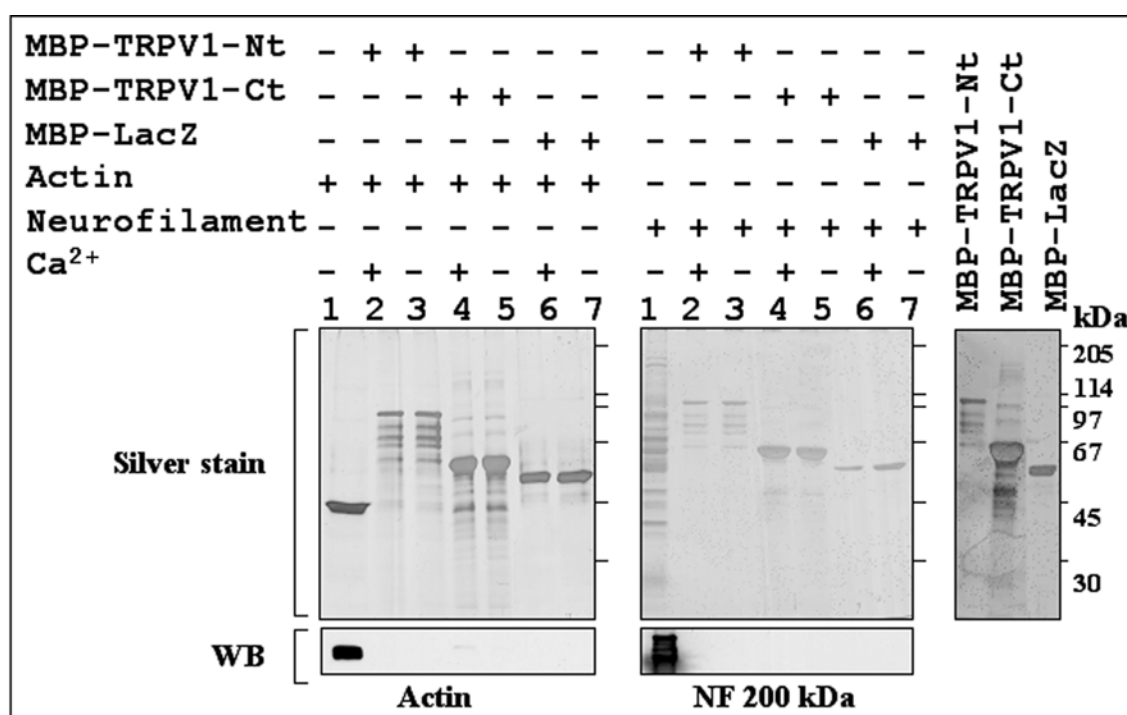
Figure 2.9. Cytosolic domains of TRPV1 do not interact with purified soluble actin or neurofilaments. MBP-TRPV1-Nt, MBP-TRPV1-Ct and MBP-LacZ, all immobilized on amylose resin material, were incubated with purified actin (left panel) or purified enriched neurofilaments (middle panel) either in presence (lane 2, 4 and 6) or absence of Ca^{2+} (lane 3, 5 and 7). Neither soluble actin nor neurofilaments bound to the MBP-TRPV1-Nt (lanes 1 and 2) or to the MBP-TRPV1-Ct (lane 4 and 5). MBP-LacZ was used as control (lanes 6 and 7). The proteins were eluted from the amylose resin with 10 mM maltose and resolved by 10% SDS–PAGE. Proteins were stained with silver stain (upper panel). Western blot analysis (lower panel) of corresponding samples with anti-actin antibody, and anti-neurofilament antibody 200 kDa confirming the absence of actin and neurofilament in the pull down elutes. The input amount of MBP-TRPV1-Nt, MBP-TRPV1-Ct and MBP-LacZ are shown (right side) by silver stained SDS-PAGE. Input of actin and neurofilaments are shown in lane 1. Enriched neurofilament fraction was kindly supplied by O. Bogen.

2.1.6. MBP-TRPV1-Ct, but not MBP-TRPV1-Nt, interacts also with polymerized forms of tubulin.

In order to assess if the C-terminal domain of TRPV1 also interacts with polymerized forms of tubulin, a co-sedimentation experiment was performed. Microtubules (MTs) can be formed from preparations of soluble dimers by adding GTP. The addition of taxol® favours MT formation and also stabilizes the MTs formed. MBP-TRPV1-Ct, MBP-TRPV1-Nt, or MBP were incubated with preformed MTs in the presence and absence of free Ca^{2+} at room temperature. The microtubules that formed along with bound proteins were separated from soluble dimers and unbound proteins by centrifugation. Proteins corresponding to supernatants and pellets were separated by SDS-PAGE, and analyzed by silver staining of proteins and by Western blots using anti-MBP antibodies. It was observed that approximately 50% of the total MBP-TRPV1-Ct co-sedimented with the polymerized microtubules (figure 2.10). In contrast, MBP-TRPV1-Nt, and MBP alone, failed to co-sediment with polymerized microtubules, and all of the MBP-TRPV1-Nt, or MBP, respectively, remained in the
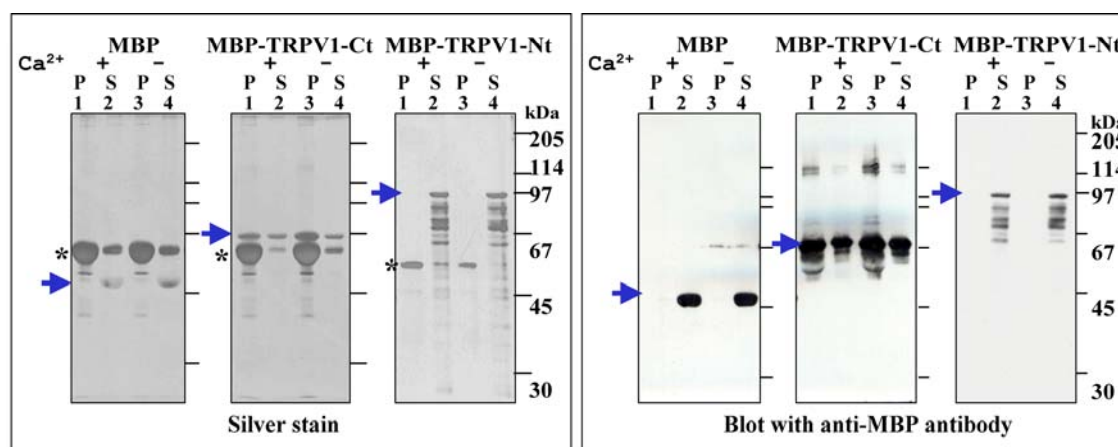
Fig 2.1.10. MBP-TRPV1-Ct, but not MBP-TRPV1-Nt, or MBP alone, co-sediments with polymerised microtubules. Purified αβ-tubulin dimers were incubated with taxol® and GTP to form microtubules (MT). Taxol®-stabilized MTs were incubated with 5 µg of purified MBP alone, MBP-TRPV1-Ct, or of MBP-TRPV1-Nt, in the presence (+) or absence (-) of Ca^{2+} (1 mM). Supernatant (**S**) and pellet (**P**) were separated by centrifugation and analysed by 10% SDS-PAGE. Distribution of the proteins between microtubule pellet (**P**) and supernatant (**S**) as visualised by silver staining of the proteins (left box). Only MBP (left), MBP-TRPV1-Ct (middle), or MBP-TRPV1-Nt (right) were assayed for co-sedimentation with MT. Tubulin on the gel is indicated by ∗ (asterisk). Coloured arrows indicate the positions of the MBP and fusion proteins. Only MBP-TRPV1-Ct co-sediments with MT. Western blot analysis of samples corresponding to those shown in silver staining using the anti-MBP antibody. Only when MBP-TRPV1-Ct was assayed for co-sedimentation with MT, anti-MBP immunoreactivity appeared in the pellet fractions (middle panel). In contrast, when MBP-TRPV1-Nt or MBP alone were assayed for co-sedimentation with MT, anti MBP immunoreactivity was only detected in the supernatants.
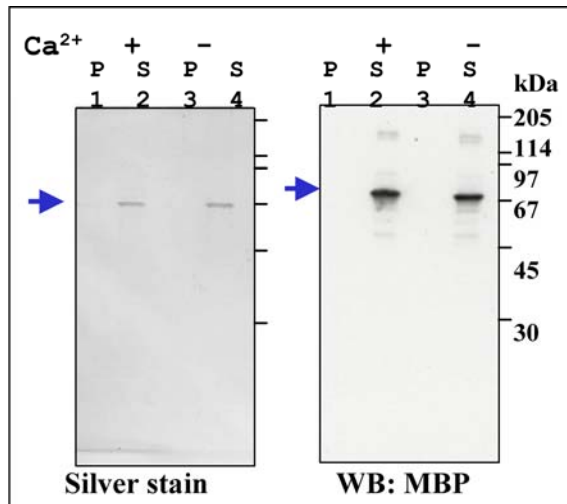
Fig 2.1.11. MBP-TRPV1-Ct does not appear in the pellet fractions in absence of polymerized microtubules.
MBP-TRPV1-Ct remain in the supernatant as confirmed by silver stain (left panel) and by anti MBP Western blot (right panel).

supernatants. This result was further confirmed by western blot analysis of the same samples using an anti-MBP antibody (figure 2.10). These data suggest that MBP-TRPV1-Ct, but not MBP-TRPV1-Nt, is capable of interacting not only with tubulin dimers, but also with polymerized microtubules. In the absence of polymerized microtubules, MBP-TRPV1-Ct was not found in the pellet fraction. Instead, it remained in the supernatant after centrifugation under these conditions (figure 2.11). The interaction of MBP-TRPV1-Ct with polymerized microtubule or soluble tubulin is also observed in the presence of high salt concentrations (500mM NaCl), indicating that the interaction is strong enough (data not shown).

All these results support the conclusion that the presence of the MBP-TRPV1-Ct in the pellet fraction is due to its direct interaction with polymerized MT. In this experiment, no significant effect of Ca^{2+} on the interaction was observed.

2.1.7. Tubulin interaction with MBP-TRPV1-Ct, but not MBP-TRPV1-Nt, allows microtubule formation under conditions that otherwise destabilise microtubules

To explore if the interaction of MBP-TRPV1-Ct with polymerised MT changes the physico-chemical properties of MTs, the "stability as polymers" was assessed. Tubulin dimers were allowed to form MTs in the absence of fusion proteins, or in the presence of MBP-TRPV1-Ct, MBP-TRPV1-Nt, under conditions that interfere with MT formation (presence of the MT-destabilizing agent nocodazole and Ca^{2+}). In the presence of nocodazole or a combination of nocodazole and Ca^{2+}, MT formation from tubulin dimers in the absence of fusion proteins was poor (figure 2.12, upper panel). Strikingly, when MBP-TRPV1-Ct was
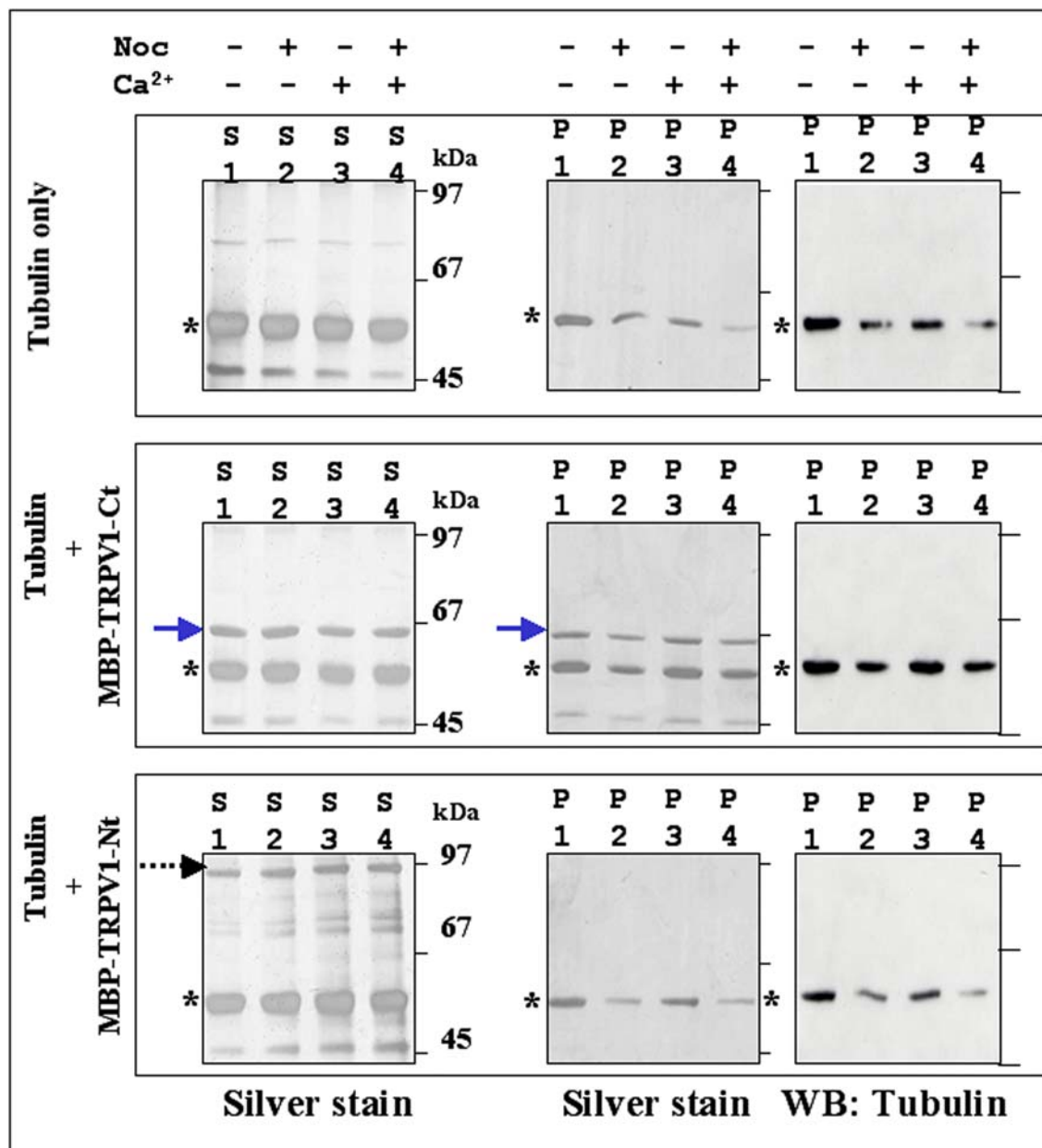
Figure 2.12. MBP-TRPV1-Ct, but not MBP-TRPV1-Nt, allows MT polymerization in the presence of nocodazole. Comparison of tubulin distribution between supernatant (indicated by **S**), and pellet corresponding to MT polymer (indicated by **P**), formed from αβ-tubulin dimer alone (upper panel), in the presence of MBP-TRPV1-Ct (middle panel), and in the presence of MBP-TRPV1-Nt (bottom panel), in buffer (lane 1), with nocodazole (lane 2), with Ca^{2+} (lane 3) and in presence of both nocodazole and Ca^{2+} (lane 4). Proteins were visualized by SDS–PAGE followed by silver staining of proteins in the supernatants and pellets, and anti tubulin western blot of the pellets. The asterisks (*) indicate the position of tubulin; MBP-TRPV1-Nt is indicated by the dotted arrow, and MBP-TRPV1-Ct by the solid arrow. Note that the amount of MT polymer formed in the presence of nocodazol or nocodazol/Ca^{2+} is significantly increased in the presence of MBP-TRPV1-Ct as compared to the 'tubulin-only' control. In contrast, the presence of the same amount of MBP-TRPV1-Nt has no effect.
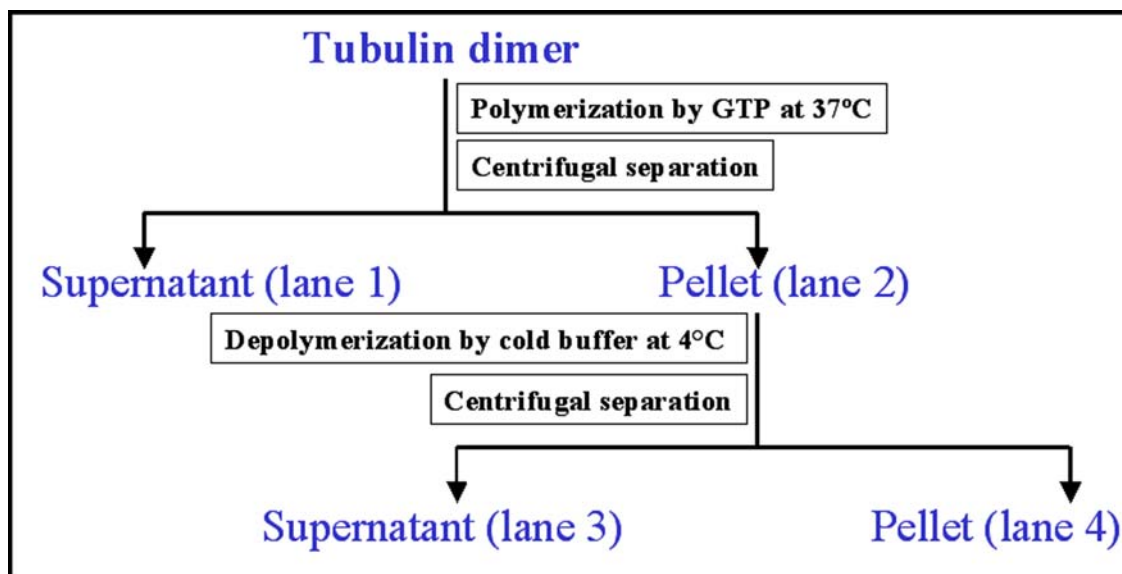
Figure 2.13. Flow chart of the experiment to analyze the effect of TRPV1 cytosolic fragments on microtubule stability. First, MTs were allowed to form from tubulin dimers, followed by separation of MT polymers from remaining dimers by centrifugation. Then, the MT polymer pellet was subjected to cold-temperature-induced depolymerization on ice. Subsequently, cold-stable MT polymers were separated from disassembled tubulin by another round of centrifugation. This sequential polymerization/depolymerization was performed with tubulin alone, in the presence of MBP-TRPV1-Ct, or MBP-TRPV1-Nt, in the presence or absence of Ca^{2+}, respectively. The distribution of tubulin and added proteins between supernatant and pellet fractions was monitored.

present, MT formation was considerably enhanced even in the presence of nocodazole or a combination of nocodazole and Ca^{2+}, and a significant portion of MBP-TRPV1-Ct was found in the MT pellet (figure 2.12, middle panel). In contrast, in the presence of MBP-TRPV1-Nt, MT polymer formation was not altered and similar to the "tubulin-only"-sample. No MBP-TRPV1-Nt was observed in the pellet fraction and the entire amount of fusion protein remained in the supernatant (figure 2.12, bottom panel). These results suggest that MBP-TRPV1-Ct is able to provide stability to the MT polymers even in the presence of nocodazole.

2.1.8. MBP-TRPV1-Ct, but not MBP-TRPV1-Nt, stabilizes microtubules against cold-induced depolymerization in a Ca^{2+}-sensitive manner.

MTs are known to be susceptible to depolymerization at temperature below 15°C. In order to test if MBP-TRPV1-Ct affects this property, tubulin polymerization from tubulin
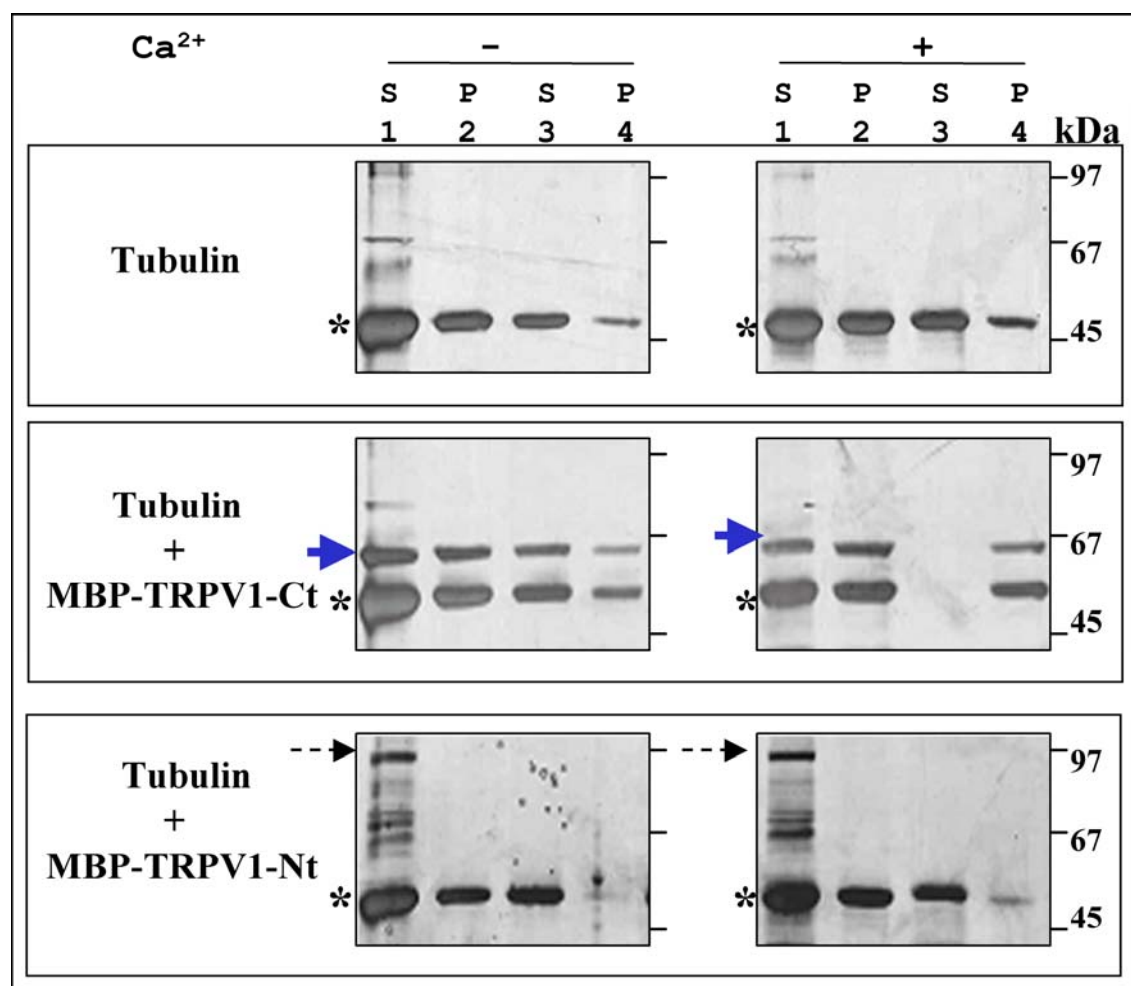
Figure 2.14. MBP-TRPV1-Ct provides stability to the MT towards depolymerization at low temperatures. $\alpha\beta$-Tubulin dimers alone (top panel) or in the presence of MBP-TRPV1-Ct (middle panel), or in the presence of MBP-TRPV1-Nt (bottom panel), were subjected to polymerization either in the absence of Ca^{2+} (–, left side) or presence of Ca^{2+} (+, right side). After the first cycle of polymerization, free dimers and unbound proteins (which remained in the supernatant, **S**, lane 1) were separated from MT polymers and associated proteins (pellet, **P**, lane 2) by centrifugation. The MT polymers were subsequently depolymerized by ice-cold buffer, followed by the centrifugal separation of disassembled tubulin dimers (**S**, lane 3) and cold-stable MTs (**P**, lane 4). Samples were analyzed by 10% SDS–PAGE followed by silver staining. The position of tubulin is indicated by an asterisk (*), MBP-TRPV1-Ct is indicated by a solid arrow, and MBP-TRPV1-Nt by a dotted arrow. In contrast to MBP-TRPV1-Nt, which remained in the supernatant in step 1 (lanes 1, bottom panel), MBP-TRPV1-Ct co-sedimented with polymerized MT both in the presence or absence of Ca^{2+} (lanes 2, middle panel). Strikingly, the association of MBP-TRPV1-Ct with MT in the presence of Ca^{2+} results in an increased amount of cold-stable MT polymer (middle panel, right side, lanes 3 and 4).

dimer was performed in the absence of fusion proteins, or in the presence of MBP-TRPV1-Ct or MBP-TRPV1-Nt respectively. The MT polymerization was carried out either with or without Ca^{2+}, followed by depolymerization at low temperature (4°C, on ice, see figure 2.13 for a flow chart of the experiment). In the "tubulin-only" sample (figure 2.14, upper panel), a

portion of tubulin dimers polymerized to form MT polymers at 37°C, the latter of which could be pelletted by centrifugation (lane 2). When subjected to ice-cold temperatures, the MT polymers were partially depolymerized under the experimental conditions used, and tubulin occurred in a supernatant (lane 3) and in a pellet (lane 4) fraction after another round of centrifugation. It was observed that after the first cycle of polymerization, the amount of formed MT polymer pellet was unaffected by the presence or absence of Ca^{2+}. A comparable amount of MT polymers formed in the presence of MBP-TRPV1-Ct. In agreement with the experiments shown above, a significant portion of the MBP-TRPV1-Ct was detected in the MT pellet fraction (figure 2.14, middle panel). Strikingly, in the presence of Ca^{2+} and MBP-TRPV1-Ct, cold-induced MT depolymerization was dramatically reduced (figure 2.14, middle panel). The presence of MBP-TRPV1-Nt had no such effect. In fact, MBP-TRPV1-Nt was never observed in a MT polymer pellet, not even after the first round of MT polymerization from tubulin dimers (figure 2.14, bottom panel). This suggests a specific Ca^{2+}-sensitive stabilizing effect of the TRPV1 C-terminus on microtubules against cold-induced depolymerization.

In summary, there appears to be not only an interaction of the C-terminal domain of TRPV1 with tubulin dimers and with polymerized microtubules, but – at least under some experimental conditions - also a Ca^{2+}-sensitivity of this interaction. Furthermore, obtained results suggest that the C-terminus of TRPV1 affects the properties of microtubules.

2.2. Characterization of the TRPV1-tubulin interacting region.

The C-terminal cytoplasmic domain of TRPV1 was observed to interact not only with soluble αβ-tubulin dimer, but also with polymerized microtubules. This indicates that the C-terminus of TRPV1 harbours some element, which retains the important structural information required for tubulin binding. In absence of a three-dimensional crystal structure or any characterized motifs located within the C-terminus of TRPV1, a systematic deletion approach and other biochemical methods were used to identify the tubulin-binding site/s and to characterize the TRPV1 region/s interacting with tubulin. The results indicate that the C-terminal cytoplasmic domain of TRPV1 preferably interacts with β-tubulin rather than with α-tubulin, suggesting a possible mode of interaction of TRPV1 at the plus end of microtubules. The results also indicate the presence of two short - basic amino-acid stretches located within the C-terminal sequences of TRPV1, which can positively influence the tubulin interaction. One of these two stretches is highly conserved in all mammalian TRPV1 orthologues. The same sequence stretch is also partially conserved in some TRPV1 homologues belonging to the TRPV subfamily (discussed in chapter 3.1). In agreement with the presence of such a sequence stretch, the C-terminus of a few other members of the TRPV subfamily, namely TRPV2 and TRPV4, also interact with soluble tubulin and with polymerized microtubules. Considering the homology and diversity among the TRP channels, this might imply that these TRPV members interact with tubulin and polymerized microtubules through a novel and unique tubulin-binding motif sequence (also see the discussion section 3.1 for details).

2.2.1. β-tubulin, but not α–tubulin interacts with TRPV1.

The tubulin preparation from brain tissue can be expected to consist predominantly of αβ-tubulin heterodimers. In order to analyze, which subunit of the tubulin dimer interacts with the C-terminal domain of TRPV1, a cross-linking experiment was performed (figure 2.15). A mixture of αβ-tubulin dimer and MBP-TRPV1-Ct was cross-linked by using dimethyl suberimidate (DMS), a homobifunctional cross-linking agent, which reacts with amino groups. Cross-linked products of tubulin dimers and MBP-TRPV1-Ct were subsequently analyzed by gel electrophoresis and Western blot analysis with the appropriate antibodies. The cross-linking occurred fast and the entire amount of MBP-TRPV1-Ct appeared as a high-molecular weight complex after only 1 minute of cross-linking. All β-tubulin in the reaction mixture also appeared in the same high-molecular weight cross-linked product. α-Tubulin was also found in that complex, but approximately 50% of the α-tubulin did not react and failed to form this high-molecular weight complex. Even after 60 minutes of reaction, this α-tubulin population occurred at its monomeric molecular weight on the SDS-PAGE. The high-molecular weight complex was not observed when purified MBP was used instead of MBP-TRPV1-Ct for cross-linking experiment with αβ-tubulin dimer (data not shown). In a similar manner, MBP-TRPV1-Nt also does not form any specific cross-linked product (data not shown). From these data it can be concluded that the MBP-TRPV1-Ct interacts with the tubulin dimer predominantly via β-tubulin.
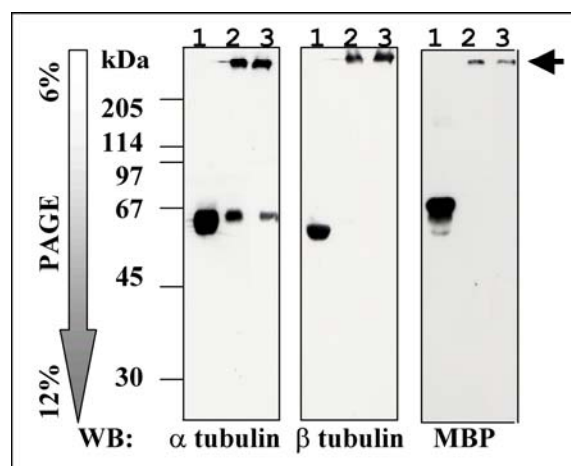

Figure 2.15. MBP-TRPV1-Ct interacts directly with β–tubulin. MBP-TRPV1-Ct and αβ–tubulin dimer mixture was cross-linked with DMS cross-linker. Protein mixtures before cross-linking (lane 1), 1 minute after cross-linking (lane 2) and 60 minutes after cross-linking (lane 3) were seperated by SDS-PAGE and transferred to a nitrocellulose membrane. Blots were probed with the anti α–tubulin antibody (left), the anti-β–tubulin antibody (middle) and the anti-MBP antibody (right). The arrow indicates the high-molecular-weight cross-link product. After cross-linking, all MBP-TRPV1-Ct and all β-tubulin shows up in a high-molecular weight complex, whereas a significant amount of α-tubulin remains in a monomeric state.

2.2.2. TRPV1 interacts with tubulin and microtubules through two small, basic sequence stretches located in the C-terminal cytoplasmic domain.

To identify the tubulin-binding region located within the C-terminus of TRPV1, a systematic deletion approach was applied. Initially, three MBP-fused C-terminal deletion constructs, namely MBP-TRPV1-Ct-Δ1, MBP-TRPV1-Ct-Δ2 and MBP-TRPV1-Ct-Δ3 were prepared. These constructs are approximately 30 to 40 amino acids shorter from the C-terminal end, respectively (figure 2.16). All these constructs were expressed in *E.coli,* purified and confirmed by western blot analysis (data not shown). An MBP-pull-down experiment was performed with these deletion-proteins (MBP-TRPV1-CtΔ1, MBP-TRPV1-CtΔ2 and MBP-TRPV1-CtΔ3) to identify the tubulin-binding region. Pulled-down eluate samples were first analyzed by silver staining and then probed for bound tubulin by Western blot analysis. It was observed that all these MBP-TRPV1-Ct deletion proteins pulled-down tubulin when used as baits (figure 2.17). As expected, no tubulin was observed in the pull-down samples where an unrelated protein (MBP-LacZ) was used as bait (data not shown). However, the amount of tubulin pulled down by different deletion-proteins (MBP-TRPV1-CtΔ1, MBP-TRPV1-CtΔ2 and MBP-TRPV1-CtΔ3) varies from each other, indicating that different regions of C-terminus of TRPV1 influence the tubulin interaction (figure 2.17). A significant amount of tubulin was observed
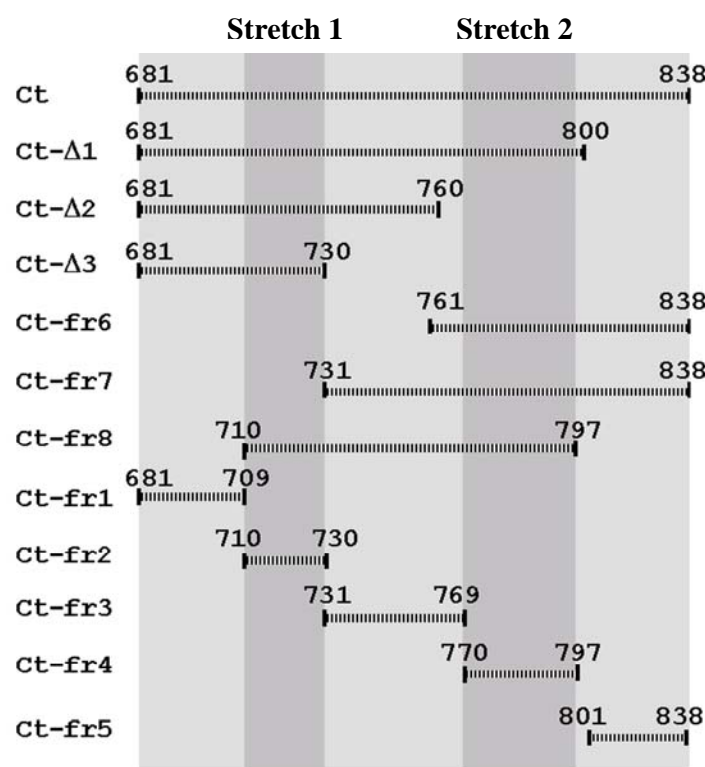

Figure 2.16. Constructs used to identify the tubulin-binding site located in the C-terminus of TRPV1. Schematic representation of constructs prepared to express the deletion-proteins and fragments corresponding to the different regions of C-terminus of TRPV1. Positions of the amino-acids are written in top. Different deleted and fragmented parts of the C-terminal of TRPV1 are expressed as MBP-fusion protein (MBP is at the N-terminus of each fusion constructs). Dark background indicates the regions with high pI (short basic stretches 1 and 2), whereas light background indicates the regions with lower pI.

when MBP-TRPV1-CtΔ1 was used. Tubulin binding in MBP-TRPV1-Δ1 was slightly more when compared with MBP-TRPV1-Ct. This probably indicates that amino acid region 800 to 838 is not important for the tubulin interaction, and deletion of this region may actually favour tubulin interaction. Similarly, a significant amount of tubulin binding was observed for MBP-TRPV1-Δ3, which contains amino acids 681 to 730 of TRPV1. Interestingly, a significantly reduced amount of tubulin binding was observed for MBP-TRPV1-CtΔ2, which expresses amino acid residues 681 to 760 of TRPV1. Taken together, these results indicate that a stretch of 50 amino acids from position 681-730 amino acids is sufficient for tubulin interaction. This also suggests that the sequence from 731-760 and from 800 to 838 of TRPV1 probably have some inhibitory effect on the tubulin binding, while the sequence of residues 760 to 800 exerts a positive influence on tubulin binding.

The exposed C-terminal over-hanging region of αβ-tubulin through which most of the microtubule-binding proteins interact is strongly negatively charged (Nogales E. 2001). Due to the fact that multiple genes encode both, α- and β-tubulin, much heterogeneity among the tubulin monomer as well as dimers exists. Their isoelectric points therefore differs from each other. The calculated and measured isoelectric points of different α− and β-tubulin monomers are generally very low and range between 4.8 to 5.2 (Verdier-Pinard et al. 2003; Towbin et al. 2001; Stracke et al. 2002). However, the measured pI around 4.2 for the αβ-tubulin dimer (the predominant form in which both the monomer exist) is significantly lower than the pI of the monomers alone (Stracke et al. 2002). Interestingly, many tubulin- and microtubule-binding proteins contain more than one short basic-repeat structure mediating the interaction with tubulin and/or microtubules (discussed in details in chapter 3.1).

To explore, if the C-terminal cytoplasmic domain of TRPV1 contains similar basic-sequence stretches for tubulin binding, the theoretical pI of the entire C-terminal of TRPV1 as well as of short sequence stretches were calculated (see discussion section 3.1.3 and figure 3.1 for details). This leads to the identification of two short sequence stretches, which consist of basic amino-acid residues and thus have high pI. The first of these two stretches ranges from residue 710-730 (calculated pI is 11.17). The second sequence stretch ranges from residue 770 to 797 (calculated pI is 12.6). Interestingly, these two sequences are flanked by sequence stretches, which consist of negatively charged amino acids. Such a motif of a short - basic sequence flanked by acidic amino acids correlates well with the observed tubulin interaction with MBP-TRPV1-CtΔ1 and MBP-TRPV1-CtΔ3, but not with the MBP-TRPV1-CtΔ2.

To identify the exact regions, which mediate the tubulin interaction, the entire C-terminus of TRPV1 was further fragmented in five short sequence stretches. These short fragments are referred to as MBP-TRPV1-Ct-fr1 to MBP-TRPV1-Ct-fr5 (figure 2.16). Fragment 1, 3 and 5 contain negatively charged amino acids (with low pI), while fragments 2 and 4 represent basic stretch 1 and basic stretch 2, respectively. Two more fragments were prepared, where the basic stretch 2 is present with an acidic stretch to the right side (referred
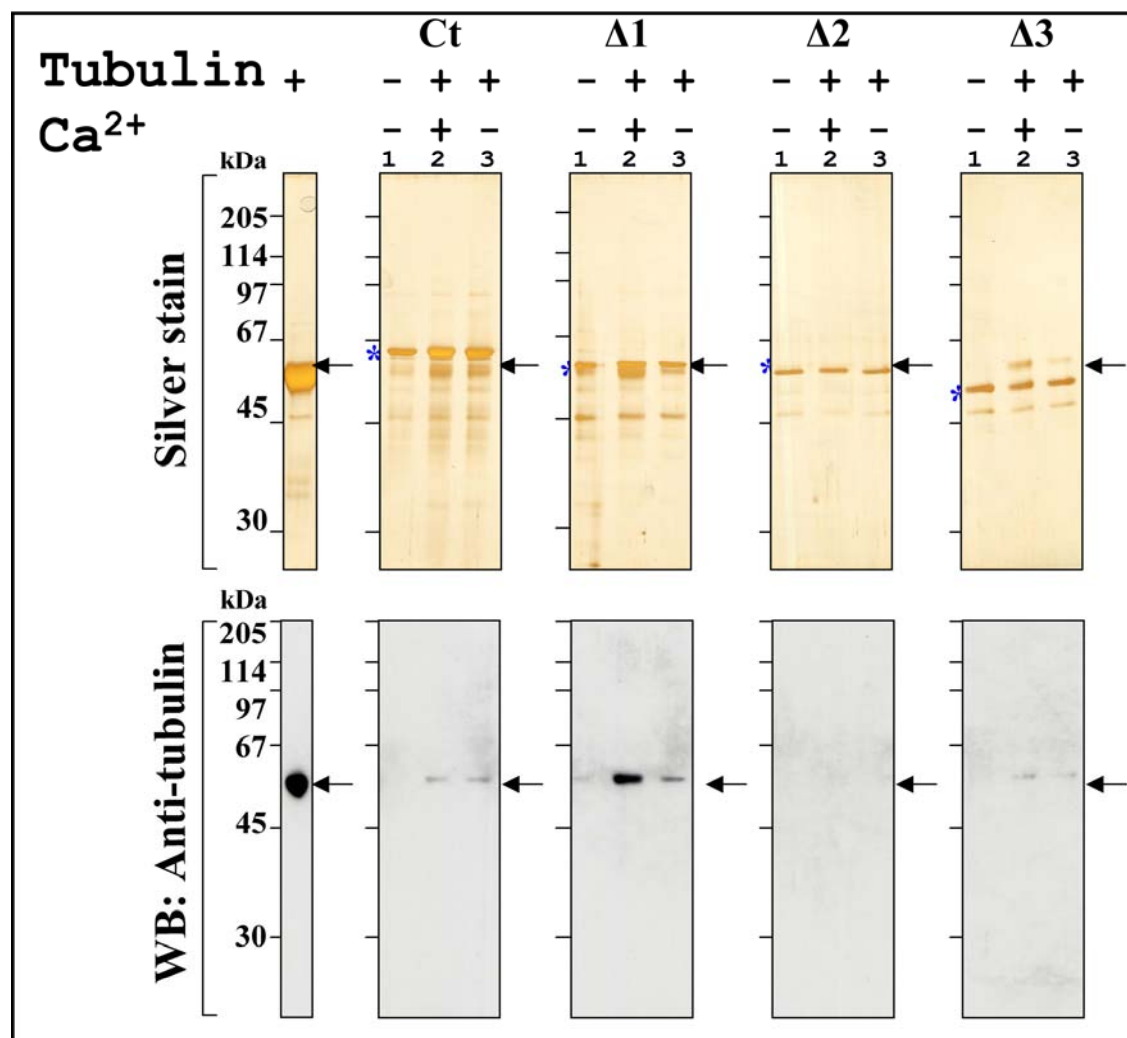
Figure 2.17. Differential binding of tubulin to the different deletion constructs. MBP-TRPV1-Ct, MBP-TRPV1-Ct-Δ1, MBP-TRPV1-Ct-Δ2 and MBP-TRPV1-Ct-Δ3, all immobilized on amylose resin (lane 1), were incubated with purified tubulin dimer either in the presence (lane 2) or absence of Ca^{2+} (lane 3) to analyze the relative affinity of the deletion fragments for tubulin. The proteins were eluted from the amylose resin with 10 mM maltose and resolved by SDS–PAGE. Proteins were stained with silver stain (upper panel). Western blot analysis (lower panel) of corresponding samples with anti-tubulin antibody shows the differential presence of tubulin (arrow) in the different pull down elutes. A significant amount of tubulin binds to the MBP-TRPV1-Ct, MBP-TRPV1-Ct-Δ1 and MBP-TRPV1-Ct-Δ3. MBP-TRPV1-Ct-Δ2 in contrast binds much less tubulin. The input amount of tubulin is shown by silver stained SDS-PAGE (left, upper panel) and by Western blot analysis (left, lower panel).
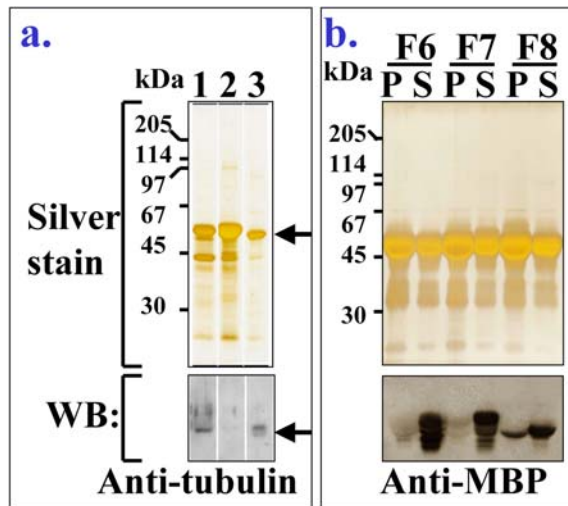
Figure 2.18. Presence of the short basic sequence stretches influences the interaction of TRPV1 with tubulin dimers and with microtubules. a. MBP-TRPV1-Ct-fr6 (lane 1), MBP-TRPV1-Ct-fr7 (lane 2) and MBP-TRPV1-Ct-fr8 (lane 3), all immobilized on amylose resin, were incubated with purified tubulin dimers to analyze the relative affinity of the deletion fragments for tubulin. Bound proteins were eluted from the amylose resin with 10 mM maltose and resolved by SDS–PAGE. Proteins were visualized by silver stain (upper panel). Western blot analysis (lower panel) of corresponding samples with anti-tubulin antibody shows the differential presence of tubulin in the pull down elutes. A significant amount of tubulin binds to MBP-TRPV1-Ct-fr6 and MBP-TRPV1-Ct-fr8. Much less tubulin binds to MBP-TRPV1-Ct-fr7 (Note the excess amount of MBP-TRPV1-Ct-Fr7 in the silver stain). Arrows indicate the position of tubulin. **b.** MBP-TRPV1-Ct-fr8 co-sediments with polymerized microtubules. Purified αβ-tubulin dimers were incubated with taxol® and GTP to form microtubules. Taxol®-stabilized MTs were incubated with 6 μg of purified MBP-TRPV1-Ct-fr6, MBP-TRPV1-Ct-fr7 and MBP-TRPV1-Ct-fr8 respectively. Microtubules and bound proteins were separated by centrifugation and analyzed by 10% SDS-PAGE. The distribution of the proteins between microtubule pellet (**P**) and supernatant (**S**) fractions was visualized by silver staining of the proteins (upper panel) and Western blot analysis of the same samples with anti-MBP antibody (lower panel). A significant amount of MBP-TRPV1-Ct-fr8 and a small amount of MBP-TRPV1-Ct-fr6 co-sediment with microtubules. The majority of MBP-TRPV1-Ct-fr6 and MBP-TRPV1-Ct-fr7 remain in the supernatant.

as MBP-TRPV1-Ct-Fr6, figure 2.16) or with the acidic sequences on both sides (referred as MBP-TRPV1-Ct-Fr7, figure 2.16). One more fragment was prepared which contained both basic sequence motifs connected by the acidic stretch in between. This fragment is referred to as MBP-TRPV1-Ctfr8 (figure 2.16).

All these deletion constructs and fragments of the C-terminus of TRPV1 were created as fusion proteins with an N-terminal MBP and expressed in *E.coli*. The whole set covers all possible combinations; two short basic sequences are present in combination, alone, and excluded completely. The expressed proteins were used for MBP-pull-down assays and also for microtubule binding assays. These proteins were additionally tested for their binding to SDS-PAGE-separated-denatured tubulin dimer or to native tubulin dimers spotted on membranes in a blot-overlay experiment (data not shown).

When tubulin binding (by MBP-pull-down assay) and microtubule binding (by co-sedimentation assay) were compared among MBP-TRPV1-Ct-fr6, MBP-TRPV1-Ct-fr7 and MBP-TRPV1-Ct-fr8, it was observed that MBP-TRPV1-Ct-fr7 has the lowest affinity while

MBP-TRPV1-Ct-fr8 has the highest affinity for both soluble tubulin dimer and also to the polymerized microtubules exerts most. MBP-TRPV1-Ct-fr6 also reveals significant affinity to tubulin as well as to the microtubules (figure 2.18). Similar results were obtained, when these fragments were used in a blot overlay experiment with SDS-PAGE-separated tubulin (data not show). The complete characterization by using all these generated fragments and deletion proteins are ongoing and not yet complete (figure 2.19). The results so far support a positive modulation of tubulin binding by the presence of the two short basic amino acid stretches. The first motif stretch acts as the primary tubulin-binding region.

Ca^{2+}	Pull-down +	Pull-down −	MT binding +	MT binding −	Blot overlay +	Blot overlay −
Ct	●●●	●●	●●●●	●●●●	●●	●
Δ1	●●●●	●●●	x	x	●	○
Δ2	○	○	x	x	●	○
Δ3	●●●	●●	x	x	●	●
F6	●●	●●	●●	●●	x	●
F7	○	○	○	○	x	○
F8	●●	●●	●●	●●	x	●
F1	?	?	?	?	x	○
F2	?	?	?	?	x	●●
F3	?	?	?	?	x	●
F4	?	?	?	?	x	●
F5	?	?	?	?	x	○

Figure 2.19. Summary of different experiments with deletion and fragments of MBP-TRPV1-Ct. Tubulin-binding affinity of each MBP-fusion proteins corresponding to fragments of TRPV1-Ct domain were assessed by three independent experiments: MBP-pull-down assay, microtubule binding assay (co-sedimentation) and blot-overlay on tubulin. The strong binding is indicated by a filled circle (●), poor binding is indicated by an open circle (   ). The number of circles indicates the relative strength of binding. The complete characterization of all fusion-proteins still ongoing. Experiments that await evaluation are indicated by a question mark (?). Experiments that have not been done yet are indicated by a cross (x).

2.2.3. Tubulin interaction is conserved in some other members of the TRPV subfamily.

To explore if tubulin interaction is conserved in some other members of TRPV subfamily, the C-termini of TRPV2, and TRPV4 were expressed as MBP-fusion proteins.

Tubulin interaction with purified MBP-TRPV2-Ct and MBP-TRPV4-Ct was tested in the pull-down assay. Both, MBP-TRPV2-Ct and MBP-TRPV4-Ct interacts with soluble tubulin (figure 2.20). Purified MBP-TRPV2-Ct and MBP-TRPV4-Ct were further tested for microtubule binding in the co-sedimentation assay, where they interacted as well with the polymerized microtubules and thus appear in the pellet fraction (figure 2.20). This shows that the tubulin interaction through the C-terminal cytoplasmic domain of the channel is conserved for at least three members (TRPV1, TRPV2 and TRPV4) of the TRPV subfamily (discussed in chapter 3.1, see figure 3.3).
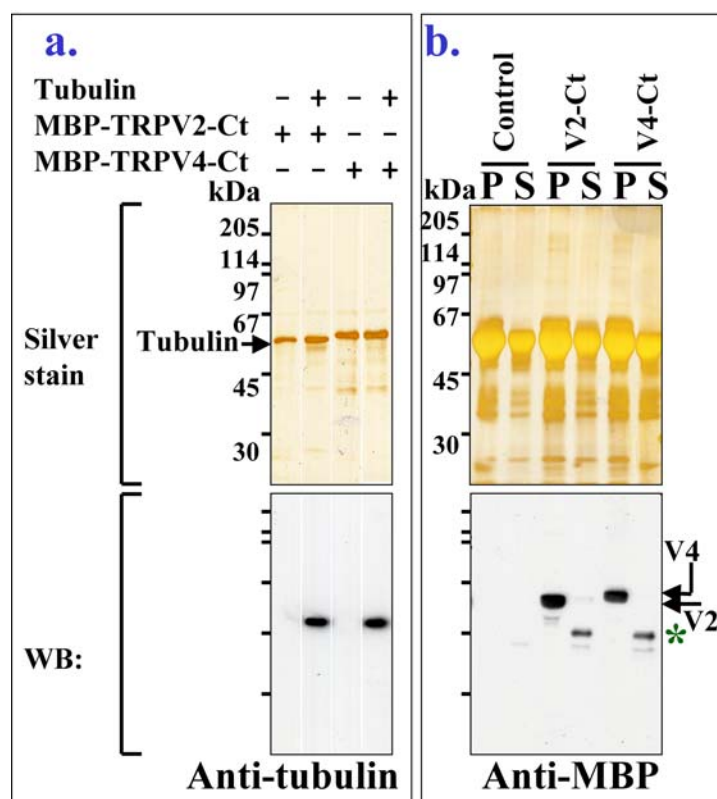
Figure 2.20. Interaction of MBP-TRPV2-Ct and MBP-TRPV4-Ct with soluble tubulin and with polymerized microtubules. a. Purified MBP-TRPV2-Ct and MBP-TRPV4-Ct were incubated with tubulin dimers. The fusion protein along with bound tubulin were eluted from the resin and separated by SDS-PAGE. Proteins were visualized by silver stain (upper panel) and the presence of tubulin (indicated by arrow) in the eluate was confirmed by western blot analysis with anti-tubulin antibody (lower panel). A significant amount of tubulin was pulled down with the MBP-TRPV2-Ct and MBP-TRPV4-Ct.

b. Taxol®-stabilized microtubules were incubated with purified MBP-TRPV2-Ct or MBP-TRPV4-Ct and separated by centrifugal separation of a pellet (**P**) of polymerized microtubules from a supernatant (**S**) of unbound soluble proteins. The pellet and supernatant fractions were separated by SDS-PAGE. Proteins were visualized by silver stain (upper panel). Distribution of the MBP-TRPV2-Ct and MBP-TRPV4-Ct were confirmed by western blot analysis with anti-MBP antibody (lower panel). A significant amount of MBP-TRPV2-Ct and MBP-TRPV4-Ct was observed in the pellet fraction (indicated by arrows). Note that some amount of MBP (∗) (generated by the degradation of fusion proteins) is present in the binding-mixture and appears exclusively in the supernatant. This confirms that the interaction of MBP-TRPV2-Ct and MBP-TRPV4-Ct with polymerized microtubules is specific and mediated only through the C-terminal cytoplasmic domain of TRPV proteins.

2.3. Regulation of cytoskeleton by TRPV1.

Previously, involvement of cytoskeletons, especially the microtubule cytoskeleton in the pain pathway has been reported (Dina et al. 2003; Topp et al. 2000). Identification of tubulin as a TRPV1 interacting protein, and the direct physical interaction of the TRPV1-C-terminus with polymerized microtubules indicated that the microtubule cytoskeleton is directly linked with the TRPV1 and may be a down-stream effector of TRPV1 activation. Therefore, it was justified to test if TRPV1 can regulate cytoskeletons, especially the microtubule cytoskeleton in a cellular context. In this study, regulation of cytoskeleton by TRPV1 was analyzed by a combination of biochemical, cell-biological and microscopic methods. The results obtained indicate that TRPV1 activation causes rapid disassembly of dynamic microtubules but does not affect the actin nor neurofilament cytoskeletons. The C-terminal cytoplasmic domain of TRPV1 exerts a stabilizing effect on microtubules *in vivo* too. These suggest that TRPV1 activation may contribute to cytoskeleton remodelling and thereby to influence nociception.

2.3.1. TRPV1 co-localizes with tubulin.

To assess the TRPV1–tubulin interaction at the cellular level, co-localization experiments were performed. Full-length TRPV1 was transiently expressed in F11 cells, and visualized with endogenous tubulin by indirect immunofluorescence. It was observed that TRPV1 is localized both in intracellular regions and also at the plasma membrane. Significant co-localization was observed between anti-TRPV1 immunoreactivity and anti-tubulin immunoreactivity (figure 2.21a). In neurite-like extensions of F11 cells, a dot-like anti-TRPV1 immunoreactivity was observed. Many of these distinct TRPV1-immunoreactive structures also stained positive with anti-tubulin antibodies. Tubulin accumulation in such structures at TRPV1-enriched patches at plasma membrane is in full agreement with the fact that TRPV1 can stabilize microtubules. Such accumulation of anti-tubulin immunoreactivity pattern at the plasma membrane was not observed in non-transfected F11 cells (figure 2.21b).

To analyze the status of actin in TRPV1-expressing cells, F-actin was stained with fluorescent phalloidin (figure 2.22). In contrast to what was observed with tubulin and TRPV1, only minimal colocalization of TRPV1 with actin filaments was observed. In particular, no overlap with actin was observed in areas enriched with TRPV1. No overlap was also found in areas that reveal intense F-actin staining.

In a similar manner, the status of neurofilaments in TRPV1-expressing cells was tested by indirect immunostaining with specific antibodies raised against neurofilaments. No significant co-localization was observed between TRPV1 and neurofilaments (figure 2.23).

2.3.2. Activation of TRPV1 alters the microtubule-cytoskeleton pattern.

To understand the effect of TRPV1 activation on the tubulin cytoskeleton in a cellular context, TRPV1-transfected cells were treated with the selective agonist resiniferatoxin (RTX), and the integrity of microtubule cytoskeletal structures was monitored after RTX-activation (figure 2.24). The bright immunostaining of TRPV1 in some cells distinguished TRPV1-expressing cells from the non-transfected cells. It was observed that after RTX activation (1 minute), the microtubule cytoskeleton was altered in TRPV1-expressing F11 cells (figure 2.24a). In these cells, the microtubule structure was lost and the immunostaining against tubulin revealed a dispersed immunoreactivity all over the cell body. However, the non-transfected cells showed the normal microtubule structures after RTX treatment (figure 2.24a). Microtubules in TRPV1 expressing cells reveal normal fibrous structure even after RTX activation when the cells were preincubated with 5'I-RTX, an antagonist for TRPV1
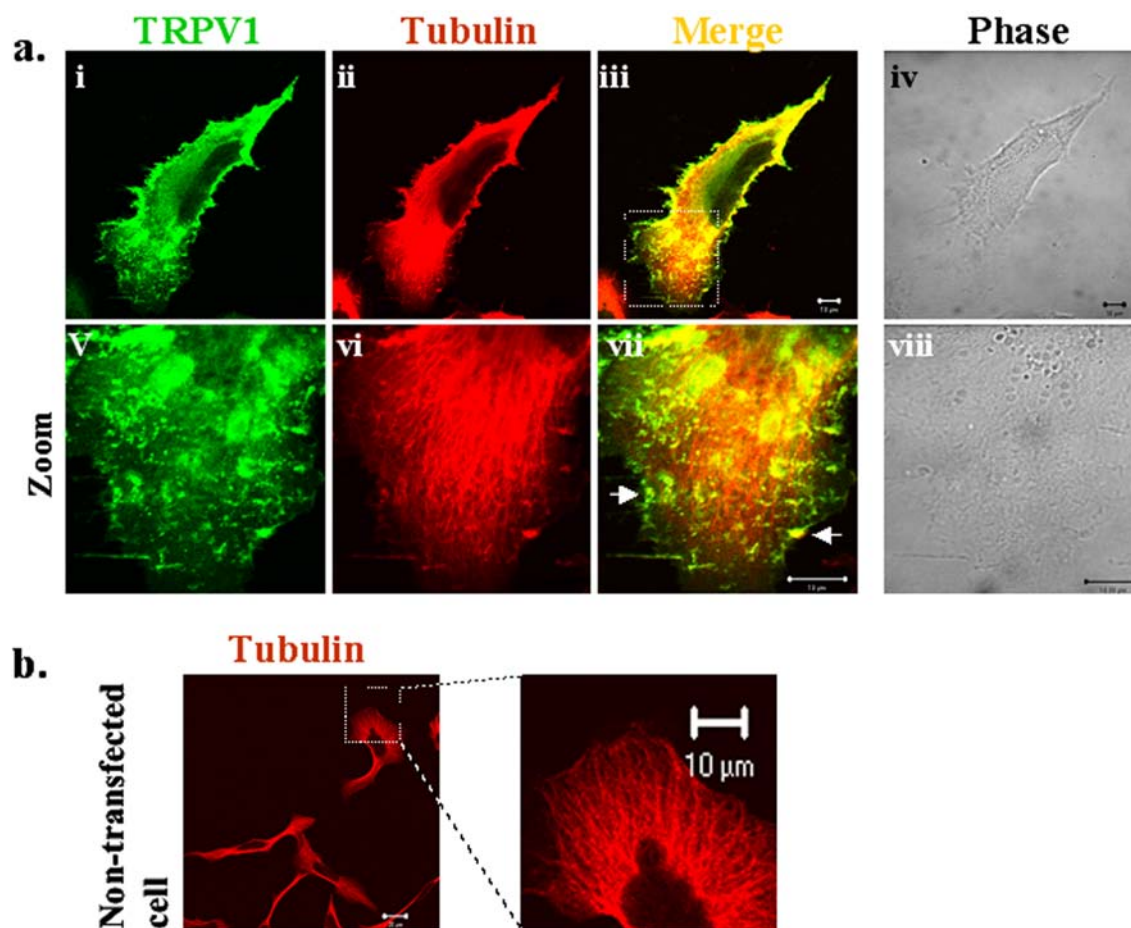
Figure 2.21. TRPV1 co-localizes with tubulin in transfected F11 cells. a. Confocal images (i-iv) and enlarged sections of the same images (v-viii) of F11 cells transiently expressing TRPV1. There is some distinct co-localization (yellow in the overlay) of TRPV1 (green) and tubulin (red) immunoreactivity. TRPV1 (i and v) and tubulin (ii and vi) were visualized by indirect immunofluorescence with an anti-TRPV1 antibody and an anti-tubulin antibody. Regions of co-localization appear as yellow (iii and vii). Distinct spots of co-localization near the plasma membrane are marked with arrows. Phase-contrast pictures (iv and viii) of the same cell are shown. Scale bar: 20 µM. **b.** Confocal images of non-transfected F11 cells (scale bar 20 µM) and an enlarged image of the indicated area (scale bar 10 µm) stained for anti-tubulin immunoreactivity. No tubulin accumulation at plasma membrane is observed.

(data not shown). In a similar manner, microtubules in TRPV1-expressing cells reveal the normal pattern when cells were incubated with buffer only. When the same experiment was performed in HEK 293 cells transfected with TRPV1, a similar effect on microtubules due to TRPV1 activation was observed (figure 2.24b). These results indicate that it is the activation of TRPV1, but not its over-expression that affects the micotubular structures.

The status of the actin cytoskeleton after TRPV1 activation was also analyzed. In contrast to the microtubule cytoskeleton, no significant change in the actin (figure 2.25) nor
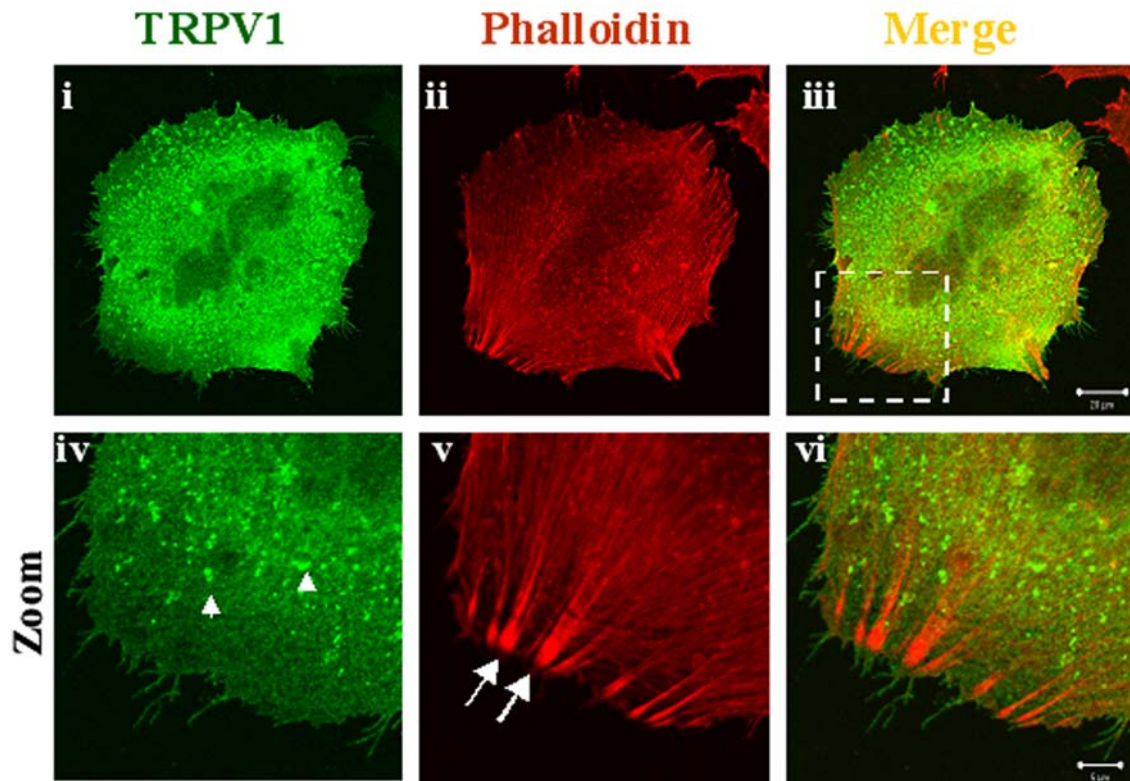
Figure 2.22. TRPV1 co-localizes minimally with actin. Shown are the confocal images of an F11 cell expressing TRPV1 after transient transfection (upper panel, i-iii) or an enlarged area (indicated by white dashed line) of the same cell (lower panel, iv-vi). Cells were stained for TRPV1 (green, i and iv) with anti-TRPV1 antibody and F actin with Alexa-594-labelled phalloidin (red, ii and v). No accumulation of actin was observed in TRPV1-enriched structures (indicated by arrow heads), nor any significant co-localization was observed between TRPV1 with actin in actin-enriched structures (indicated by arrow). The actin cytoskeleton remains normal even after over-expression of TRPV1. Scale bar 20 μm (for upper panel) and 5 μm (for lower panel).

the neurofilament cytoskeleton (data not shown) in TRPV1-expressing F11 cells was observed. The filamentous actin structure was observed in TRPV1-expressing F11 cells even after RTX treatment.

2.3.3. Activation of TRPV1 results in increased tubulin solubility due to disassembly of microtubules.

The apparent dispersal of microtubules subsequent to activation of TRPV1 detected by indirect immunofluorescence suggests that the microtubules may have been disassembled into small tubulin oligomers and dimers. To analyze whether activation of TRPV1 renders an increased fraction of tubulin soluble, the cells were extracted with digitonin in an isotonic buffer immediately after the activation with RTX. Under these conditions, elements of the stable cytoskeleton and associated proteins are expected to remain unaffected while all

soluble cytoplasmic proteins will be extracted. After extraction, it was observed that all cells which express TRPV1, showed a significantly reduced tubulin content (figure 2.26a). Some remaining immunostaining for tubulin, which was observed in the cell body appeared diffuse (figure 2.26a, iii). In some instances, it could be assigned as fragmented microtubules (figure 2.27). However, a perinuclear structure retained anti-tubulin immunoreactivity even after RTX-activation (figure 2.26a and 2.27). No effect of RTX was observed in non-transfected cells (figure 2.26a). To prove further that the observed disassembly of microtubules is indeed due to the TRPV1 activation, the cells were incubated with antagonist 5' I-RTX for 10 minutes before activation with RTX and subsequent extraction with digitonin. As expected, 5' I-RTX-treated TRPV1-expressing F11 cells do not reveal loss of microtubules from the cell body after RTX activation. Microtubules reveal the normal fibrous pattern in these cells (figure 2.26b). Additionally, TRPV1-transfected, but unstimulated cells displayed a normal microtubule structure and comparable to non-transfected cells after digitonin extraction (figure 2.26c). This indicates that the loss of microtubule structures in the cell body is rapid and occurs within a minute upon TRPV1 activation. After RTX treatment and digitonin
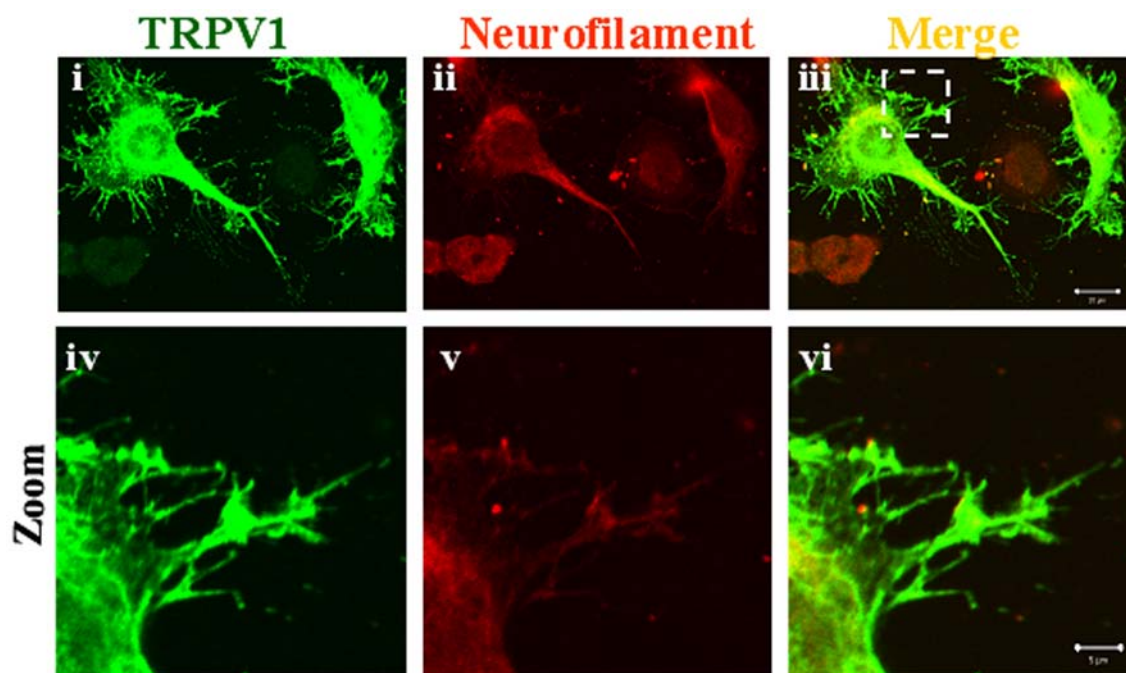

Figure 2.23. TRPV1 co-localizes minimally with neurofilaments. Shown are the confocal images of F11 cells expressing TRPV1 after transient transfection (upper panel, i-iii) or an enlarged area (indicated by white dashed line) of the same cells (lower panel, iv-vi). Cells were immunostained for TRPV1 (green, i and iv) and 160 kDa neurofilament (red, ii and v) with specific antibodies. No significant co-localization between TRPV1 and neurofilaments was observed. Scale bar 20 μm (for upper panel, i-iii) and 5 μm (for lower panel, iv-vi).
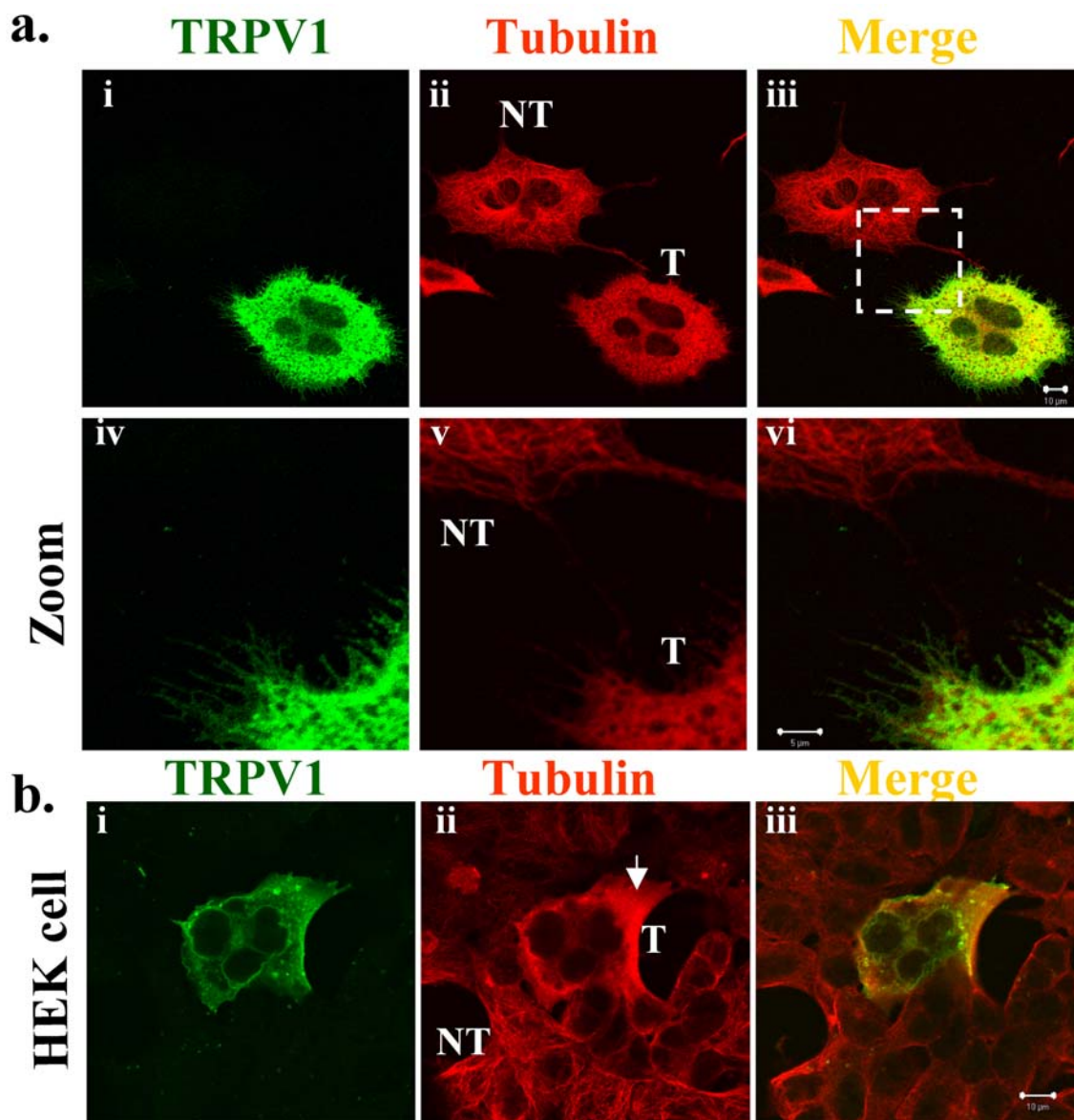
Figure 2.24. Activation of TRPV1 affects microtubule structures. Shown are the confocal images of F11 cells (**a**) or HEK cells (**b**) transiently expressing TRPV1 (indicated by T). NT indicates non-transfected cells. Cells were treated with RTX to activate the TRPV1 channel and subsequently immunostained for TRPV1 (green) and tubulin (red). TRPV1-expressing cells show a dispersed pattern of tubulin staining whereas TRPV1-non-expressing cells show normal microtubule staining. An enlarged area (indicated by white dashed line) of the F11 cells is shown (a, iv-vi). Scale bar 10 μm (a, i-iii and b) and 5 μm (a, iv-vi).

extraction, the actin and neurofilament cytoskeleton remain unchanged, visible all over the TRPV1 expressing cells, and comparable to the control cells (figure 2.28). This indicates that activation of TRPV1 has no effect on the polymeric nature of actin and neurofilament cytoskeletons.
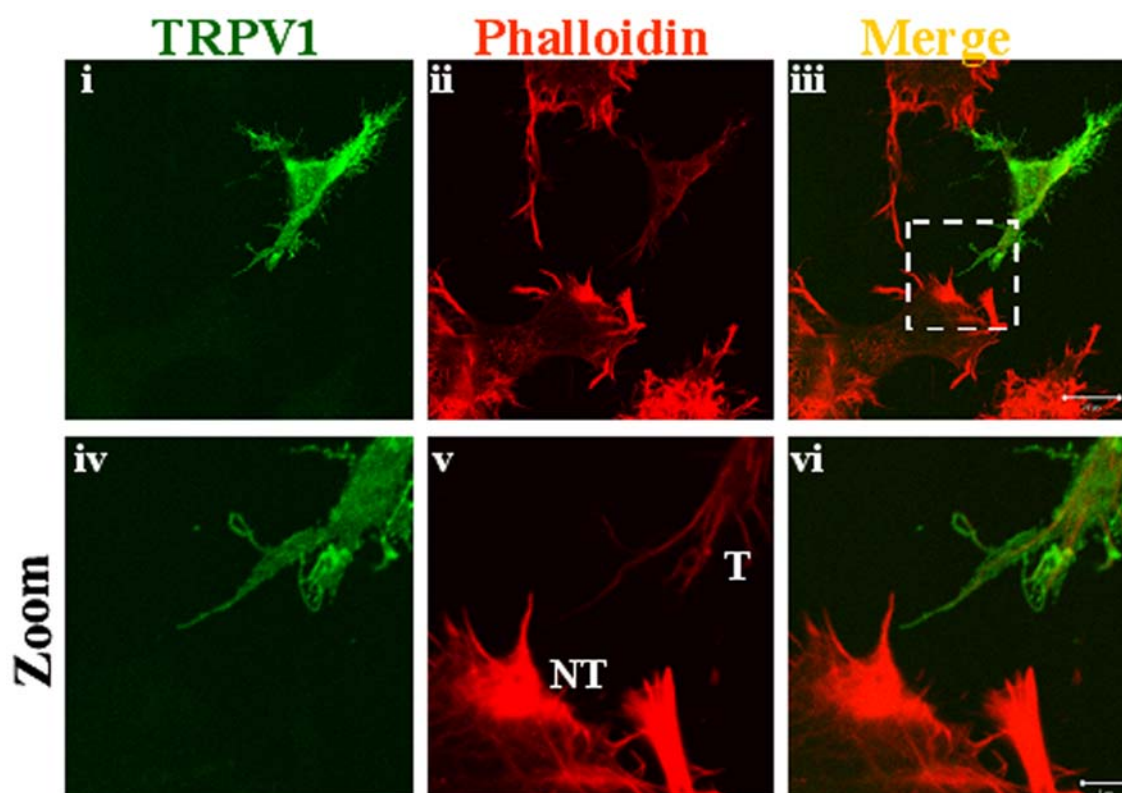
Figure 2.25. Activation of TRPV1 does not alter actin filaments. Shown are the confocal images of F11 cells transiently expressing TRPV1 (indicated by T) and non-transfected cells (indicated by NT). TRPV1 was activated with RTX and the cells were subsequently stained for TRPV1 (green) and actin (red). Normal filamentous actin filaments remain visible in TRPV1-expressing cells even after RTX treatment. An enlarged area (indicated by white dashed line) of the cells is shown below (iv-vi). Scale bar 20 μm (i-iii) and 5 μm (iv-vi).

2.3.4. Visualizing microtubule disassembly due to TRPV1 activation in live cells.

To visualize the effect of TRPV1 activation on microtubule disassembly in live cells, TRPV1 and CFP-tubulin were co-expressed in F11 cells by transient transfection. CFP-tubulin was observed to be localized strongly at the microtubule-organizing centre (MTOC) located at the perinuclear region and also in the fine filamentous structure all over the cell body representing microtubules respectively (figure 2.29a). The status of CFP-tubulin in live cell was observed for a longer duration with a confocal microscope. The change in the microtubule structure upon RTX treatment was prominent and loss of filamentous microtubules over time was visible (figure 2.29b). In agreement with the results obtained from fixed cells, it was observed that the MTOC region was not disassembled even 10 minutes after RTX application.
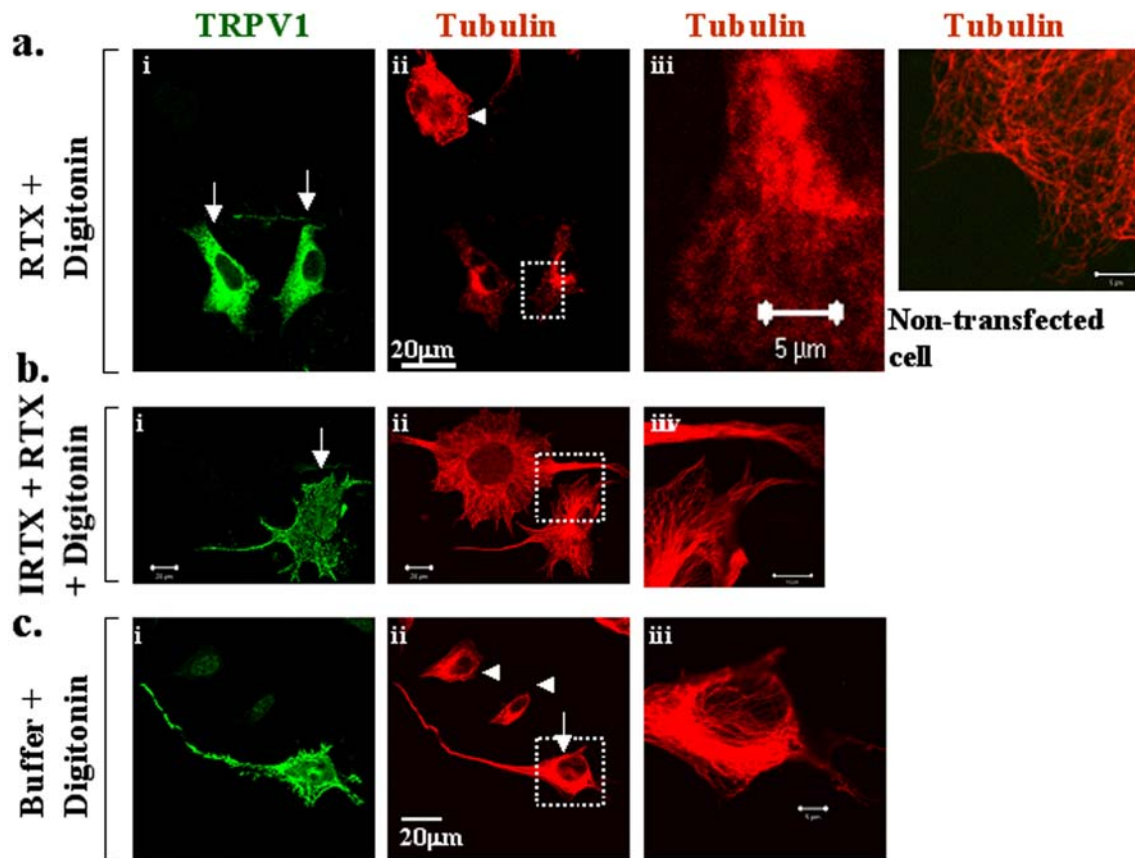
Figure 2.26. Activation of TRPV1 results in the rapid disassembly of microtubules at specific cell sites. F11 cells expressing TRPV1 (indicated by arrows) and non-expressing cell (indicated by arrowheads) were treated with RTX (**a**), with RTX in presence of the antagonist IRTX (**b**) or with HBSS buffer (**c**) for 1 minute before extraction with digitonin in an isotonic buffer. Cells were subsequently immunostained for TRPV1 (green) and tubulin (red) with specific antibodies. All images were taken on a confocal microscope. **a**. Strongly reduced tubulin immunoreactivity was observed in TRPV1-expressing cells with comparison to the non-expressing cells when cells were treated with RTX only (ii). An enlarged area (iii) of the TRPV1-expressing cells (indicated by dashed white line in ii) reveals "smeary" presence of tubulin all over the cell body except the microtubule-organizing centre at the perinuclear region. Complete absence of normal microtubular structures was observed in TRPV1-expressing cells. Under the same conditions, there is no effect of RTX in the TRPV1-non-expressing cells, and normal microtubular structures are retained (iv). Scale bar 20 μm (for i-ii) and 5 μm for (iii-iv). **b.** Cells treated with RTX in presence of I-RTX and subsequently extracted with digitonin reveal no change in the microtubular structure in TRPV1-expressing cells. Tubulin immunoreactivity of an enlarged area (indicated by white box) is provided right (iii). Scale bar 20 μm (for i-ii) and 10 μm for (iii). **c.** Both TRPV1-expressing as well as non-expressing cells retain normal microtubular structures all over the cell including the neurites when the cells were treated with only buffer instead of RTX, extracted with digitonin in isotonic buffer and immunostained for TRPV1 (i) and tubulin (ii). An enlarged area of the TRPV1-expressing cell (indicated by dashed white line in ii) is provided (iii). This indicates that in the absence of TRPV1 activation microtubule disassembly does not occur. Scale bar 20 μm (for i-iii) and 5 μm for (iv).
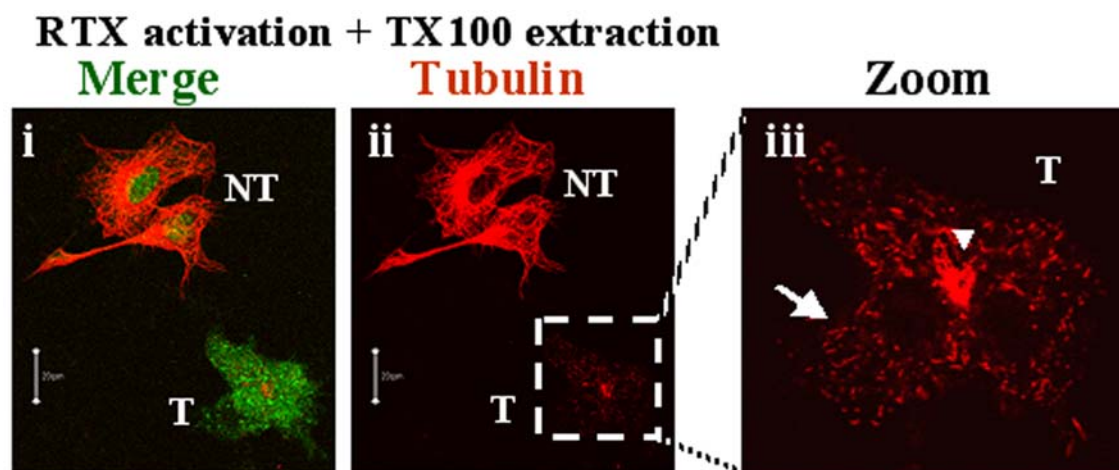
Figure 2.27. Destabilization and fragmentation of microtubules due to TRPV1 activation is cell-site specific. Shown are the indirect immunofluorescence confocal images of F11 cell transiently expressing TRPV1 (i-ii) and an enlarged area depicting the status of microtubules in a TRPV1-expressing (indicated by T) cell (iii) after activation and detergent extraction. Cells were activated with RTX, extracted with Triton X-100 in an isotonic-buffer and immunostained for TRPV1 (green) and tubulin (red) with specific antibodies. A merged image of both TRPV1 and tubulin immunofluorescence is shown on the left (i). When compared to the non-transfected cells (NT), TRPV1-expressing cell (T) reveals a marked reduction in the tubulin immunoreactivity (ii, indicated by a white box). The remaining anti-tubulin immunoreactivity appeared as fragmented microtubules (indicated by arrow) and the stable microtubule-organizing centre (MTOC, indicated by arrow head) at the perinuclear area (iii). Scale bar 20 μm.

2.3.5. TRPV1-mediated microtubule dispersal in stably transfected cells

In order to achieve a homogeneous TRPV1-expressing cell population for biochemical studies, F11 cells stably transfected with TRPV1 cDNA were prepared[*]. Stably transfected F11 cells were obtained by using a viral transduction method and subsequent fluorescence-activated cell sorting, according to a method described in Liu et al (Liu et al., 2000). Expression of TRPV1 in this cell line was confirmed by Western blot analysis and immunofluorescence analysis (data not shown). Expression of TRPV1 was detected in all cells by indirect immunofluorescence analysis with anti-TRPV1 antibody, and the expression level was much lower as compared to transiently transfected cells (data not shown). These cells are referred as TRPV1-F11 cells. Due to low and homogeneous expression of TRPV1 in this cell line, it was used to study the effect of TRPV1 activation biochemically.

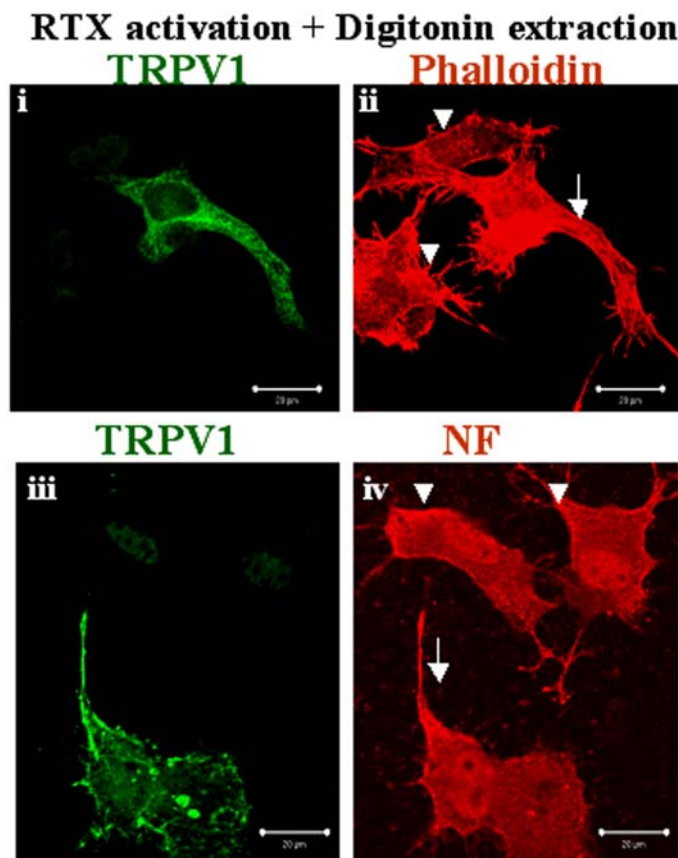∗ (B. Schwappach generated this cell line at Heidelberg).

Figure 2.28. Activation of TRPV1 does not result in disassembly of actin or neurofilaments. Shown are the confocal indirect immunofluorescence images of F11 cells transiently expressing TRPV1. Cells were treated with RTX, extracted with digitonin in an isotonic buffer and immunostained for TRPV1 (green) and actin (red, ii) with alexa-594-labelled phalloidin or TRPV1 and neurofilament (red, iv) with specific antibodies. The actin and the neurofilament cytoskeleton remain unchanged and insoluble in the TRPV1-expressing cells (indicated by white arrows) and are comparable to the non-transfected cells (indicated by white arrow heads) even after RTX activation and detergent extraction. Scale bar 20 μm.

Immunofluorescence analysis after RTX treatment of TRPV1-F11 cells reveals that activation of TRPV1 again resulted in disassembly of the microtubules but not of the actin cytoskeleton from the majority of cells (figure 2.30). Co-staining of both actin and microtubules in TRPV1-F11 cells confirmed that cells, which showed a drastic reduction in the microtubules in the cell body, retained a normal actin cytoskeleton even after activation of TRPV1 and subsequent detergent extraction (figure 2.31). This effect resembles the results with transiently transfected cells. This also suggest that the observed disassembly of microtubules due to activation of TRPV1 is not dependent on the level of TRPV1 expression as stably transfected TRPV1-F11 cells also exhibit the same effect.

To confirm the apparent increase in soluble tubulin subsequent to activation of TRPV1 by an independent method, the detergent extraction of TRPV1-F11 cells was applied again. The soluble and the insoluble fractions were separated by centrifugation, analysed by SDS-PAGE, and finally probed for the abundance of cytoskeletal compounds across the fractions by Western blot analysis (flow chart in figure 2.32). The amount of tubulin
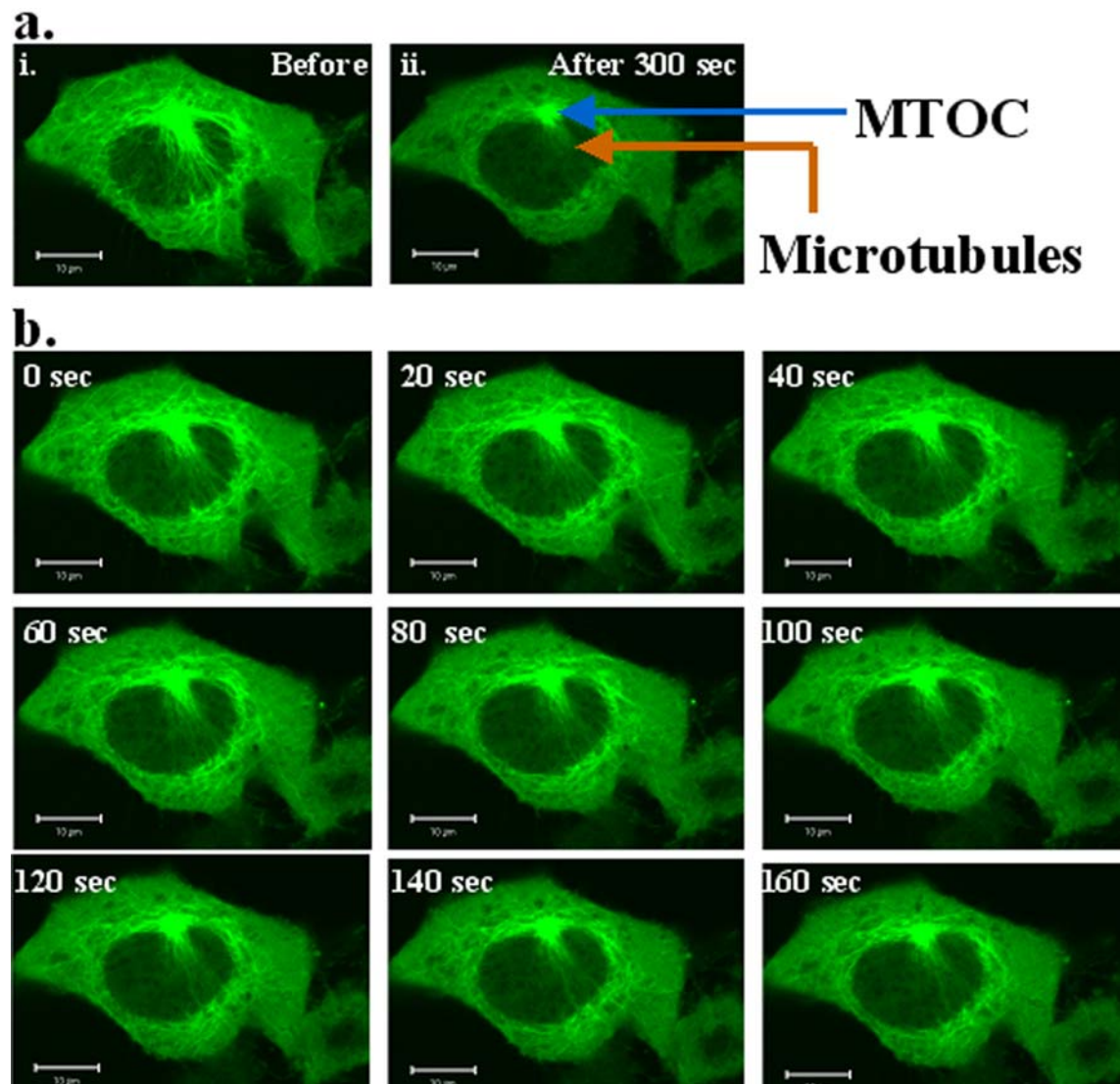
Figure 2.29. Live cell imaging of microtubule disassembly due to TRPV1 activation. a. Shown are the live cell confocal images depicting CFP-tubulin fluorescence pattern in a F11 cell transiently expressing TRPV1 and CFP-tubulin before (i) and after 300sec (ii) of adding RTX. Distribution of microtubule filaments become restricted to the MTOC region as majority of microtubules disassembled into soluble tubulin. Stable MTOC and disassembled dynamic microtubules after TRPV1 activation are indicated by a blue arrow and by a yellow arrow respectively. Scale bar 10 μm. **b.** Time series of the same cell in 20 sec intervals are provided.

increased significantly in the soluble fraction and decreased in the insoluble fraction after activation of TRPV1 (figure 2.33). In contrast, only a little change of actin and almost no change of neurofilament protein were observed in the soluble and insoluble fractions after TRPV1 activation when compared to non-stimulated cells. These results suggest that disassembly of the tubulin cytoskeleton is a downstream effect of TRPV1 activation.
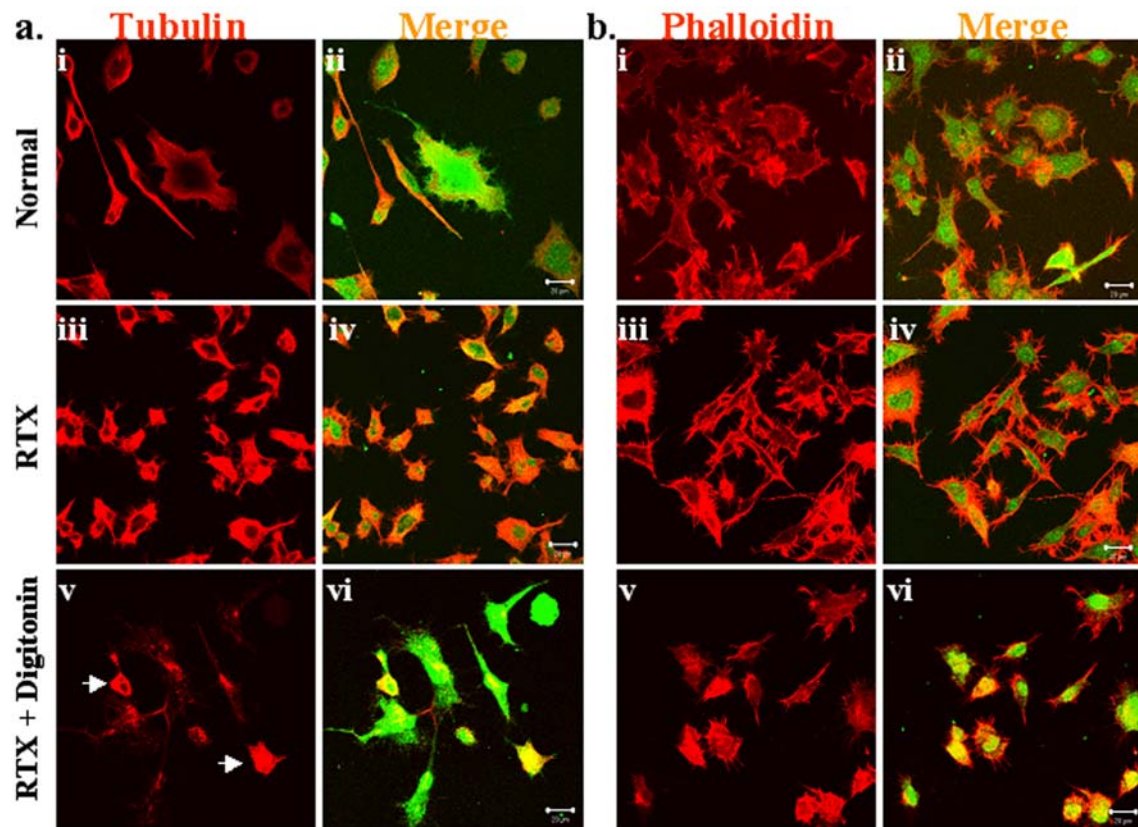
Figure 2.30. Microtubule disassembly after TRPV1 activation is an effect independent of TRPV1 expression level. TRPV1-F11 cells (upper panel), which express a low level of TRPV1 were activated with RTX for 1 minute (middle panel) or further extracted with digitonin after RTX activation (lower panel). Cells were further immunostained for TRPV1 (green) and tubulin (red in figure a) or TRPV1 (green) and phalloidin (red in figure b). Majority of the cells reveal loss of microtubules from cell body (a, v-vi). Arrow indicates cells that reveal no loss of microtubules after TRPV1 activation and detergent extraction. However, all the cells retain normal actin filamentous staining under the same conditions (b, v-vi). Scale bar 20μm.

2.3.6. Dynamic microtubule structures are affected by TRPV1 activation.

Near the perinuclear zone, it was always observed that an area retained strong tubulin immunoreactivity even after activation of TRPV1 and extraction with detergent. These data suggested that this structure was made of mainly stable microtubules that are resistant against Ca^{2+} influx and detergent extraction. One candidate structure for this is the microtubule-organizing centre (MTOC), which characteristically contains gamma-tubulin (Joshi 1993; Okley et al. 1999). To analyze if the TRPV1 activation-resistant structures contain gamma-tubulin, RTX-activated and detergent-extracted TRPV1-F11 cells were co-immunostained with antibodies against tyrosinated α-tubulin and gamma tubulin. It was
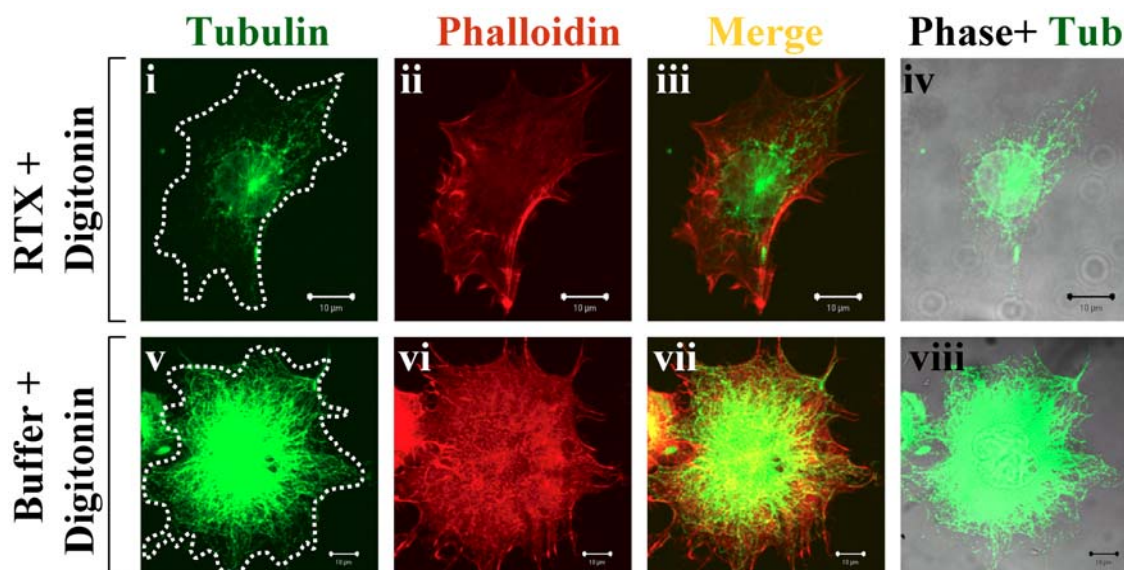
Figure 2.31. Low levels of TRPV1 are sufficient to destabilize the microtubules. Confocal immunofluorescence images of stably transfected TRPV1-F11 cells extracted with digitonin in isotonic buffer after activation with RTX (upper panel i-iv) or after mock activation with only buffer (lower panel, v-viii) are shown. Cells were immunostained for tubulin (green, i and v) with the rat monoclonal antibody YL1/2 and for actin (red, ii and vi) with alexa-594-labelled phalloidin. The tubulin staining reveals normal microtubular structures even after detergent extraction in case of mock activation (lower panel, v), but tubulin is lost from most parts of the cell body when TRPV1 is activated (upper panel, i). In contrast, the activated TRPV1-F11 cell, which reveals reduced microtubular structure after detergent extraction, still contains a normal actin cytoskeleton (ii). Dashed white lines indicate the borders of the cells. Phase contrast images superimposed with the tubulin fluorescence (iv and viii) are provided right. Scale bar 10μm
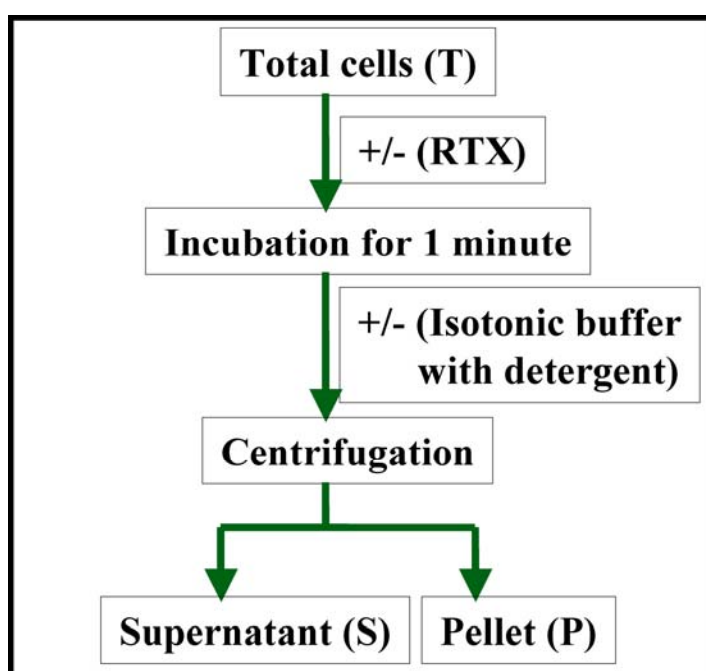

Figure 2.32 . Flow chart depicting the experimental method for TRPV1 activation and for the assessment of tubulin solubility by detergent extraction. TRPV1-F11 cells (**T**) were suspended in HBSS buffer and either activated with RTX (+) or with buffer only (-) for 1 minute. Thereafter, the cells were extracted with an isotonic buffer with (+) or without (-) detergent and fractionated into a soluble (**S**) and a pellet (**P**) fraction by centrifugation. In absence of detergent, all cellular proteins are expected to appear in the pellet fraction.
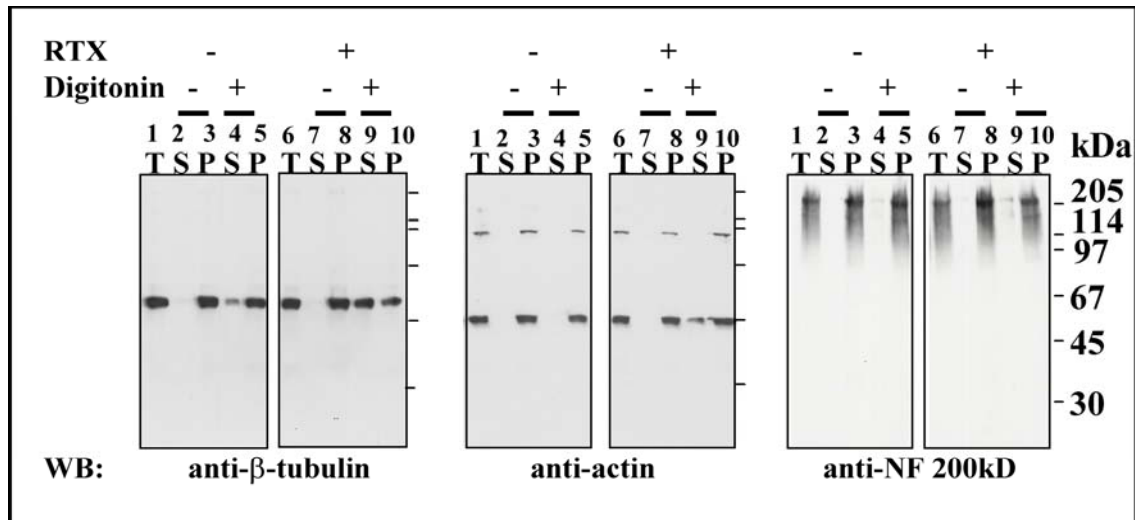
Figure 2.33. Activation of TRPV1 results in the disassembly of the microtubule cytoskeleton. Western blot analysis of total TRPV1-F11 cell extracts (**T**), the supernatant (**S**) and the pellet (**P**) fractions were probed for tubulin, actin and neurofilament. TRPV1-F11 cells were either activated with RTX (right side, lane 6-10) or incubated with buffer only (left side, lane 1-5). Cells were further extracted with detergent (lane 4 and 5, 9 and 10) or with buffer only (lane 2 and 3, 7 and 8). The immunoreactivity for tubulin in the detergent-extracted supernatant from activated cells (lane 9) increased significantly as compared with the same detergent-extracted supernatant from non-activated cells (lane 4). The pellet fraction derived from RTX-activated and detergent-extracted cells (lane 10) revealed a much lower immunoreactivity for tubulin in comparison to the detergent extracted pellets from non-activated cells (lane 5). Little increase in soluble actin and virtually no presence of neurofilament 200kD in the supernatant of RTX-activated and detergent-extracted TRPV1-F11 cells (lane 9) were observed indicating that the actin and the neurofilament cytoskeleton are not as much affected by TRPV1 activation as the microtubule cytoskeleton.
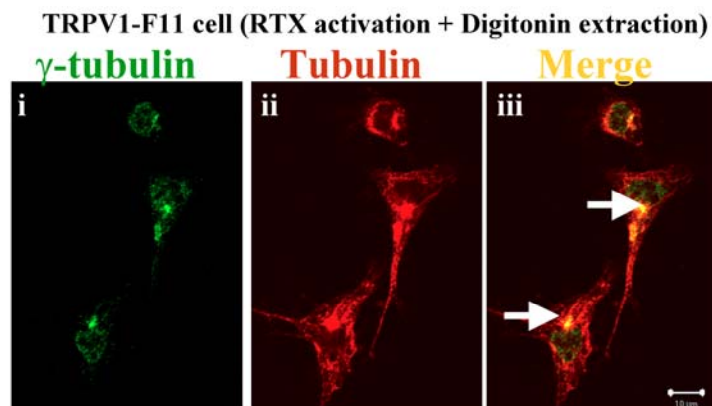

Figure 2.34. Microtubule organizing centre (MTOC) is not affected by TRPV1 activation. Shown are the indirect immunofluorescence images of TRPV1-F11 cells activated with RTX and immunostained for gamma-tubulin (green, i) and tyrosinated α-tubulin (red, ii) with specific antibodies. The merged image is shown on the right side (iii). Immunoreactivity for tyrosinated tubulin was much reduced all over the cell, especially in the cell body. However strong immunoreactivity for tyrosinated tubulin was observed at the perinuclear region, which co-localized with gamma-tubulin (indicated by arrow).

observed that the centre of this anti-tubulin immunoreactive region indeed contained gamma-tubulin and thus confirms the identity of this structure as MTOC (figure 2.34). Also, tubulin staining was retained in some cell extensions even after RTX treatment and digitonin extraction (data not shown). This suggests that the effect of TRPV1 activation on the microtubule cytoskeleton is cell-site specific and that the peripheral dynamic microtubules in the cell body are most affected, while microtubules at the MTOC and in neurite-like processes are relatively stable.

To analyze this effect of TRPV1 activation on microtubule subpopulations in more detail, the fractionation scheme according to the flow chart (figure 2.32) was applied again, but the insoluble and the soluble fractions were probed with antibodies specific for various post translationally modified tubulins. Post-translational modifications of tubulin are known
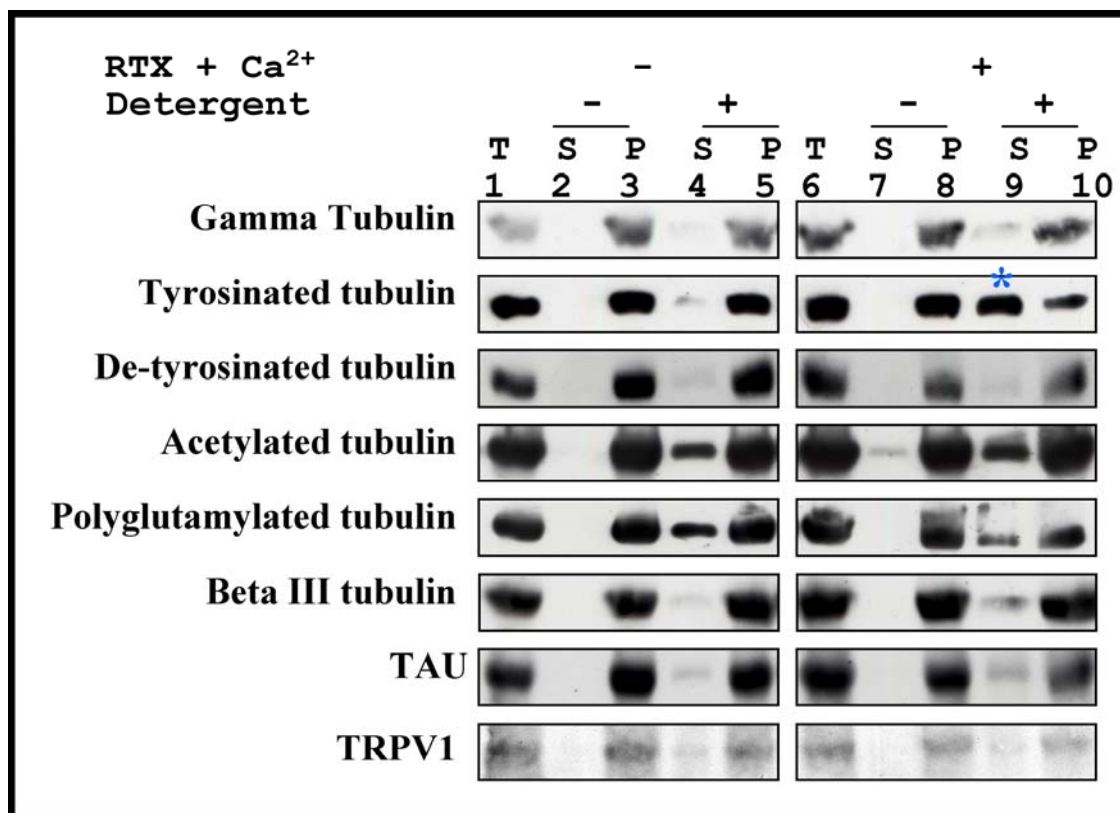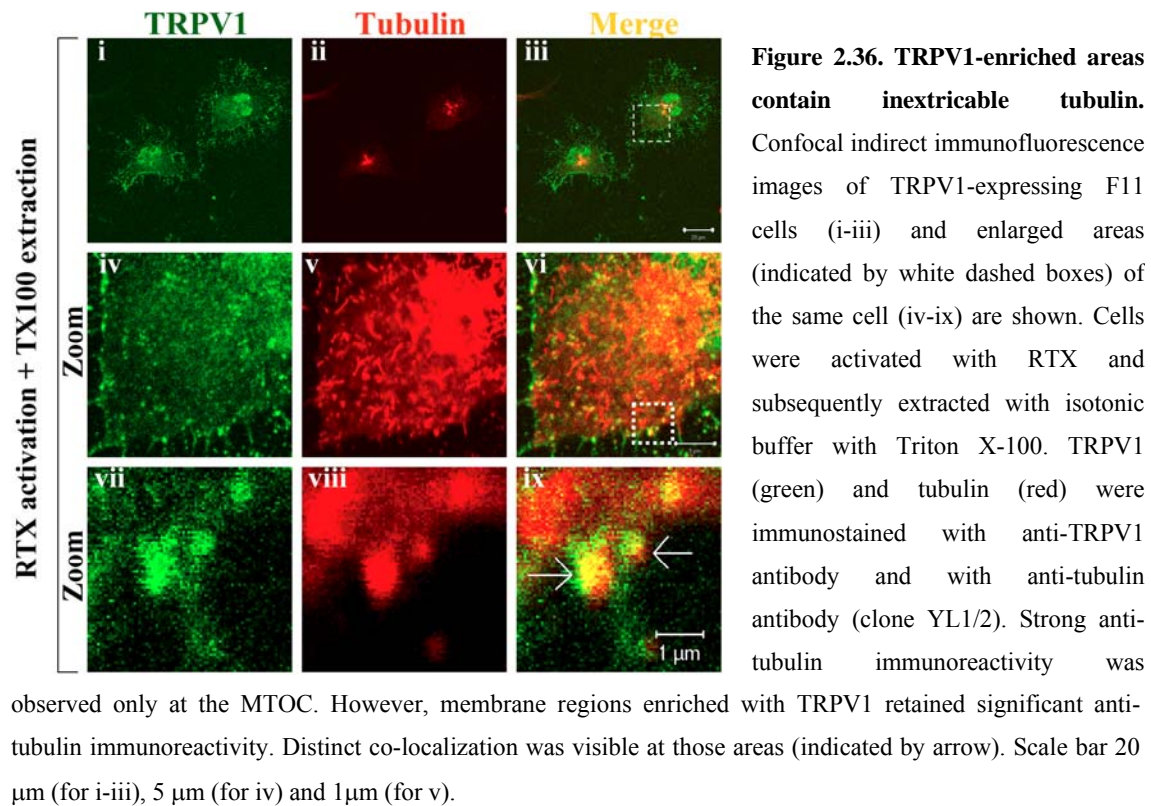

Figure 2.35. TRPV1 activation affects dynamic microtubules. Samples produced as described in fig 4b were probed for gamma-tubulin, tyrosinated tubulin, detyrosinated tubulin, acetylated tubulin, polyglutamylated tubulin, neuron-specific β-tubulin subtype III, TAU, and TRPV1. Only the amount of tyrosinated tubulin increased significantly in the supernatant (lane 9, indicated by an asterisk ∗), and decreased in the corresponding pellet fraction (lane 10) after RTX activation as compared to the same fractions from non-activated cells (lane 4 and 5). The distribution of other modified tubulins and components of the microtubule cytoskeleton remained unchanged upon activation. The majority of TRPV1 remains associated with the insoluble pellets after activation with RTX.

to alter the physico-chemical properties of the microtubules (MacRae, 1997; Westermann and Weber, 2003). Other microtubule cytoskeleton proteins, namely gamma tubulin (as a component of MTOC), the neuron-specific β-tubulin subtype III, and TAU were also probed for the same purpose. Under conditions of RTX activation of TRPV1-F11 cells, no change in the distribution of gamma-tubulins in comparison to the non-activated cells was observed, and the majority of the gamma-tubulin remains in the insoluble fraction (figure 2.35). This is in line with data obtained from the immunofluorescence studies (figure 2.34). It suggests that indeed the MTOC, a rigid and stable structure composed of mainly stable microtubules, gamma-tubulin and other modified tubulins, remains unaffected upon TRPV1 activation. In contrast, tyrosinated tubulin, a marker for dynamic microtubules (Gundersen et al., 1984; Kreis 1987; Wehland and Weber, 1987) increased significantly in the soluble fraction after TRPV1 activation as compared to control conditions (figure 2.35). A certain amount of tyrosinated tubulin, however, remained in the insoluble fraction even after TRPV1 activation and detergent extraction. This is in full agreement with the immunostaining analysis that revealed that stable microtubules at the MTOC and neurites contain a considerable amount of tyrosinated tubulin, too (figure 2.34). In contrast to the tyrosinated tubulin, the proportion of detyrosinated tubulin (known as glu-tubulin), polyglutamylated tubulin, and acetylated tubulin was not significantly altered in the soluble fraction after TRPV1 activation. Distribution of neuron-specific β-tubulin subtype III did also not change upon TRPV1 activation. It is important to note that detyrosinated tubulin, acetylated tubulin, polyglutamylated tubulin and neuron-specific beta tubulin subtype III are all attributed to stable microtubules. After TRPV1 activation, no significant change in the soluble fraction was observed for the neuron-specific TAU, which provides stability to the microtubules (Weingarten et al. 1975). Collectively these results suggest that the dynamic microtubules (enriched with tyrosinated tubulin and/or non-modified tubulins) were affected, while stable microtubules were not affected by TRPV1 activation.

2.3.6. TRPV1-enriched membrane patches contain inextricable tubulin.

It was observed that TRPV1, when over-expressed in F11 cells, is localized at the membrane as distinct patches (figure 2.21) and accumulates tubulin there. In order to understand whether this accumulated tubulin is part of a stable structure in such TRPV1-enriched patches, F11 cells transiently expressing TRPV1 were extracted with digitonin or triton X-100 subsequent to RTX activation. Indirect immunofluorescence analysis was then

Figure 2.36. TRPV1-enriched areas contain inextricable tubulin. Confocal indirect immunofluorescence images of TRPV1-expressing F11 cells (i-iii) and enlarged areas (indicated by white dashed boxes) of the same cell (iv-ix) are shown. Cells were activated with RTX and subsequently extracted with isotonic buffer with Triton X-100. TRPV1 (green) and tubulin (red) were immunostained with anti-TRPV1 antibody and with anti-tubulin antibody (clone YL1/2). Strong anti-tubulin immunoreactivity was observed only at the MTOC. However, membrane regions enriched with TRPV1 retained significant anti-tubulin immunoreactivity. Distinct co-localization was visible at those areas (indicated by arrow). Scale bar 20 μm (for i-iii), 5 μm (for iv) and 1μm (for v).

performed. Though activation of TRPV1 followed by detergent extraction resulted in the loss of microtubule structures from the majority of the cell body, it was observed that TRPV1-enriched patches at the plasma membrane still retain some of the tubulin immunoreactivity (figure 2.36, data for Triton X-100 extraction is shown). This indicates that the tubulin at the TRPV1-enriched patches is part of stable microtubule structures.

2.3.7. Over-expression of TRPV1-Ct results in the formation of bundled microtubules and stabilizes them.

It was observed before that the C-terminus, but not the N-terminus of TRPV1 provides stability to microtubules *in vitro*. Therefore it was explored if it is the C-terminal domain of TRPV1 that confers stability to microtubules localized in the TRPV1 patches. In order to assess this, only the C-terminal cytoplasmic domain of TRPV1 was transiently expressed in F11 cells and immunostaining of the C-terminal fragment as well as of tubulin was performed. TRPV1-Ct immunofluorescence appears as distinct spots throughout the cytoplasm (figure 2.37). These spots are much bigger than the size of vesicles. Interestingly, an uneven distribution and bundling of microtubules in TRPV1-Ct-expressing cells were observed (figure 2.37a). This bundling occurs especially at the regions, which contain
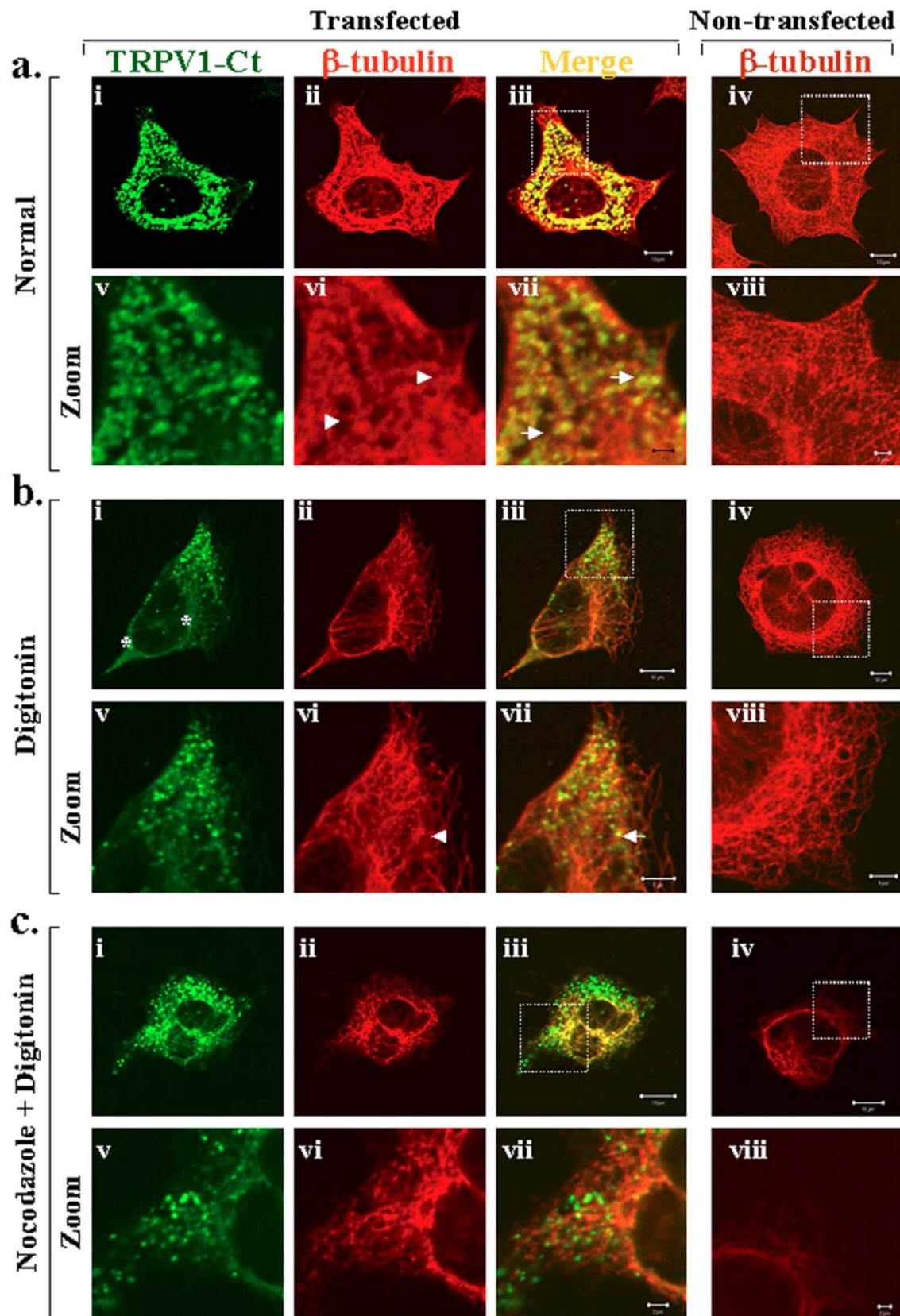
Figure 2.37. Over-expression of the C-terminus of TRPV1 results in bundled and stable microtubules. a. Confocal immunofluorescence images of a F11 cell (i-iii) or an enlarged area (indicated by a white box) of the same cell (v-vii) transiently expressing TRPV1-Ct are shown. Cells were immunostained for the C-terminus of

TRPV1 (green) with a goat anti-TRPV1 antibody (specifically recognizing the C-terminus of TRPV1) and for β-tubulin (red) with a mouse monoclonal anti-β tubulin antibody. TRPV1-Ct immunoreactivity mostly appeared as distinct spots or clusters, and regions of co-localization appeared as yellow (indicated by an arrow). TRPV1-Ct-expressing cells revealed an abnormal microtubule structure, mainly aggregated microtubules at the area where most of the TRPV1-Ct clusters were present (indicated by an arrow head). The pattern of microtubule immunoreactivity in a non-transfected cell (iv) and an enlarged area of the same cell (viii) are shown on the right side. No aggregation or bundling of microtubules was observed in non-transfected cells. Scale bar 10 μm (i-iv) and 2 μm (v-viii). **b.** Confocal immunofluorescence images of a F11 cell (i-iii) and an enlarged area of the same cell (v-vii) depicting the pattern of microtubules after the cells were extracted with detergent in an isotonic buffer are shown. Cells were immunostained for the C-terminus of TRPV1 (green, i and v) and for β-tubulin (red, ii and vi). TRPV1-Ct clusters were visible (i and v) even after detergent extraction and an arrow indicates areas of co-localization with anti β-tubulin. The appearance of anti-TRPV1-Ct immunoreactivity along the microtubule-enriched areas became prominent after detergent extraction (indicated by ∗ sign). Unextractable microtubules appeared aggregated and bundled, especially at areas that colocalized with the TRPV1-Ct clusters (indicated by an arrow head). The immunoreactivity pattern of microtubules in a detergent-extracted non-transfected cell (iv) and an enlarged area of the same cell (viii) are shown on the right side. Scale bar 10 μm (i-iv) and 5 μm (v-viii). **c.** Confocal immunofluorescence images of a F11 cell (i-iii) and an enlarged area of the same cell (v-vii) depicting the pattern of nocodazole-resistant microtubules are shown. Cells were treated with nocodazole for depolymerization of microtubules and further extracted with detergent in an isotonic buffer. Cells were immunostained for the C-terminus of TRPV1 (green, i and v) and for β-tubulin (red, ii and vi). TRPV1-Ct clusters were visible (i and v) even after nocodazole treatment and detergent extraction. Distribution of nocodazole-resistant microtubules appeared almost all over the cell including the peripheral regions of the cell. Relative distribution of the nocodazole-resistant microtubules appeared only in restricted areas near MTOC in non-transfected cell (iv). An enlarged area of the same non-transfected cell is shown on the right side (viii). Scale bar 10 μm (i-iv) and 5 μm (v-viii).

clusters of TRPV1-Ct. In contrast to the transfected cells, non-transfected cells did not reveal this kind of uneven distribution or bundling, and a normal microtubule structure was visible (figure 2.37a). These observations support a stabilizing effect of TRPV1-Ct on the microtubules *in vivo*.

Next the cells were extracted with detergent before fixing them, and a similar immunostaining was performed. It was observed that the cluster-like spots that contained TRPV1-Ct were not extractable (figure 2.37b). After detergent extraction, the cells lose soluble tubulin, but retain microtubules. In TRPV1-Ct-expressing cells, unevenly distributed microtubules all over the cell body and bundled microtubules at areas enriched with TRPV1-Ct spots became prominent after detergent extraction. Interestingly, apart from these spots, some TRPV1-Ct immunoreactivity was also observed after detergent extraction along with
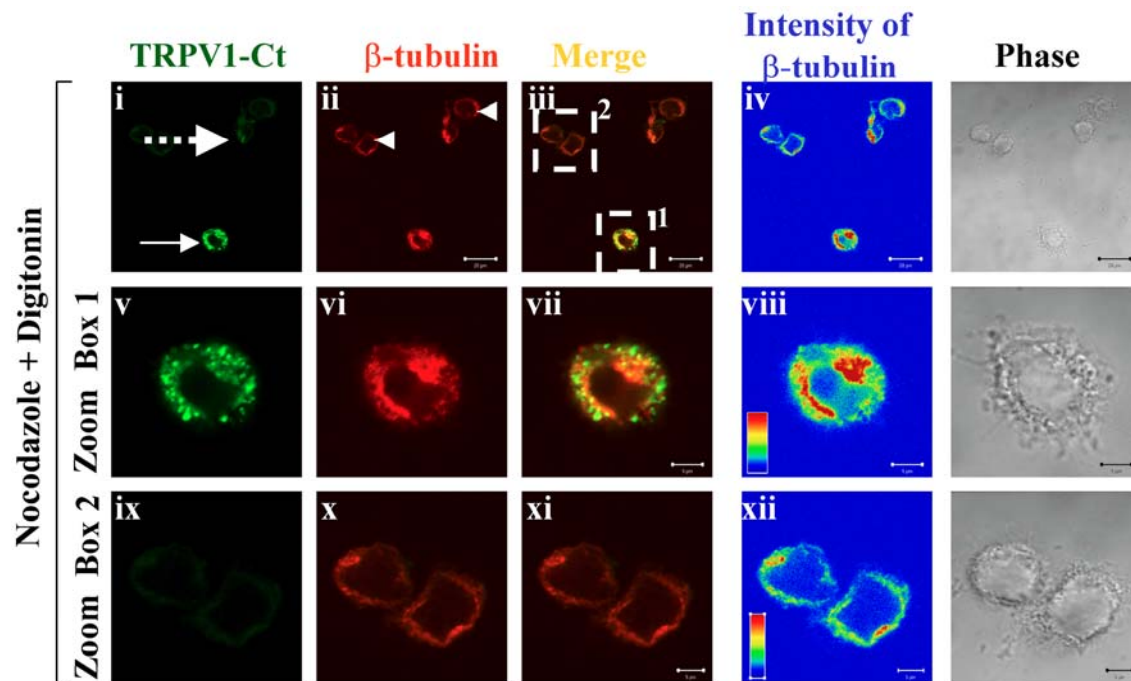
Figure 2.38. Over-expression of TRPV1-Ct provides stability to the microtubules against nocodazole. Indirect immunofluorescence confocal images of nocodazole-treated and detergent-extracted F11 cells (i-iii) or enlarged areas depicting either a cell transiently expressing TRPV1-Ct (indicated by white box 1) or non-transfected cells (indicated by white box 2) are shown. Cells were incubated with nocodazole, extracted with detergent in an isotonic buffer and immunostained for the C-terminus of TRPV1 (green, i, v and ix) and for β-tubulin (red, ii, vi and x). An arrow and a dashed arrow indicate cells expressing high and moderate amounts of TRPV1-Ct, respectively (i). Non-transfected cells are indicated by arrowheads (ii). TRPV1-Ct clusters were visible even after nocodazole treatment and detergent extraction (v). The amount of nocodazole-resistant and unextractable microtubules was significantly higher in the TRPV1-Ct-expressing cells and appears to correlate with the expression level of TRPV1-Ct. The picture on the right shows the intensities of the β-tubulin immunoreactivity in the rainbow scale (iv, viii and xii). Scale bar 20 μm (i-iv) and 5 μm (v-xii).

the microtubules, especially at areas with enriched microtubule structures (figure 2.37b). In contrast, non-transfected cells reveal uniform distribution of microtubules all over the cell body and no bundling of microtubules (figure 2.37b).

In order to further substantiate our conclusion that the C-terminus of TRPV1 provides stability to the microtubules in cultured cells, it was over-expressed and the cells were incubated with nocodazole, a microtubule-destabilizing drug. The cells were then extracted with an isotonic buffer containing digitonin. The TRPV1-Ct clusters remain visible even after nocodazole treatment and digitonin extraction (figure 2.37c). More often the presence of nocodazole-resistant microtubules all over the cell body including the distal peripheral areas in the TRPV1-Ct-expressing cells was observed, whereas the distribution of the nocodazole-

resistant microtubules in non-transfected cells was limited only to the presumed MTOC and nearby areas (figure 2.37c).

By immunofluorescence analysis it was also observed that the amount of tubulin immunoreactivity left after nocodazole treatment and detergent extraction (nocodazole-resistant microtubules) in TRPV1-Ct-expressing cells was significantly higher than in the non-transfected cells (figure 2.38). Interestingly, a correlation between the amounts of nocodazole-resistant microtubules left after detergent extraction with the expression levels of TRPV1-Ct was observed. This was confirmed by a comparative analysis of the intensity of the tubulin immunoreactivity of the nocodazole-resistant microtubules in TRPV1-Ct-expressing cells and non-expressing cells (figure 2.38). Similar results were also obtained when the cells were probed with anti-α-tubulin antibody (data not shown). These results match well with the observation that MBP-TRPV1-Ct interacts with polymerized microtubules *in vitro* and provides stabilization against nocodazole (figure 2.12). In contrast, no changes in the actin cytoskeleton, especially no accumulation of actin in TRPV1-Ct-expressing cells was observed (figure 2.39).
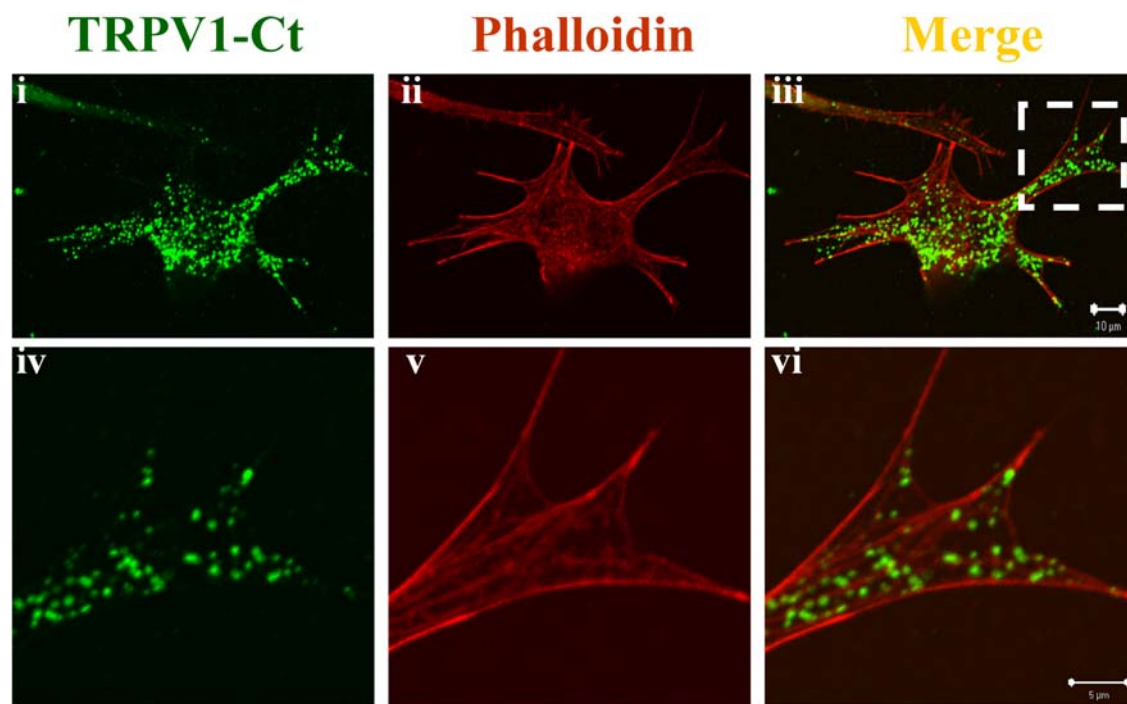

Figure 2.39. Over-expression of TRPV1-Ct does not alter the actin cytoskeleton. Shown are the indirect immunofluorescence images of a F11 cell (i-iii) transiently expressing TRPV1-Ct and immunostained for TRPV1-Ct (green) with a goat polyclonal anti-TRPV1 antibody, and for the actin with alexa-595-labelled phalloidin. Merged images of actin and TRPV1-Ct of the cell (iii) and an enlarged area of the same cell (iv) are shown on the right side. No co-localization between actin and TRPV1-Ct, nor any accumulation of actin in the TRPV1-Ct-enriched areas was observed. Scale bar 10 µm (for i-iii) and 5 µm (for iv).

In summary, these results indicate that TRPV1 activation results in destabilization of dynamic microtubules while the C-terminus of the channel has a microtubule-stabilizing effect. Such interplay between stabilizing and destabilizing effects could provide the basis for a participation of TRPV1 in microtubule cytoskeleton remodelling during pain transmission.

2.4. Presence of TRPV1 at nerve endings. Regulation of growth cone morphology and movement by TRPV1 activation.

Nerve endings, including growth cones, are a special kind of neuronal structures where microtubule dynamicity and complex signalling events determine multiple biological functions. The importance of different Ca^{2+} channels including some members of the TRPC subfamily in such regulation is established to a certain extent (Gomez and Spitzer. 2000; Gomez et al. 2001; Spitzer et al. 2000; Henley and Poo. 2004; Robels et al. 2003; Wen et al 2004; Montell C. 2004; Gomez T. 2005; Li et al. 2005; Wang et al. 2005; Shim et al. 2005; Bezzerides et al. 2004; Greka et al. 2003). However the exact mechanism by which these Ca^{2+} channels regulate growth cone movement is not known. Previous experiments demonstrated that while activation of TRPV1 results in rapid disassembly of microtubules, the C-terminal cytoplasmic domain of TRPV1 provides stabilization to the microtubules. Therefore, the ability of TRPV1 to stabilize-destabilize microtubules and the ability to detect multiple endogenous ligands, noxious physical and/or chemical stimuli makes TRPV1 an ideal Ca^{2+} channel that may be involved in axonal growth and path finding.

Though initially expression of TRPV1 was speculated to be restricted only to the DRG (Caterina et al. 1997), recently TRPV1 was detected in many parts of the brain and spinal cord (Roberts et al. 2004; Mezey et al. 2000; Toth et al. 2005) as well as in many other non-neuronal tissues (see chapter 1.3 for details). This suggests that TRPV1 is distributed widespread and is not restricted to peripheral neuronal structures. Additionally responsiveness of synaptosomes isolated from brain and spinal cord to capsaicin, the main ingredient of hot chilly pepper, was reported, indicating that functional TRPV1 is most likely present at nerve endings (Li and Eisenach. 2001; Schmid et al. 1998).

Therefore, it was justified to test if TRPV1 is present in growth cones and if so, then to investigate if it can regulate the behaviour of growth cones. Using synaptosomes, transfected F11 cells, embryonic DRG explants from mice and/or chicken, and a combination of biochemical and microscopic methods, my experiments demonstrate that TRPV1 is indeed present at nerve endings and also in synaptic structures. My results also indicate that TRPV1 regulates the growth cone behaviour and dynamicity by altering the microtubule cytoskeleton. The ability of TRPV1 to regulate the axonal morphology, movement and dynamicity may well be a new aspect of pain sensation, especially of chronification of pain.

2.4.1. TRPV1 is present in synaptic structures (synaptosomes).

Previously capsaicin sensitivity of synaptosomes was reported in various studies (Li and Eisenach. 2001; Schmid et al. 1998). Here it was examined whether TRPV1 is indeed present in synaptosomes isolated from both rat and porcine spinal cord. By western blot analysis, specific TRPV1 immunoreactivity was detected in synaptosome fractions (figure 2.40). The anti-TRPV1 immunoreactivity match well with the molecular weight attributed for monomer and glycosylated monomer of TRPV1. The same immunoreactivity was not detected when the anti-TRPV1 antibody was pre-incubated with a blocking peptide.
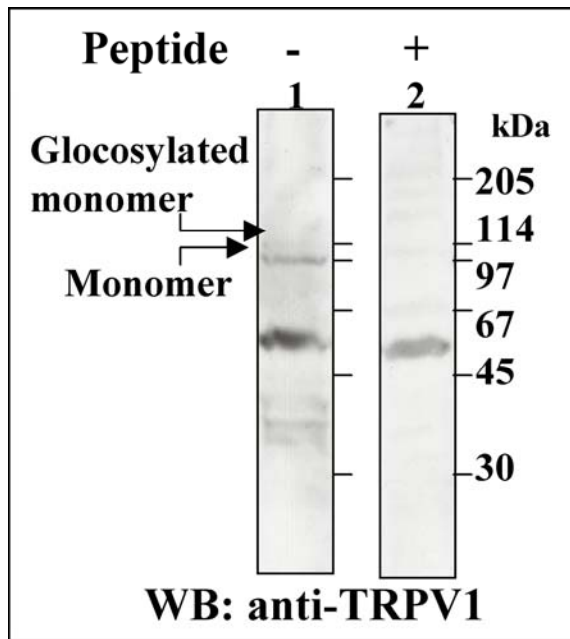
Figure 2.40. TRPV1 is present in synaptosomes. 100μg of porcine synaptosomal proteins were loaded in each lane and probed with anti-TRPV1 antibody either in the absence (lane 1) or presence (lane 2) of a blocking peptide. Arrows indicate the specific immunoreactivities against TRPV1 monomer and glycosylated monomer.

2.4.2. TRPV1 is localized at neurites and growth cones.

TRPV1 was transiently expressed in F11 cells and the localization was monitored. Upon transfection F11 cells develop multiple neurite-like extensions including growth cones. TRPV1 was detected at the neurite-like extensions of different lengths (figure 2.41). TRPV1 immunofluorescence was observed along the full length of the neurite-like extensions, and also at their branching points. Though few in numbers, the presence TRPV1 immunoreactivity in big bulge-like structures within the long neurite-like extensions were visible (figure 2.41). Similar structures are often termed as "varicosities", "beads" or "waves", respectively (Ahmad et al. 2000; Hatada et al. 1999; McNeil et al. 1999; Ruthel and Banker. 1998; Jacobs and Stevens. 1986). These structures are believed to contain densely packed vesicles with synaptic complexes and to be generated due to a local
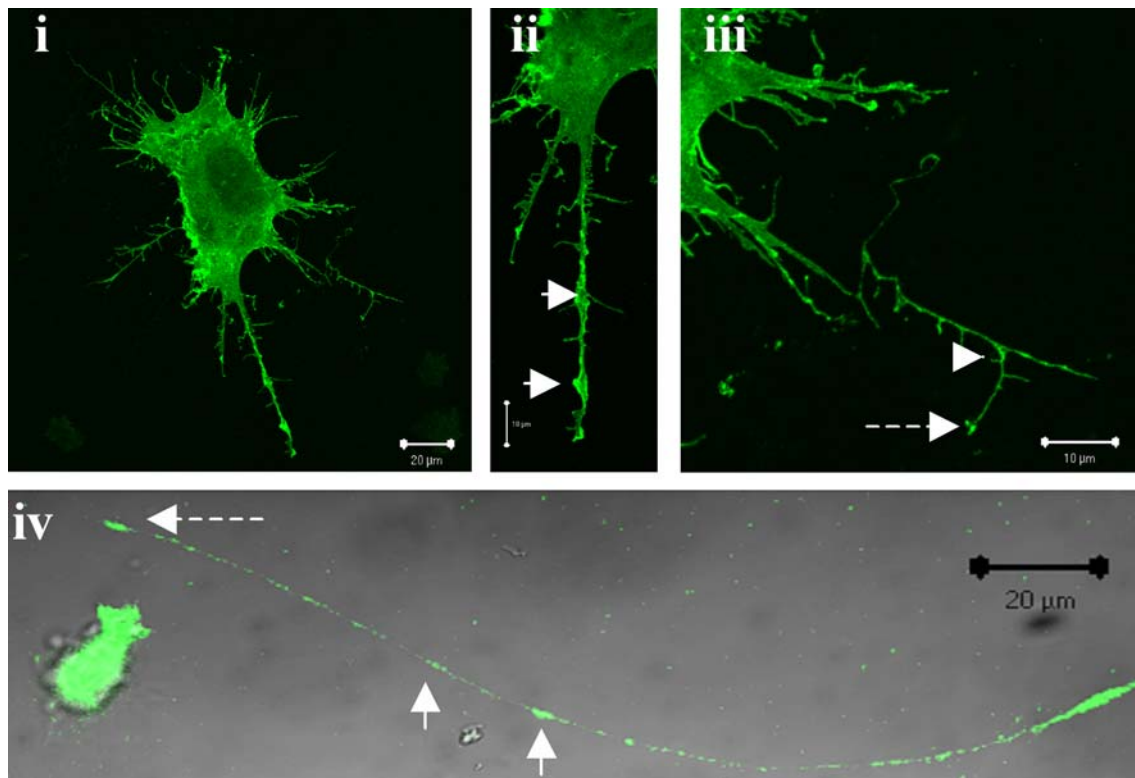
Figure 2.41. Localization of TRPV1 in neurites and at the nerve endings. Shown are indirect immunofluorescence confocal images of a F11 cell transiently expressing TRPV1 (i) and enlarged areas of the same cell (ii-iii). An enlarged area of a TRPV1-F11 stable cell depicting a long neurite is also shown (iv). Presence of TRPV1 (green) in varicosities within long neurites (white arrows, in ii and iv), branching points (arrow head, iii) and at neurite endings (dashed arrows, ii and iv), respectively is indicated. Scale bar 20μm (for i and iv) and 10μm for (ii-iii).

disassembly of microtubules or to a temporary pause of growth cones. In this study these structures are referred to as "varicosities". The presence of TRPV1 in similar "varicosities" was also observed in TRPV1-F11 cells that express low levels of TRPV1 after stable transfection (figure 2.41-iv). Significant immunoreactivity was also observed in multiple thin filopodial structures developed from the cell body and neurites.

By immunofluorescence analysis, TRPV1 was detected at the nerve endings that extend into growth cone-like structures. By co-immunostaining for growth-cone associated protein 43 (GAP43/neuromodulin), a well-characterized growth-cone marker (Jacobson et al. 1986; Strittmatter et al. 1995; Meiri et al. 1986; Skene J.H.P. 1989), the identity of such structures was confirmed as conventional axonal "growth cones" (figure 2.42).

2.4.3. TRPV1 localizes to the C- and P-zone of growth cones.

Extending growth cones display distinct structural features, e.g. a central zone (C-zone), a peripheral zone (P-zone) and a transition zone (T-zone) that correlate with the presence of different cytoskeletal proteins (Gordon-Weeks P.R., 2004; Rodriguez et al., 2003; Dent and Gertler. 2003). The C-zone of growth cones is known to be enriched with vesicles of various sizes and with microtubules, in particular their plus ends. In contrast, the P-zone is enriched with the plasma membrane and the actin cytoskeleton beneath it. Distinct morphological features correlate with different stages of the growth (Gordon-Weeks P.R., 2004; Rodriguez et al., 2003; Dent and Gertler. 2003). By immunofluorescence microscopy, TRPV1 was observed in growth cones that are at pause and at the stage of retraction (data not shown). In extending growth cones, a differential distribution of TRPV1 in distinct areas was observed (figure 2.42). Negligible TRPV1 immunoreactivity was detected in the T-zone, whereas a considerable TRPV1 immunoreactivity was observed in the P-zone and in the C-zone (figure 2.42).
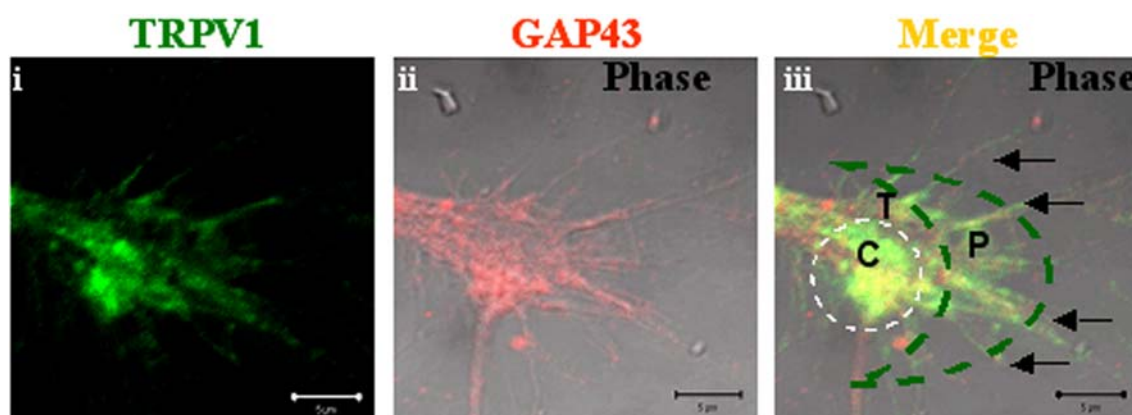

Figure 2.42. Localization of TRPV1 at extending growth cone. Shown are the confocal immunofluorescence images of a growth cone developed from F11 cell immunostained for TRPV1 (green, i) and GAP43 (red). Immunofluorescence image of GAP43 is superimposed on the phase-contrast image (ii). A merged image of TRPV1 (green) and GAP43 (red) is superimposed on the phase-contrast image (iii). Central zone (**C**), transition zone (**T**) and peripheral zone (**P**) of growth cones are indicated. Black arrow indicates filopodial structures. Scale bar 5μm.

2.4.4. TRPV1-GFP localizes to the growth cone.

In order to confirm the differential localization of TRPV1 in growth cones by another method, TRPV1-GFP was transiently expressed in F11 cells and live cell microscopy was performed. Fusion of GFP with TRPV1 does not alter the receptor's properties, as for example the capsaicin response (Hellwig et al., 2004) or the membrane localization. Fusion
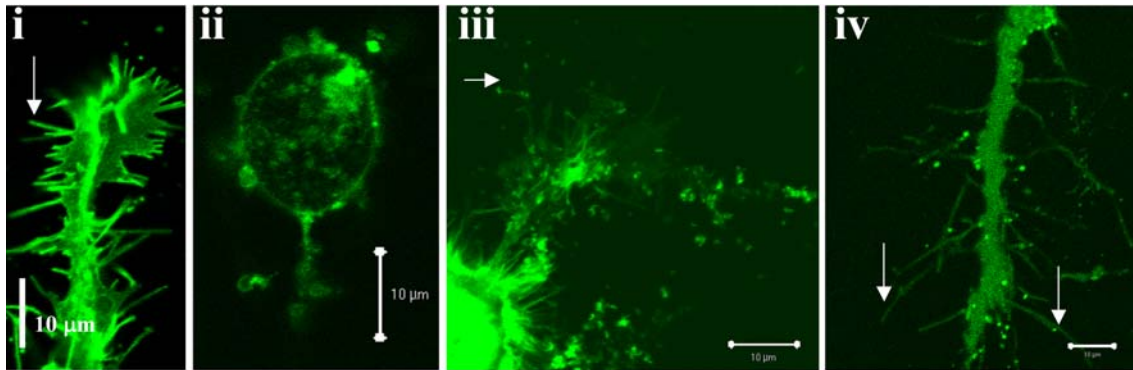
Figure 2.43. TRPV1-GFP localizes to the growth cones. Examples of growth cones with TRPV1-GFP of different stage, shape and morphology observed in this study. An extending growth cone with an extended axon-like structure (i) and a growth cone with a bulb like morphology at the end of a long axon, presumably at the "pause-stage" (ii) is shown. An immature-dynamic-extending growth cone with a short neuritic shaft (iii) reveals significant accumulation of TRPV1-GFP at the C-zone. Presence of TRPV1-GFP at the filopodial structures and enrichment of TRPV1-GFP at the tip of such structures are shown (iv). Scale bar 10μm.

of GFP at either the C- or N-terminus of TRPV1 does not alter the receptor's membrane localization, capsaicin responses or the interaction with tubulin (see figure 2.5). All live cell studies reported here were performed with TRPV1-GFP.

TRPV1-GFP was localized in intracellular regions as well as at the plasma membrane. Apart from that, TRPV1-GFP was observed to localize to the neurites of different lengths and to growth cones of different shape and morphology (figure 2.43). In agreement with the immunofluorescence analysis, TRPV1-GFP was predominantly localized at the C- and P-zones of extended growth cones (figure 2.43). A significant amount of TRPV1-GFP was observed in the region of the main axonal shaft that is known to consist predominantly of microtubules. A considerable amount of TRPV1-GFP is localized in the filopodial structures developed from extended growth cones (figure 2.43, i and iv). With live cell microscopy, it was observed that these filopodial structures were indeed dynamic in nature. Often, an enrichment of TRPV1-GFP at the tip of such filopodial structures was observed (figure 2.43, iv). Interestingly, these TRPV1-GFP-enriched structures at the tip of filopodia remain stable and were observed to be less dynamic within the filopodial structure.

2.4.5. Fast and slow transport of TRPV1 to the growth cones.

To understand how TRPV1 is transported to the growth cones, the movement of TRPV1-GFP in F11 cells was observed by live cell microscopy. It was observed that

TRPV1-GFP is transported to the growth cone by mobile small vesicles as well as with much larger units (figure 2.44). A saltatory movement was observed for the small vesicular structures. The larger units either stood still for a longer time, or moved very little in hours. However, we observed that these units can change speed and direction within seconds and can accelerate to a velocity which is as fast as approximately 0.45μm per sec, a velocity matching well with the velocity of the microtubule-based transport system (Woehlke and Schliwa. 2000; Goldstein and Yang. 2000). Taken together, the observations suggest that TRPV1 is transported to the dynamic growth cones through vesicles and transport units of different sizes.
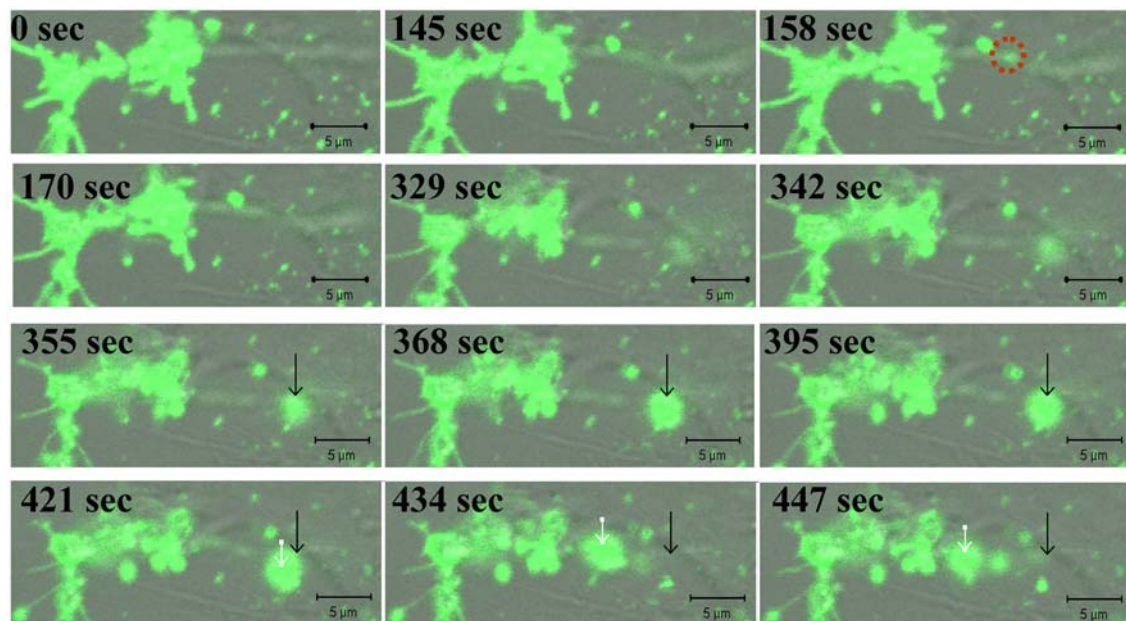

Figure 2.44. Transport of TRPV1 to the growth cone. Shown are time series of confocal images of a long neurite with a growth cone originating from a F11 cell transiently expressing TRPV1-GFP (green). Superimposed images of TRPV1-GFP and phase-contrast images are provided. The red dashed circle indicates a smaller transport unit of TRPV1. A black arrow indicates the area where a much larger transport unit first appeared. White arrows indicate the relative positions of the same transport unit at a particular time. The larger transport unit moved with a maximum velocity of 0.44μm per second. (Total 5.25μm distance covered between 421sec to 434 sec). Scale bar 5μm.

2.4.6. TRPV1-enriched patches at growth cones provide stability and guidance to pioneer microtubules.

Significant TRPV1 immunoreactivity was observed at the neurite shaft and at the C-zone, which represent the plus ends of microtubules (see figure 2.42 and 2.43). TRPV1

immunoreactivity also occurs in the P-zone as patches. Though, the majority of microtubules are restricted to the main axonal shaft and to the C-zone of the growth cone, few pioneer microtubules migrate to the P-zone. These few pioneer microtubules are "dynamic" and important for growth cone turning (Gordon-Weeks PR, 2004; Suter et al. 2004. Discussed later in section 3.3). I observed that these pioneer microtubules, which are projecting towards the P-zone, are often restricted to areas enriched with TRPV1. These TRPV1-enriched patches at the P-zone contain a considerable amount of immunoreactivity attributed to α-tubulin (figure 2.45). This accumulation of α-tubulin was not observed in other regions of the P-zone that do not harbour TRPV1-enriched patches. This again indicates a stabilizing effect of TRPV1 on the pioneer microtubules at the P-zone in the resting stage of the growth cone.

Neuronal microtubules composed of unmodified alpha-beta tubulin dimers undergo a series of sequential post-translational modifications (e.g. a tyrosination-detyrosination cycle, acetylation, discussed later in section 3.3.1) underlying a process of maturation, which provides them with different physico-chemical properties and marks their "age" (Dent and Gertler. 2003; Westermann and Weber. 2003; MacRae T.H., 1997, Idriss H.T. 2000). To investigate how TRPV1 can regulate the microtubule cytoskeleton at the growth cones, microtubules at the P-zone of growth cones were analyzed for their "physico-chemical nature" as well as their "age". Therefore microtubules at the P-zone of TRPV1 containing growth cones were analyzed for different post-translationally modified tubulins. It was observed that the TRPV1-enriched patches at the P-zone contain microtubules that are immuno-positive for tyrosinated tubulin (figure 2.21a), a marker for dynamic microtubules
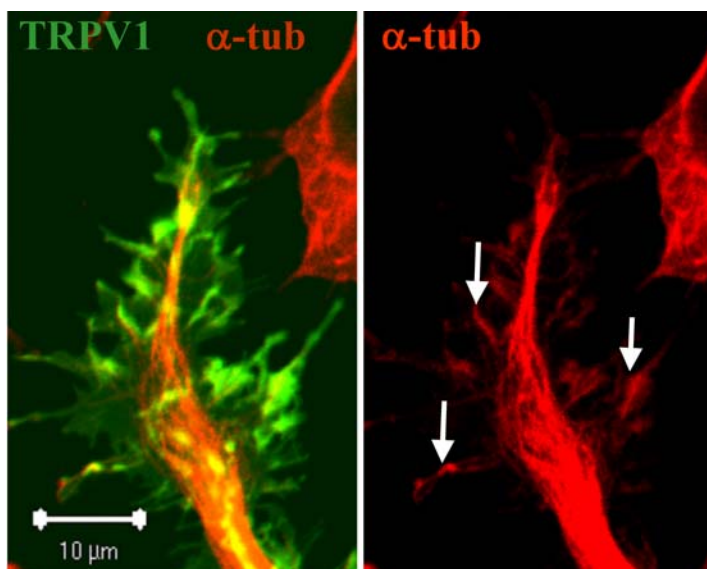

Figure 2.45. TRPV1-enriched patches at P-zone stabilize to the pioneer microtubules. Shown are indirect immunofluorescence confocal images of extending growth cones developed from F11 cells transiently expressing TRPV1. Cells were co-immunostained for TRPV1 (green) and for α-tubulin (red). The merged image is provided at the left side. Corresponding image of α-tubulin is provided at the right side. Arrows indicate restricted distribution of α-tubulin at TRPV1-enriched patches at the P-zone of the growth cones. Scale bar 10μm.
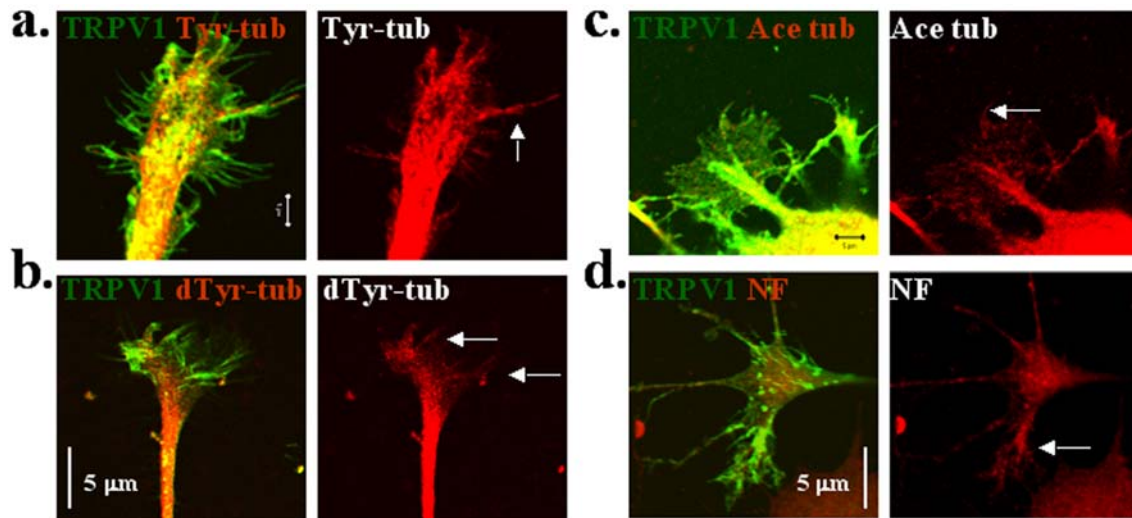
Figure 2.46. TRPV1-enriched patches at P-zone contain post-translationally modified tubulins and neurofilaments. Shown are indirect immunofluorescence confocal images of extending growth cones developed from F11 cells transiently expressing TRPV1. Cells were co-immunostained for TRPV1 (green) and for different post-translational modified tubulins or neurofilaments (red). Merged images were provided at the left side. Corresponding images of cytoskeleton elements are shown at right. Restricted distribution of tyrosinated tubulin (**a**), detyrosinated tubulin (**b**), acetylated tubulin (**c**) and neurofilament 116 kDa (**d**) at the TRPV1-enriched patches at P-zone of the growth cones is indicated by arrows. See also figure 2.45. Scale bar 5 μm.

(Gundersen et al., 1984; Kreis T.E.1987; Wehland and Weber. 1987). In agreement with the previous observations, the majority of these pioneer microtubules that are immuno-positive for tyrosinated tubulin are restricted to areas containing TRPV1-enriched patches (figure 2.46, a). Similarly, the pioneer microtubules at the TRPV1-enriched patches in the P-zone were further probed for acetylated tubulin and detyrosinated tubulin as markers for "stable microtubules" which are supposed to be present only in "matured" or "aged" microtubules (Idriss H.T. 2000). It was observed that the TRPV1-enriched patches in the P-zone contain a significant amount of detyrosinated tubulin and a moderate level of acetylated tubulin (figure 2.46, b-c). It was also tested if these TRPV1-enriched patches at the P-zone contain any neurofilaments. A considerable amount of neurofilament was also detected in the TRPV1-enriched patches (figure 2.46, d).

Taken together, the restricted distribution of microtubules and the presence of immunoreactivities characteristic for "aged" microtubules at the TRPV1-enriched patches in the P-zone suggest that the TRPV1-enriched patches may guide and/or determine the direction of dynamic microtubules by providing the necessary stability at the plus ends. This is further supported by the presence of neurofilament in these patches, as incorporation of neurofilament is considered to be a later event (Chan et al. 2003; Uchida and Brown. 2004).

2.4.7. The N-terminal sequence is important for localization at nerve endings while the C-terminus is important for the stabilization of microtubules.

Previously I observed that the TRPV1-tubulin interaction is mediated by the C-terminus of TRPV1 (TRPV1-Ct). Over-expression of TRPV1-Ct causes bundling and stabilization of microtubules (see figure 2.37 and 2.38). However, TRPV1-Ct was not observed at nerve endings (data not shown). In order to identify the molecular determinants of TRPV1 responsible for its targeting to the nerve endings, different truncated constructs of TRPV1 were expressed in F11 cells. Immunofluorescence analysis was performed to monitor their localization. TRPV1-ΔCt (this construct contains the entire N-terminal cytoplasmic domain together with the transmembrane region but lacks the entire C-terminal domain of TRPPV1) accumulated at the nerve endings (figure 2.47, a). To rule out the possibility that this localization of TRPV1-ΔCt at the neurite and nerve endings was due to the presence of the transmembrane sequences, another construct, namely TRPV1-Nt (only the N-terminal cytoplasmic domain of TRPV1) was expressed in F11 cells. TRPV1-Nt localized to the nerve endings (figure 2.47, b). However, in both cases no co-localization with tubulin or an accumulation of tubulin was observed. TRPV1-ΔNt, another construct that lacks the entire N-terminal cytoplasmic domain, was expressed. It localized to the cell body and to the plasma membrane, but failed to be localized to neurites (data not shown). Taken together the results suggest that the N-terminus of TRPV1 is necessary and sufficient for the localization at nerve endings, while the C-terminus provides stability to the microtubules.

2.4.8. Activation of TRPV1 results in retraction of growth cones.

The importance of Ca^{2+} channels in the regulation of growth-cone movements has been reported previously (Gomez and Spitzer, 2000; Gomez et al. 2001; Spitzer et al. 2000; Henley and Poo, 2004; Robels et al. 2003; Wen et al. 2004). Earlier it was observed that activation of TRPV1 has a destabilizing effect on microtubules in the cell body (see chapter 2.3). Therefore it was investigated if activation of TRPV1 can alter or regulate the cytoskeleton in growth cones and neurite extensions, too. For that purpose TRPV1-GFP was expressed in F11 cells and growth cones with TRPV1-GFP were monitored for 10 minutes before and after RTX application.

As expected, it was observed that the majority of the TRPV1-GFP-positive growth cones responded to the agonists RTX or capsaicin. Activation resulted in retraction and/or collapse of growth cones. However, the rate of retraction varied. It probably depends on the stage, on cues present in the local environment and on the morphology of the growth cones.
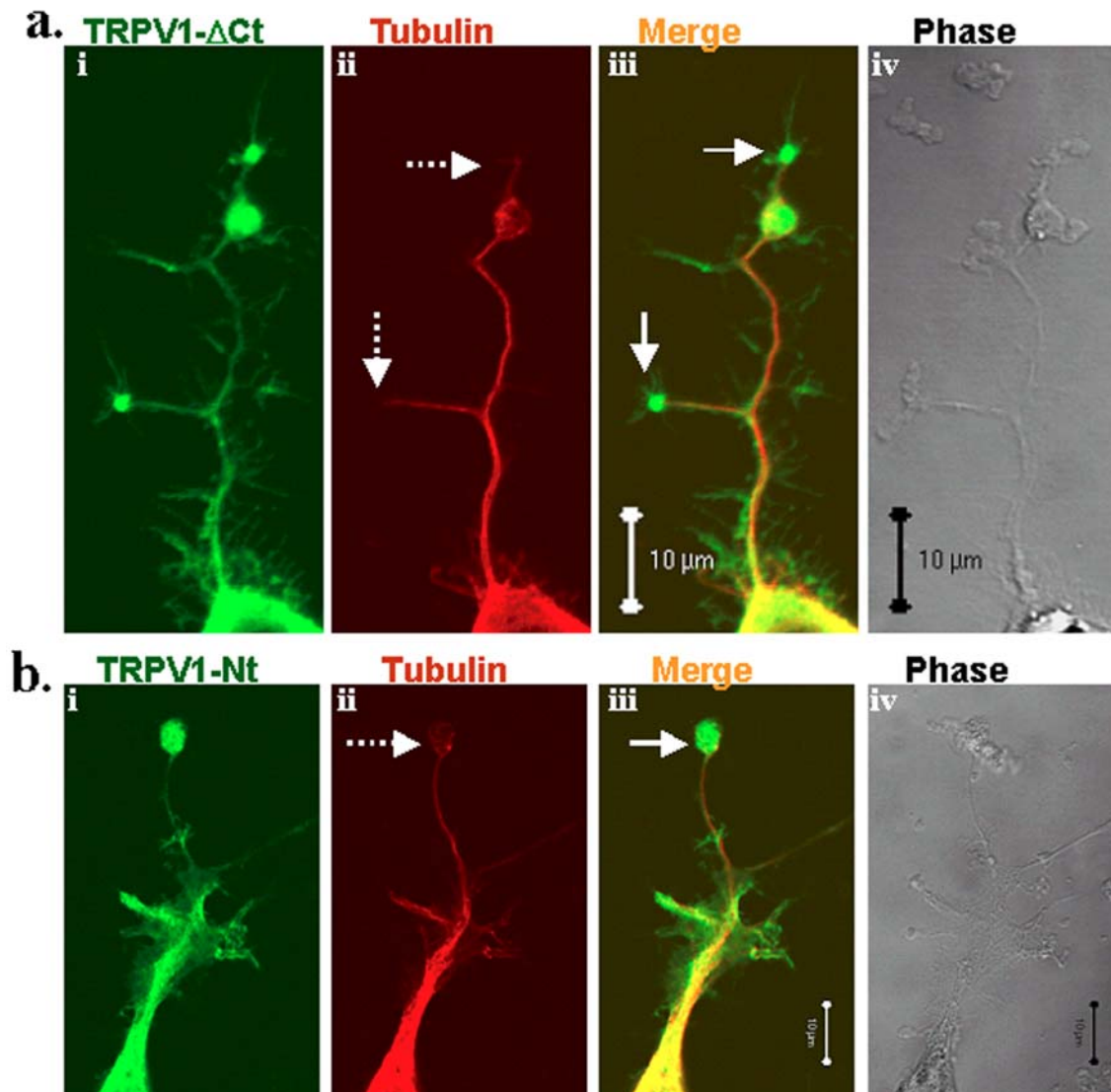
Figure 2.47. N-terminus of TRPV1 is sufficient for localization at neurite endings. a. Shown are indirect immunofluorescence confocal images of neurite endings developed from a F11 cell transiently expressing TRPV1-ΔCt. Cells were immunostained for TRPV1-ΔCt (green, i) with rabbit polyclonal anti-TRPV1 antibody and for tyrosinated tubulin (red, ii). Presence of TRPV1-ΔCt in the thin filopodial structures is indicated by white arrowheads. Localization of TRPV1-ΔCt at the neurite endings is indicated with white arrows. Merge image (iii) and phase contrast (iv) images are provided on the right side. Minimal co-localization between TRPV1-ΔCt and tubulin was observed. At neurite endings TRPV1-ΔCt enriched structures reveals no immunoreactivity for tyrosinated tubulin (indicated by dashed arrows). Scale bar 10 μm. **b.** Indirect immunofluorescence confocal images of neurite endings developed from an F11 cell transiently expressing TRPV1-Nt. Cells were stained for TRPV1-Nt (green, i) and tyrosinated tubulin (red, ii). TRPV1-Nt localizes efficiently to the neurite endings (indicated by white solid arrow), but does not co-localize with tubulin (iii). The dashed arrow indicates immunoreactivity for tubulin in TRPV1-Nt enriched neurite endings. Phase contrast image is provided on the right side (iv). Scale bar 10 μm.

Growth cones with a long axon retracted slowly. They often changed to a "pause stage" and formed multiple varicosities (data not shown). Growth cones that are presumably at pause (growth cones at pause exhibit a distinct morphology: a bulb-like structure at their end, Dent and Gertler. 2003) did not retract upon agonist application. For the purpose of better characterization, this study was restricted to growth cones that are dynamic, immature, with an extended morphology and which are not connected to any other cell or growth-cone (figure 2.43, iii). The majority of this type of growth cones (56 out of 60) retracted fast (figure 2.48). This process of retraction, due to TRPV1 activation, could be completely blocked by the presence of antagonist 5'-IRTX (5'-IRTX and RTX added together, data not shown), indicating that the retraction of growth cones was indeed due to TRPV1 activation (see also section 3.3.1).
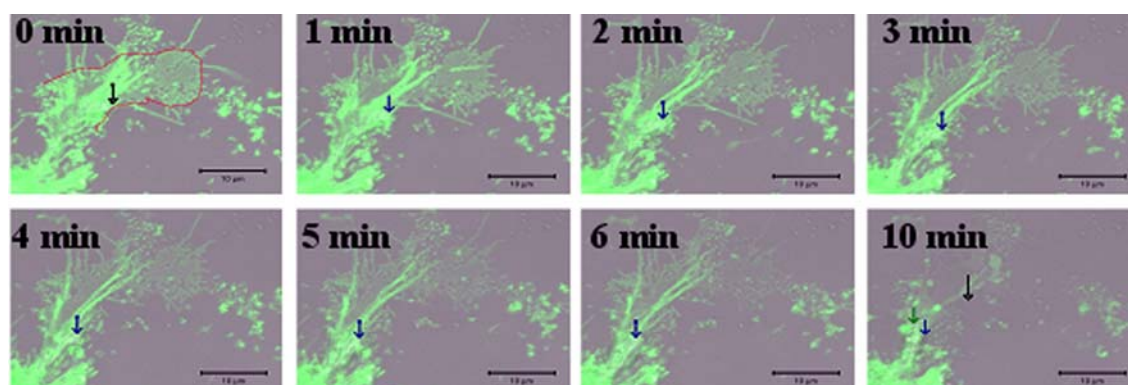

Figure 2.48. Activation of TRPV1 results in retraction of growth cone. Shown are the time-lapse confocal images of an immature dynamic extended growth cone with TRPV1-GFP (green). Images were captured in 30-second intervals and fluorescence images superimposed on phase contrast images are shown. The first image (0 minute) was captured just after adding the agonist RTX. The red line and the black arrow indicate the borderline and the centre of the main shaft of the growth cone, respectively, at time 0. The blue arrow indicates the position of the main shaft or the centre of the growth cones at a particular time point during the retraction phase. The growth cone extends very little from 6th minute to 10th minute to a different direction. The position of the main shaft at minute 10 (indicated by green arrow) differs in length and direction from the same at minute 6 (indicated by blue arrow). Scale bar 10μm.

2.4.9. Activation of TRPV1 results in changes of the microtubule organization at growth cones.

Extending growth cones maintain a fine balance between dynamic microtubules at the P-zone and stable microtubules at the shaft as well as at the C-zone. The microtubules projecting towards the P-zone represent dynamic microtubules important mainly for path finding (Gordon-Weeks P.R. 2004; Rodriguez et al. 2003; Dent and Gertler. 2003). To

understand the effects of TRPV1 activation on the change in the microtubule cytoskeleton, dynamic microtubules were analyzed by immunofluorescence analysis. For this purpose TRPV1 was activated for 1 minute and the cells were fixed immediately to avoid loss of growth cone morphology.

In the absence of TRPV1 activation, the immunoreactivity for tyrosinated tubulin was restricted to the main shaft of the microtubules. Some of these dynamic microtubules extended to the P-zone of the growth cones where TRPV1-enriched patches are present (figure 2.49). Most of the P- and T-zones do not reveal any immunoreactivity against anti-tyrosinated tubulin antibodies. In contrast, upon TRPV1 activation, an altered distribution of tyrosinated tubulin within the growth cone was observed. The immunoreactivity for tyrosinated tubulin was dispersed all over the growth cone, and the fine microtubule filament structures had disappeared. A considerable increase in tyrosinated tubulin was observed in
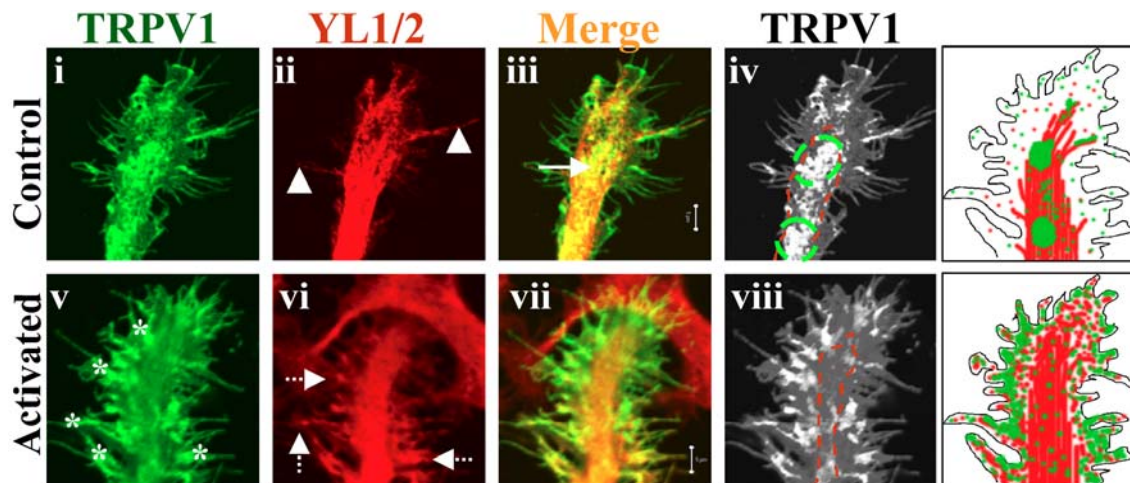

Figure 2.49. Activation of TRPV1 results in a change of the microtubule cytoskeleton at growth cones. Indirect immunofluorescence confocal images of a growth cone developed from an F11 cell transiently expressing TRPV1 (i-iii) or after activation with RTX (iv-vi). Cells were immunostained for TRPV1 (green) with rabbit polyclonal anti-TRPV1 antibody and for tyrosinated tubulin (red) with rat monoclonal antibody clone YL1/2. In the absence of activation (i-iii), immunoreactivity for tyrosinated tubulin appears only in the C-zone as a neurite shaft made of microtubules. Only few pioneering dynamic microtubules extend to the P-zone (indicated by arrow heads), keeping the majority of the P-zone and T-zone free from dynamic microtubules. Immunoreactivity for TRPV1 is mainly restricted to the C-zone (indicated by arrow) and partly to the P-zone as filopodial fingers. In an RTX-activated growth cone (iv-vi), the entire P-zone and T-zone reveal dispersed immunoreactivity for tyrosinated tubulin (indicated by dashed arrow), and extending dynamic microtubules were no more visible. Immunoreactivity for TRPV1 at the P-zone increased significantly after activation with RTX (indicated by ∗). Scale bar 5μm. In right, positions of the main microtubule shaft (indicated by red line) and the TRPV1-enriched units (indicated by green line) are drawn on the digitally enhanced TRPV1 immunofluorescence confocal images. Schematic models representing the TRPV1 (green) and microtubule (red) are provided at the extreme right.

the P- as well as in the T-zone. A significant co-localization of TRPV1 with tubulin was observed now in the peripheral extensions (figure 2.49, b). This observation matches well with the previous observation that activation of TRPV1 results in the disassembly of dynamic microtubules.

2.4.10. Activation of TRPV1 results in formation of varicosities within the neurites due to disassembly of microtubules.

It was observed that extending growth cones with a long axon-like neurite, which do not retract upon TRPV1 activation, turn to a pause state and their neurite-like structures develop multiple varicosities (data not shown). Formation of varicosities is believed to represent a change in the microtubule cytoskeleton (Ahmad et al. 2000, Jacobs and Stevens.1986). To explore if the formation of varicosities is indeed due to the TRPV1 activation-mediated disassembly of microtubules, TRPV1 was expressed in F11 cells and the status of microtubules within long neurites was compared. Neuron-specific microtubules within long neurites from TRPV1-activated and non-activated cells were analysed. In the absence of activation, immunoreactivity against β-tubulin subtype III, appears continuous along the neurites of TRPV1-expressing cells. In contrast, upon activation it was no longer visible as a continuous pattern and often appeared as distinct discontinuous accumulations within the varicosities. Interestingly, the majority of these varicosities clearly contain TRPV1 (figure 2.50, a). In contrast, non-transfected F11 cells that do not express TRPV1 reveal a normal and continuous immunoreactivity for tubulin after addition of RTX. These non-transfected cells do not form varicosities (figure 2.50, b). These data indicate that within the long neurite-like structures, TRPV1 activation results in the formation of multiple "varicosities" or "beads in a string" morphology, due to disassembly of the microtubule cytoskeleton.

2.4.11. Embryonic DRG explant-derived growth cones collapse due to the activation of TRPV1

Due to transient over-expression of TRPV1, and F11 cells being hybridomas, the observed results may be considered as artificial. To confirm that activation of TRPV1 results in similar changes in the microtubule cytoskeleton in a truly neuronal system, DRG explants from E12 mice embryos were used. As a negative control, the DRG explants from E7 chicken were used, as the chicken homologue of TRPV1 does not respond to capsaicin or
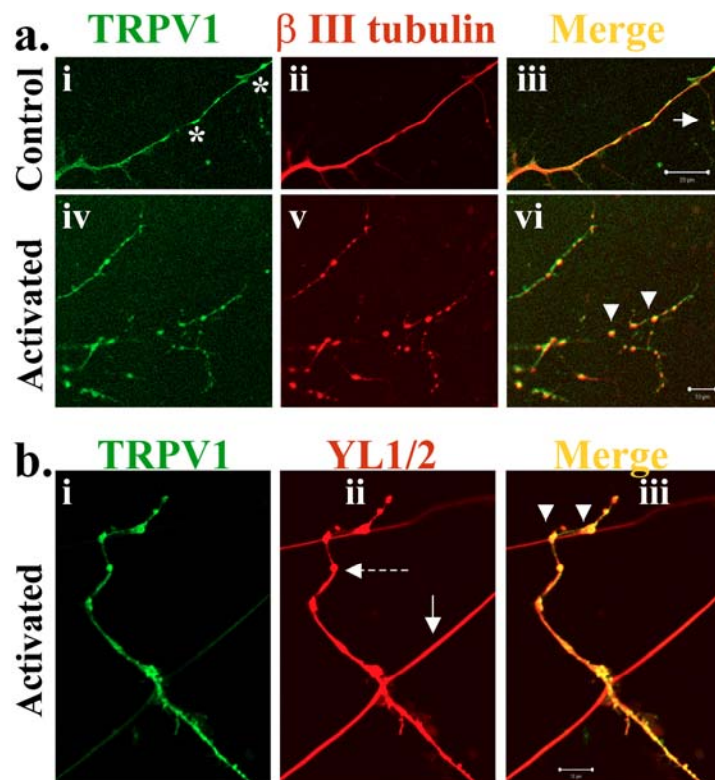
Figure 2.50. Activation of TRPV1 results in the formation of varicosities in F11 cells. a. Shown are indirect immunofluorescence confocal images of an extended neurite-like structure developed from F11 cells transiently expressing TRPV1. Unstimulated cells (i-iii) or RTX-activated cells (iv-vi) were immunostained for TRPV1 (green) and β-tubulin subtype III (red). Several varicosities (indicated by arrow heads) formed after activation with RTX. In unstimulated cells (i-iii), immunoreactivity for TRPV1 appeared as distinct units (indicated by ∗) with some residual amount throughout the neurite-like structures whereas the immunoreactivity for β- tubulin subtype III appeared continuous. An arrow indicates accumulation of tubulin at the end of a small neurite-like structure in an unstimulated cell, which co-localized with anti-TRPV1 immunoreactivity. Immunoreactivity for TRPV1 and β-tubulin subtype III appeared discontinuous throughout the neurites and appeared only within the beads/varicosities (indicated by arrow heads). At right, a schematic model of normal and activated neurites is provided. Scale bar 20μm (for i-iii) and 10μm (for iv-vi). **b.** Shown are indirect immunofluorescence confocal images of extended neurite-like structures developed either from non-transfected F11 cells (indicated by white arrow) or cells transiently expressing TRPV1 (indicated by white arrow heads). Cells were immunostained for TRPV1 (green) and tyrosinated tubulin (red). After activation with RTX, multiple varicosities were observed only in neurites originating from TRPV1-expressing F11 cells, but not from non-transfected F11 cells. Significant co-localization between TRPV1 and tyrosinated tubulin appeared only within the beads/varicosities (indicated by arrow heads). Scale bar 10μm.

RTX (Jordt and Julius. 2002). Immunofluorescence microscopy of these explants was used to visualize the effect of endogenous TRPV1 activation on the cytoskeleton. DRG explants isolated from mice and chicken developed multiple growth cones within a day (figure 2.51). All growth cones revealed a normal extended phenotype and no neurites with varicosities were found (total 437 neurites from 5 explants were counted). Application of RTX to the murine DRG explant revealed distinct changes of the growth cones and neurite structures. As TRPV1 expression is restricted to a subset of DRG neurons, it is expected that there will be
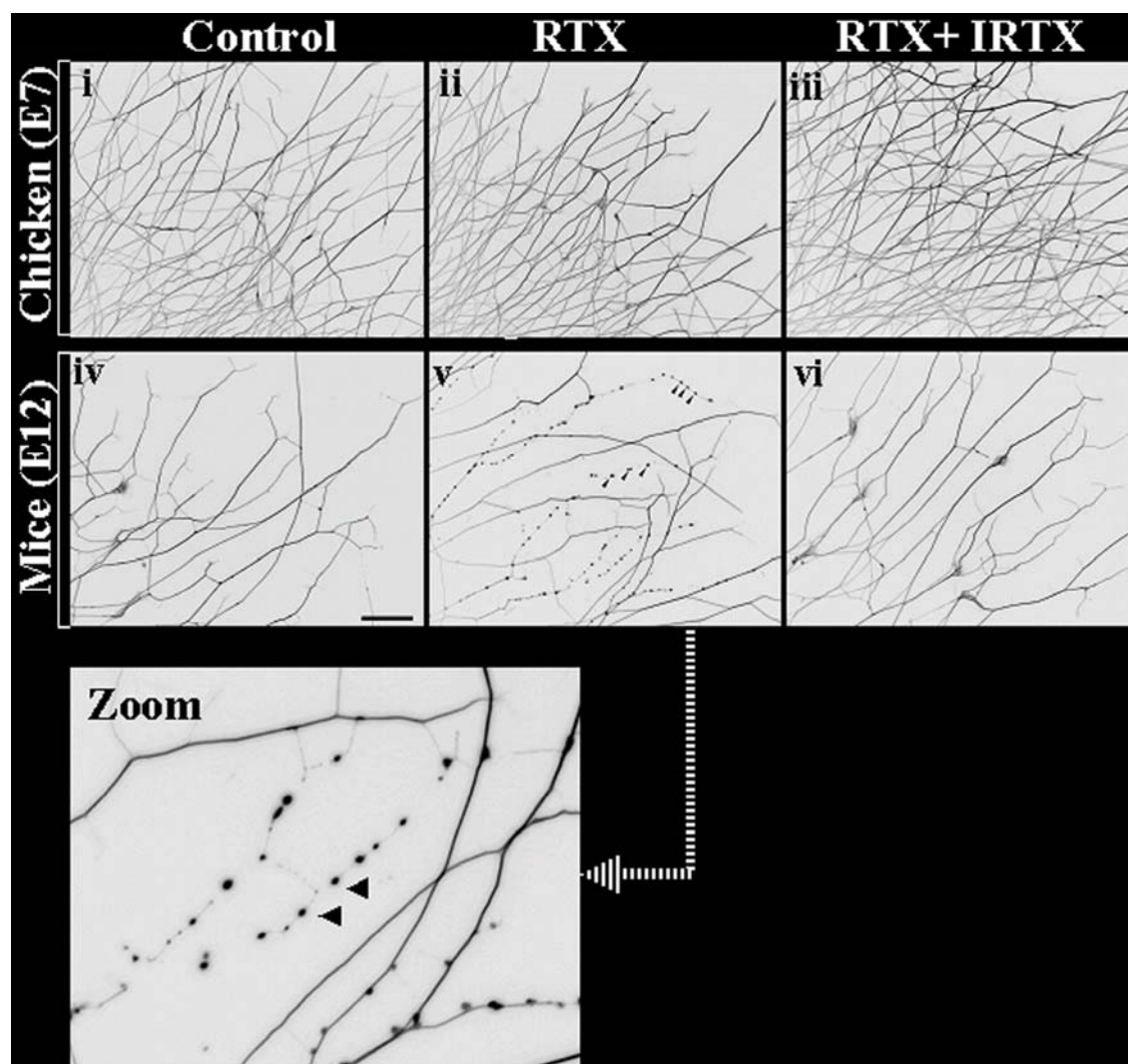
Figure 2.51. Activation of TRPV1 cause formation of "varicosities" due to disassembly of the microtubule cytoskeleton of embryonic DRG explants. Shown are the immunofluorescence images of neurites and growth cones originating from E12 mice (lower panel, iv-vi) and E7 chicken (upper panel, i-iii) DRG explants. Untreated explants (left side, i and iv), treated with agonist RTX in absence (middle, ii and iv) or presence of the antagonist IRTX (right side, iii and vi) are fixed and stained for tubulin. Growth cone collapse and formation of multiple varicosities were observed in 36.54% of the neurites developed from E12 mice explants when incubated with RTX. Arrowheads indicate neurites with collapsed growth cones and discontinuous immunoreactivity for tubulin at the varicosities. An enlarged area of RTX activated mice explant (v) is provided in below. Neurites originating from an E7 chicken DRG explant are insensitive to RTX application and do not form varicosities. Inverted images are provided for better visibility. Scale bar 20 μM.

∗**Note**: All these embryonic DRG explant studies were done at MDC (Buch) along with Dr. Hannes Smith.

some growth cones responding to RTX while others will not. In response to RTX, 36.54% of growth cones (129 out of 353) revealed a "collapsed" morphology and developed multiple varicosities within the neurites (figure 12). This not only proves that the embryonic DRG at

this stage (E12) is sensitive to RTX, but also indicates the presence of TRPV1. Immunoreactivity for tubulin was discontinuous in the "responding" neurites and was found only in the varicosities. However, "non-responding" growth cones remained unaffected, and retained normal neurites with expanding morphology even in the presence of RTX. As expected, a similar treatment of RTX had no effect on any of the DRG explants from chicken. All neurites in this tissue behaved as "non-responding". When preincubated with 5´-IRTX, an antagonist of TRPV1, the application of RTX resulted in the formation of varicosities or growth-cone collapse in only 0.9 % (only 4 out of 433, from a total of 5 DRG explants from mice) of the neurites. Under this condition, DRG explants from E7 chicken revealed a normal phenotype and formation of varicosities was not observed. This proves that the observed growth-cone collapse and varicosity formation was indeed mediated by TRPV1 activation.

Preliminary results show that addition of RTX in explants preincubated with thapsigargin (pre incubation of thapsigargin results in depletion of internal store house Ca^{2+}) also results in the formation of varicosities. This most likely suggest that the observed varicosity formation is due to the activation of TRPV1 located on the plasma membrane, but not at the ER which is responsible for this varicosity formation (see also section 3.3.1).

In summary, there appears to be a presence and functional significance of TRPV1 at neurites and neurite endings including growth cones. Overall the results suggest that TRPV1 regulates the microtubule cytoskeleton and affects growth-cone morphology and movement.